Regulator of G-protein signaling 5 is expressed in hepatic stellate cells and moderates the fibrotic response to injury

Arya J. Bahrami

A dissertation submitted in partial fulfillment of

the requirements for the degree of

Doctor of Philosophy

University of Washington

2014

Reading committee:

William M. Mahoney, Jr., PhD, Chair

Jean S. Campbell, PhD

April S. Stempien-Otero, MD

Program Authorized to Offer Degree:

Pathology -

Molecular Basis of Disease

University of Washington

Abstract

Regulator of G-protein signaling 5 is expressed in hepatic stellate cells

and moderates the fibrotic response to injury

Arya J. Bahrami

Chair of the Supervisory Committee:

William M. Mahoney, Jr., PhD

Pathology

Liver fibrosis is mediated by hepatic stellate cells (HSCs), which respond to a variety of cytokine and growth factors to moderate the response to injury and create extracellular matrix at the site of injury. G-protein coupled receptor (GPCR)-mediated signaling, via endothelin-1 (ET-1) and angiotensin II (AngII), increases HSC contraction, migration and fibrogenesis. Regulator of G-protein signaling-5 (RGS5), an inhibitor of vasoactive GPCR agonists, functions to control GPCR-mediated contraction and hypertrophy in pericytes and smooth muscle cells (SMCs). Therefore we hypothesized that RGS5 controls GPCR signaling in activated HSCs in the context of liver injury. In this study, we localize RGS5 to the HSCs and demonstrate that *Rgs5* expression is regulated during carbon tetrachloride (CCl_4)-induced acute and chronic liver injury in $Rgs5^{LacZ/LacZ}$ reporter mice. Furthermore, CCl_4 treated RGS5-null mice develop increased hepatocyte damage and fibrosis in response to CCl_4 and have increased expression of markers of HSC activation. Knockdown of *Rgs5* enhances ET-1-mediated signaling in HSCs *in vitro*. Taken together, we demonstrate that RGS5 is a critical regulator of GPCR signaling in HSCs and regulates HSC activation and fibrogenesis in liver injury.

Table of Contents

List of Figures

Chapter 1: Introduction

Liver fibrosis is responsible for 29,000 deaths a year in the United States, making it the 12th leading cause of death [1]. It is caused by a chronic liver injury, commonly resulting from viral hepatitis, nonalcoholic steatosis, and alcoholic liver disease[2]. Five million people in the United states suffer from a form of chronic liver disease[3] and associated co-morbidities, including hepatorenal syndrome or hepatic encephalopathy[4]. The liver has tremendous capacity for self-repair; however, chronic injury, repair, and scaring results in the gradual loss of hepatocytes and replacement with scar tissue[5]. Liver fibrosis often progresses to cirrhosis, which is characterized by poorly perfused nodules of regenerated hepatocytes encased in scar tissue, resulting in diminished function, and ultimately, liver failure[6]. This chapter reviews liver fibrosis, co-morbidities, diseases of the liver and animal models of these diseases. Next, we detail the signaling pathways which control fibrosis, underscoring the role of GPCR signaling in control of fibrosis and the role of Regulator of G-protein Signaling (RGS) proteins in the control of these pathways. Finally, we present our hypothesis that RGS5 is a regulator of stellate cell activation in liver fibrosis and controls the stellate cell response to liver injury.

1.1 Structure and cells of the liver

The liver is comprised of heterogeneous cell-types: the parenchyma and the non-parenchyma. The parenchyma of the liver is comprised of hepatocytes; these maintain the body's metabolic homeostasis. Hepatocytes control the levels of amino acids, carbohydrates, lipid, and vitamins. They also synthesize plasma proteins and detoxify endogenous waste products and xenobiotics[7]. Hepatocytes are arranged in plates radiating out from the central vein (Figure 1.1A). Blood from the intestines enters the portal vein, while blood from the heart enters via the hepatic artery. These separate blood sources mix at the edges of the hepatic lobule and enter the sinusoids. Blood flows through the sinusoids from the portal vein, between the rows of hepatocytes, and exits via the central vein.

In addition to hepatocytes, the liver is comprised of non-parenchymal cells, including endothelial cells, Kupffer cells, and stellate cells. The lumens of the sinusoids are lined with endothelial cells, which are fenestrated and highly porous, making them permeable to blood components[8]. The pores allow blood plasma to interact with the hepatocytes (Figure 1.1B). Kupffer cells are the resident macrophage of

the liver[9]. They adhere to the luminal surface of the sinusoidal endothelial cells, scavenging dead cells, endotoxin, and pathogens in the blood. The area between the permeable endothelial layer and the hepatocytes is known as the space of Disse. Hepatocyte microvilli project into this space, increasing the membrane area in contact with plasma while being protected from blood flow. Hepatic stellate cells (HSCs) are found in the space of Disse, surrounding the sinusoidal endothelium. HSCs are astrocyte-like, with fine projections which branch through the space of Disse[10]. HSCs also store large amounts of vitamin A in lipid droplets. In a normal liver, HSCs exist in a quiescent state: astrocyte-like and non-contractile. However in response to liver injury, HSCs are responsible for synthesizing collagen, which can result in hepatic fibrosis, and eventually cirrhosis[10].

1.2 Liver Injury and cirrhosis

Injury to the liver is rapidly repaired by hepatocyte regeneration; therefore, it is only detected in cases of acute liver failure or severe fibrosis and cirrhosis. With severe cirrhosis, progressive scar tissue deposition leads to sinusoidal remodeling, loss of parenchyma, formation of intrahepatic shunts, and increased hepatic resistance[4]. This induces portal hypertension and a series of cascading failures, culminating in multiple organ failure. The appearance of esophageal varices, ascites or other complications indicates decompensated cirrhosis, leading to significant morbidity and mortality[4].

Increased hepatic resistance increases shear stress in the portal and splanchnic vasculature, inducing endothelial production of nitric oxide ($NO^{\bullet}$) and vasodilation as a compensatory mechanism[11]. The combination of portal hypertension and vasodilation increases plasma exudate in intestinal capillaries, leading to the formation of ascites in advanced cirrhosis[12]. Compensatory high levels of $NO^{\bullet}$ induce systemic vasodilation, leading to hepatopulmonary and hepatorenal syndromes. In hepatopulmonary syndrome, $NO^{\bullet}$ vasodilation of the pulmonary vasculature leads to perfusion/ventilation mismatch. Higher blood volume than can be effectively oxygenated flows through the lungs, causing arterial hypoxemia[13]. In hepatorenal syndrome, systemic dilation and ascites reduce effective blood volume. This activates the renin-angiotensin-aldosterone system and the parasympathetic nervous system, inducing a constriction of the afferent renal artery and production of anti-natriuretic factors. The resulting reduction in sodium excretion and urine production causes fluid retention and kidney failure[11].

Hepatorenal syndrome occurs in 10% of cirrhosis cases and accounts for nearly 20% of acute kidney failures in the United States.

Hepatic encephalopathy occurs in up to 50% of cirrhosis patients[14], resulting in attention deficits, cognitive impairment, personality changes and decreased coordination in minor cases, and stupor, coma, and in severe cases, death [3]. One-year mortality of cirrhosis patients with encephalopathy is 64%[4]. Portal hypertension and splanchnic vasodilation induces the formation of portal-systemic shunts. This, in combination with decreased liver function, allows intestinal contaminants to bypass hepatic metabolism and enter the systemic circulation. Intestinal bacteria derived ammonia is the major contributor to hepatic encephalopathy[3], causing cerebral edema and inflammation.

Hepatocellular carcinoma (HCC) is one of the greatest complications and risks of liver cirrhosis, being the third most common cause of cancer death worldwide[15]. While it is most associated with hepatitis B and hepatitis C infection[16], HCC can develop in cirrhosis induced by any cause[4]. Heavy alcohol use, nonalcoholic fatty liver disease (NAFLD), and carcinogen exposure are significant risk factors. With early detection, via screening of at risk patients, tumors can be resected or the entire liver can be transplanted. Early detection and treatment boost survival to 50% at 5 years[15]. In the case of inoperable tumors or lack of a suitable transplant, treatment with the tyrosine kinase inhibitor sorafenib can delay tumor progression (5.5 months vs 2.8 months with placebo)[15].

Cirrhosis, liver failure, and the consequences of decompensation are significant causes of mortality and morbidity, with 525,000 chronic liver disease coded discharges annually[17]. Current therapeutic strategy is to stabilize disease progression and delay decompensation and the eventual need for liver transplantation[4](Figure 1.2). A better understanding of the causes of liver fibrosis and cirrhosis may provide a possible mechanism to limit their progression.

1.3 Causes of liver injury and fibrosis

While the common endpoint of most liver diseases is cirrhosis, the cause of different liver diseases may vary. Damage to hepatocytes can occur by toxin exposure, viral infection, or genetic disease. Though understanding of these causes provides insight to treatment, transplantation remains as

the only curative therapy. Shortage of transplantable livers has led to a relaxation of donor organ requirements[18] and underscores the need for additional anti-fibrotic therapies.

Alcoholic liver disease is caused by excessive consumption of alcohol, and causes symptoms ranging from fatty liver to cirrhosis[19]. A hallmark of alcoholic hepatitis is alcoholic steatosis, the accumulation of fat in hepatocytes. The metabolite of alcohol, acetaldehyde, directly inhibits proliferator-activated receptor-α (PPAR-α) and suppresses fatty acid oxidation[20]. Acetaldehyde is toxic to hepatocytes, depleting glutathione and causing lipid peroxidation that induces apoptosis or necrosis[21]. Alcohol increases intestinal permeability, allowing enteric bacterial lipopolysaccharide (LPS) release into the portal blood flow. LPS triggers Kupffer cells to release TNFα and other inflammatory cytokines[21], causing neutrophilic infiltration. HSCs express TLR4, and are also activated by LPS. Stimulated HSCs, in combination with activated Kupffer cell signaling, leads to the persistent activation of HSCs which proliferate and generate extracellular matrix, eventually causing cirrhosis[21]. Management of alcoholic hepatitis requires cessation of alcohol intake, and corticosteroid treatment is used to reduce inflammation, at the cost of increased risk of infection. Patient compliance is critical as transplant programs require 6 months of abstinence from alcohol prior to transplant[21,22].

Currently, acetaminophen toxicity accounts for 50% of all cases of acute liver failure in the United States[23]; 48% of these cases were due to unintentional overdose[24]. With very high doses, normal metabolism by glucuronidation, sulfation and renal excretion are overwhelmed. Acetaminophen is therefore metabolized by cytochrome-P450, which creates the toxic metabolite *N*-acetyl-*p*-benzoquinoneimine (NAQI)[9]. NAQI depletes glutathione and covalently arylates proteins, leading to centrilobular necrosis and fulminant liver failure. Toxicity is exacerbated by alcohol or drugs which up-regulate cytochrome-P450 and accelerate the production off NAQI[9]. The resultant acute liver failure induces coagulopathy and encephalopathy, with a 65% survival rate[24].

Hepatitis B and C virus, infecting approximately 450 million people worldwide, account for the 57% of cirrhosis cases globally. One million of these patients die each year, typically from decompensated cirrhosis, liver failure, and HCC[25]. Antiviral therapy with nucleoside analogues treat infections, however 70% of Hepatitis C patients and 8% of hepatitis B patients develop chronic

infections[25]. Inflammation present in chronic infection induces persistent immune infiltration, cytokine secretion causes liver damage, and hepatocyte death. HSC are activated in response to this milieu, causing scar tissue deposition, fibrosis, and eventually cirrhosis. Hepatitis B infection accounts for 50% of HCCs[15]. Vaccination against hepatitis B is effective in preventing infection and thus the major cause of HCCs[26]. Antiviral treatment reduces the risk of HCC[27] and slows the progression of fibrosis, and reduces the risk of post-transplant recurrence. Successful viral response improves fibrosis, but does eliminate the risk of HCC[4].

Cholestatic liver injury occurs with the accumulation of bile in the liver, leading to hepatocyte death, fibrosis and cirrhosis. Obstructive cholestasis occurs when the extra-hepatic or intrahepatic bile ducts are blocked. Bile retention causes inflammation of the portal tracts, and results in bridging periportal fibrosis[28]. This eventually progresses to biliary cirrhosis. Removal of the obstruction leads to substantial reversal of fibrosis, over the course of years. Non-obstructive destruction of the intrahepatic bile ducts occurs in primary biliary cirrhosis, wherein autoimmune attack leads to the destruction of small intrahepatic bile ducts. This disease is progressive, leading to biliary fibrosis and cirrhosis. The current standard of care for cholestatic disease is ursodeoxycholic acid (UDCA), a secondary bile that acid reduces cholesterol absorption, symptoms of jaundice, and delays progression to cirrhosis[29].

Non Alcoholic Fatty Liver Disease (NAFLD) is now the leading cause of chronic liver disease in the United States[30]. It is concomitant of the increased obesity and metabolic syndrome incidence worldwide[31]. Confirmation of fibrosis requires liver biopsy, and NAFLD is typically recognized by elevated levels of the liver enzyme alanine transaminase (ALT)[30,32]. While elevated ALT may be detected in severe NAFLD cases, progressive NAFLD often remains undetected. NAFLD is characterized by lipid accumulation in hepatocytes, ranging in appearance from steatosis to ballooned hepatocytes, with nuclei displaced to the side of the cell[31]. Histological confirmation is determined by the presence of Mallory-Denk bodies, comprised of condensed cytoplasmic proteins[31] and the loss of cytokeratins K8 and K18 in ballooned hepatocytes. Collagen deposition occurs in the perisinusoidal space surrounding hepatocytes, appearing in a “chicken wire” pattern[31]. The molecular mechanisms of NAFLD are not well understood, but are thought to be due to “multiple hits” inducing inflammation and fibrosis in the liver.

Increased visceral fat leads to elevated production of adipokines (IL-6, TNFα), which are pro-inflammatory[33]. There is also evidence for increase intestinal permeability[34], allowing endotoxin into the portal blood flow. The combination of these factors activates Kupffer cells, which then activate stellate cells, generating ECM and fibrosis. Management of NAFLD revolves around treating risk factors such as obesity and insulin resistance[32]. Bariatric surgery has been noted as improving insulin resistance, obesity, steatohepatitis, and fibrosis, however more studies are needed[32].

In summary, treatment of liver fibrosis and cirrhosis, of any etiology, revolves around managing the cause of hepatocyte injury and limiting progression to cirrhosis and liver failure. Ultimately, transplantation is the only curative treatment for progressive liver disease. There are currently no therapeutic strategies inhibiting the fibrosis that actually destroys the liver architecture and disrupts function.

1.4 Animal models of liver disease

The processes of liver injury, repair, and fibrosis have been studied extensively in mice and rats, with various models replicating different aspects of hepatic injury and repair[35–37]. These models are used to study fibrosis, with the goal of understanding the fibrotic process and identifying targets for therapy. The most commonly used fibrotic injury models include carbon tetrachloride (CCl_4) exposure or ligation of the bile duct (BDL).

Acute CCl_4 exposure is a necrotic inflammatory model, causing rapid death and necrosis of hepatocytes surrounding the central vein of a hepatic lobule. CCl4 is a teratogen[38] and it is metabolized by hepatocytes, via oxidation by cytochrome P450[39]. This generates a $CCl_3^{\cdot}$ radical that reacts with proteins, lipids, and DNA, which causes rapid cell death and necrosis. The expression of cytochrome P450 is restricted to the hepatocytes surrounding the central vein. These hepatocytes specialize in the metabolism of xenobiotics[40], such as drugs and toxins; thus, CCl_4 treatment causes rapid necrosis of these cells.

The damaged hepatocytes release tumor necrosis factor-α (TNFα), which activates the Kupffer cells (Figure 1.3). Necrotic hepatocytes release damage-associated molecular patterns (DAMPs)[41]

which also stimulate the Kupffer cells to release an array of cytokines including TNFα, IL-1β, and IL-6[35]. IL-1β provokes the infiltration of neutrophils and macrophage, which absorb the necrotic hepatocytes[9]. IL-6 is anti-apoptotic in injured hepatocytes, balancing TNFα-mediated pro-apoptotic signaling [35]. Kupffer cells also release TGFβ, which activates the HSCs[9]. Activated HSCs become contractile, exocytose their lipid droplets and proliferate. In this myofibroblast state, the activated HSC is the primary source of collagen and extracellular matrix (ECM) in liver fibrosis[42]. HSC migrate to the injury[43], secreting ET-1 and TGFβ, which are activating and profibrotic stimuli[44]. Active HSCs secrete matrix to stabilize the wound. Over time, hepatocytes proliferate to replace lost parenchyma. Subsequently, activated HSCs may revert to a quiescent state[45], or become senescent and apoptose, terminating the progression of fibrosis[46,47].

Experimental models of both acute and chronic liver injury have been described. A single CCl_4 injection is an acute toxicity model, which follows the progression outlined above and is repaired over the course of 7 days[48]. A variation of this model is the chronic CCl_4 exposure model. This model of continuous injury is used to replicate severe liver fibrosis and cirrhosis. Mice are injected with CCl_4 2-3 times a week for up to 8 weeks. Injury, inflammation, and HSC activation occur as in acute CCl_4 exposure. Chronic damage and subsequent repair of the liver results in fibrogenesis and diminished liver function, replicating human disease. Resolution of fibrosis occurs with the cessation of CCl_4 exposure.

Thioacetamide is an alternative necrotic inflammatory model, however it induces both periportal and pericentral fibrosis[49]. Administration is via drinking water, making exact dosage difficult. Fibrotic progression requires 10 weeks of treatment, and long term treatment can cause HCC[36].

Another model of liver fibrosis is ligation of the bile duct. This method mimics biliary cirrhosis in humans, where bile drainage from hepatocytes is prevented due to occlusion of the bile duct[7]. Experimentally, the bile duct is surgically ligated, causing cholestasis. Bile accumulation results in oxidative stress to hepatocytes and apoptosis[50]. Kupffer cells engulf apoptotic bodies, causing inflammation[51]. HSCs are activated by the inflammation, causing progressive fibrosis around the bile ducts. Bile toxicity also causes proliferation of duct epithelial cells, portal inflammation, and fibrosis[36]. Cirrhosis is evident 4-8 weeks after ligation of the bile duct. The associated complications of portal

hypertension, portosystemic shunting and ascites, have been observed in rats, making this model useful for studies of decompensated cirrhosis.

Many transgenic murine models mimic fibrosis by overexpressing profibrotic cytokines in hepatocytes. TGFβ and PDGFs are potent HSC mitogens[52] and thus replicate fibrosis by activating these cells. Overexpression of TGFβ in hepatocytes, under the direction of the albumin promoter, causes widespread fibrosis and collagen secretion[53]. Another model induces severe liver fibrosis through the overexpression of PDGF-C in the liver [54]. PDGF-C induces the activation and proliferation of HSCs, which secrete excessive collagen and causes rapid liver fibrosis. The environment of elevated inflammation and increased PDGF-C expression eventually progress to hepatocellular carcinoma (HCC). By 9 months of age, the livers of these mice are fibrotic and have large vascularized tumors, making it useful as a model of HCC. Other models such as the *Tsc1*$^{fl/fl}$*;Alb*^{Cre} and Pten$^{fl/fl}$*;Alb*^{Cre} mice have disregulated mTOR or AKT signaling, leading to the development of HCC[55]. Only the PDGF-C transgenic and the Pten$^{fl/fl}$*;Alb*^{Cre} models develop fibrosis in addition to HCC, making them valuable for the study of carcinogenesis in cirrhosis.

In my studies, I have chosen to use CCl_4 exposure as a method of inducing fibrosis. This allows for the investigation of both the acute and severe injury response, and treatment can be stopped, allowing study of the resolution of fibrosis. The exposure procedure is a simple intraperitoneal injection of CCl_4, allowing treatment of mice from any genetic background, such as the transgenic RGS5-LacZ reporter mouse used in these studies. Alternatively, if a PDGF-C mediated fibrosis model were used, it would require breeding the RGS5-LacZ mice with PDGF-C transgenic mice. While this genetic approach would allow the investigation of Rgs5's role in chronic fibrosis and development of HCC, it is beyond the scope of my thesis work.

Injury to the liver can be experimentally induced by numerous means, but in general, damage to the parenchyma incites a Kupffer cell-mediated inflammatory response which activates the HSCs. Activated HSCs proliferate, migrate, become contractile, and secrete ECM. The collagen and ECM secreted by active HSCs provide a scaffold for regeneration of the wound. The liver regenerates lost parenchyma and the activated stellate cells become quiescent and apoptose. Because the activation of

HSCs is central to fibrogenesis, understanding factors that control HSC activation and behavior is critical for managing disease.

1.5 Stellate cell activation: a critical role for cytokines.

The process of HSC activation can be initiated by growth factor signaling, inflammatory signaling, fibrogenic signaling, and many other pathways[56]. Each of these pathways can also influence the behavior and fibrogenesis of activated HSCs, prolonging and intensifying fibrosis. While many cytokines have been implicated in hepatic fibrogenic signaling, the most studied are the platelet derived growth factor (PDGF), transforming growth factor-β (TGFβ), tumor necrosis factor-α (TNFα) and endothelin-1 (ET-1)-mediated signaling.

PDGF: Platelet derived growth factor-mediated signaling induces rapid proliferation of HSCs[57]. As HSC are activated, expression of PDGFRβ receptors is up-regulated[58]. This is followed by an increase in contractility[59]. PDGF signaling is one of the most studied pathways in HSC activation. Sorafenib is a general inhibitor of receptor tyrosine kinases, and it therefore blocks signal transduction downstream of PDGF receptors. In rats, sorafenib treatment reduces collagen expression and liver fibrosis[60], and it remains the standard of care in human HCC.

TGFβ: Transforming Growth Factor-β is secreted in an inactive form, bound to a latency-associated protein. In this form, it binds to type IV collagen, fibronectin and fibrillin[61]. It remains bound to ECM and stored until activated by matrix metalloproteinases, plasmin, and thrombospondins[61], which can be secreted by macrophages or released from platelets. Quiescent HSCs are activated by TGFβ and subsequently secrete collagen. TGFβ also regulates the growth of hepatocytes: it can be pro-apoptotic during fibrosis, and anti-proliferative during hepatocyte regeneration[61,62]. Inhibition of TGFβ as treatment for hepatic fibrosis is difficult due its varied roles in liver disease[63]. It has been reported that TGFβ intracellular signaling is altered depending on the injury; the TGFβ signal transduction proceeds via ERK in CCl_4–induced injury and by Smad3 and p38 in the bile duct ligation injury model[64].

TNFα: Tumor Necrosis Factor-α is secreted by injured hepatocytes, which activates Kupffer cells. Activated Kupffer cells initiate an acute phase response, secreting IL-1, IL-6, TGFβ, and TNFα[9]. The acute phase response attracts macrophages and other immune cells to the site of injury. TNFα signaling induces both pro-apoptotic and anti-apoptotic signaling[65]. Pro-apoptotic signaling is FADD- and caspase-8-mediated. To counter balance this, anti-apoptotic effects are mediated by NF-κB, inducing the expression of pro-survival genes[9]. The balance of these pathways can be influenced by IL-6 and other cytokines, determining hepatocyte survival. TNFα signaling is mediated by 2 receptors, TNFR1 and TNFR2. Mice lacking TNFR1 do not develop fibrosis in response to CCl_4 exposure[66], suggesting that TNFα-mediated activation of Kupffer cells is required to activate HSCs.

1.6 G-proteins coupled receptors in stellate activation

Several G-Protein Coupled Receptor (GPCR) signaling pathways also contribute to liver fibrosis. They do not directly activate HSCs like the above growth factors; however they have significant effects during HSC activation, and can alter survival, migration, and fibrogenesis. G-protein coupled receptors are the most pharmaceutically targeted receptors in the body[67]. With many drugs already available and high selectivity, GPCRs are attractive targets for therapeutic intervention.

AngII: Angiotensin II is a vasoconstrictor peptide, which is cleaved from an inactive form by angiotensin converting enzyme (ACE). Active AngII induces inflammatory cytokines and promotes contractility and hypertrophy[68]. Activated HSCs express AngII, ACE, and Angiotensin receptor 1 (AT_1)[69]. HSCs contract, proliferate, and up-regulate collagen mRNA in response to AngII stimulation *in vitro*, and infusion of AngII in BDL-injured rats exacerbates fibrosis[70]. Blockade of AngII signaling reduces HSC activation and fibrosis in cirrhotic rats after surgical resection[71].

S1P: Sphingosine-1-phosphate is a lipid with both intra- and extracellular signaling roles. S1P is bound to albumin in the serum. S1P stimulates the fibrotic activation of myofibroblasts[72], and fibrosis in general[73]. Mice lacking the S1P2 receptor had reduced fibrotic area following chronic CCl_4 injury[74]. S1P induces HSC contractility and

proliferation in culture[75]. *In vitro* studies demonstrate S1P enhances migration and expression of fibrotic markers in HSCs[76].

Shh: Sonic Hedgehog promotes the survival of HSCs *in vivo*, and blocking Shh leads to increased apoptosis of activated HSC[77]. Pretreatment of mice with Shh-neutralizing antibodies or cyclopamine, an inhibitor of the Shh signaling cascade, reduced markers of activation and collagen expression in isolated HSCs and in healthy mice[78]. Hepatocytes which show ballooning degeneration secrete increased Shh to stromal cells[79]. Loss of Shh signaling in mouse models of cirrhosis abrogated fibrosis in a conditional knock out of the Shh co-receptor, Smoothened (Smo), in HSCs [80]. Liver regeneration was also inhibited in these Smo conditional knock-out mice, as hepatocyte progenitor cells did not proliferate[81]. Control of Shh signaling in the liver may provide a useful target for future anti-fibrotic therapies.

ET-1: Endothelin-1 is an established mediator of HSC activation and hepatic fibrosis. Prior to injury, the main source of ET-1 is the sinusoidal endothelial cell, but over the course of the injury, production shifts to the HSCs [82]. Inhibition of ET-1 signaling in HSCs reduces markers of HSC activation and fibrogenesis *in vitro*[83], and ET-1 antagonism also reduces fibrotic markers *in vivo* [84,85]. HSCs have been identified as the primary target of ET-1 in the liver, as after injury they express more ET receptors than any other hepatic cell type[86]. ET-1 signaling plays a complex role in HSCs, which have abundant ET_A and ET_B receptors. ET-1 also induces proliferation of quiescent cells, yet is anti-proliferative in active HSCs[87]. The anti-proliferative effect is thought to be ET_B-mediated, as HSCs up-regulate ET_B receptors as they are activated [88,89]. The fibrotic effect of ET-1 may be due to an interaction with TGFβ signaling. TGFβ has been shown to stimulate ET-1 production in HSCs[90], and ET-1 induces TGFβ expression and secretion [89,91]. This is an autocrine loop to promote collagen secretion and fibrosis in HSCs (Figure 1.3). However it has been reported that TGFβ down-regulates ET-1 binding sites in HSCs *in*

vitro[92]. We have observed a down-regulation of ET_B mRNA in response to TGFβ (see Fig. Figure 2.4B), but the question is remains unresolved.

In summary, the pathogenesis of liver fibrosis is affected by numerous GPCR signaling pathways that alter HSC survival, contraction or migration; however, ET-1 signaling is directly implicated in the activation of HSCs and the autocrine production of TGFβ. The importance of ET-1 signaling in HSC activation implicates it as a prime target for therapeutic intervention.

1.7 Endothelin-1 signaling regulates vascular tone and vascular injury.

ET-1 is a potent vasoconstrictor peptide that is produced primarily in endothelial cells of vessels and in the uninjured liver. It is produced as preproET-1, which is cleaved to big-ET and then again cleaved by endothelin converting enzyme (ECE). ET-1 induces the contraction and proliferation of vascular smooth muscle cells (vSMCs)[93,94]. Production of ET-1 in endothelial cells counter-balances $NO^{\cdot}$ production, with both pathways signaling to regulate vSMC tone and blood flow[94]. The two ET-1 receptor subtypes (ET_A and ET_B) signal through the large Gα proteins: ET_A via $G\alpha_i$, $G\alpha_q$, and $G\alpha_{12/13}$; ET_B via $G\alpha_q$ and $G\alpha_i$[95] (Figure 1.4). Both receptor subtypes are expressed in medial vSMCs[94]. ET receptors are also expressed in the vascular adventitia; adventitial ET_B has been shown to aid in ET-1 clearance from the blood[96]. Sequestration of ET-1 prevents excessive signaling in the media of arteries, reducing constriction, pathogenic remodeling, and hypertrophy.

ET-1 signaling has been implicated in vascular diseases such as scleroderma, and pulmonary hypertension[97]. The involvement of ET-1 in numerous human diseases has led to the development of a series of selective and general ET receptor agonists and antagonists, which have been used in clinical trials [44]. More relevant to our study, the drugs BQ-123 and BQ-788 have both been used to treat cirrhosis and portal hypertension, targeting ET_A and ET_B, respectively[44]. These strategies have had mixed results, as ET-1 antagonism leads to side effects in the cardiovascular system and the drugs are hepatotoxic[98]. Targeting intracellular signaling downstream of ET-1 receptors could provide an alternative strategy for the inhibition of hepatic fibrosis. RGS proteins are endogenous inhibitors of GPCR signaling, and provide another mechanism by which ET-1 signaling may be selectively inhibited.

1.8 Regulator of G-protein signaling proteins regulate signaling through GPCRs.

The Regulator of G-protein Signaling (RGS) family are GTPase activating proteins (GAP) which accelerate the termination of Gα signaling downstream of GPCRs. More than 30 family members have been identified[99], many inhibiting specific GPCRs. The presence of a RGS protein allows a rapid termination of signaling after activation of the receptor. RGS-mediated termination of GPCR signaling was proposed as a receptor desensitization mechanism after known mechanisms, such as receptor inactivation and internalization, were determined to be too slow[100]. The first RGS protein described was sst2p in yeast, which activates GAP activity of Gα downstream of pheromone receptors, thereby blocking the mating response[101]. RGS proteins in mammalian cells were subsequently demonstrated to block GPCR signaling [102]. There are 6 subfamilies of RGS proteins, defined by an RGS domain that interacts with Gα subunits. These families include G-protein coupled receptor kinases (GRKs), Guanidine exchange factors (GEFs), AKAPs and others, subdivided by structural similarities (as reviewed in [99]).

The RGS-R4 subfamily, of which RGS5 is a member, are small proteins consisting of the RGS domain and a short N-terminal domain[99] The N-terminus is responsible for receptor selectivity and cellular localization[103]. Several members of this family have physiological importance in regulating GPCR signaling in the cardiovascular system and the regulation of metabolism. RGS2 has been shown to control blood pressure: mutant mice are hypertensive [104] and transplantation of RGS2 deficient kidneys into normal mice can induce hypertension[105]. RGS4 is highly expressed in the sinoatrial node of the heart, thereby suppressing parasympathetic nervous system stimulation of the heart by blocking $G\alpha_i$ signaling downstream of the M2 muscarinic receptor[106]. RGS4-null mice show increased bradycardia in response to parasympathetic stimulation. A metabolic syndrome phenotype has been identified in RGS4-null mice[107], as RGS4 also controls the release of catecholamines by the adrenal glands. Loss of RGS4 results in increases in circulating catecholamines and free fatty acids. RGS4-null mice have liver steatosis, decreased insulin production, and higher glucose intolerance. RGS16 expression is diurnally regulated in mouse brains, and expression is up-regulated in the liver in response to fasting and down-regulated in response to feeding[108]. RGS16 is an inhibitor of fatty acid oxidation in the liver[109], causing knockout mice to have higher expression of fatty acid oxidation genes and fatty acid oxidation.

RGS proteins have also been implicated in numerous cancers[110,111]. Lysophosphatidic acid (LPA) is a GPCR-mediated growth factor promotes the progression of ovarian cancer. RGS2, RGS6, RGS9 inhibit LPA receptor G-protein pathways, and thus their expression is altered in ovarian cancer cell lines[112]. Angiogenesis in tumors can allow continued expansion and metastasis[113]. RGS5 has been identified as a marker of tumor vasculature[114], and decreased RGS5 expression normalizes this vasculature[115]. Further, RGS5 and RGS17 expression are altered in hepatocellular carcinoma (HCC).

1.9 Regulator of G-protein Signaling 5 in the cardiovascular system

The expression of RGS5 reduces sensitivity to a number of vasoactive GPCR agonists, including AngII, ET-1, serotonin[116], and bradykinin[117,118]. RGS5 has also been shown to regulate Shh[119] and S1P[120]. Aortic banding studies demonstrate that RGS5 is down-regulated at early time points following injury and up-regulated late after hypertrophic remodeling is complete. RGS4 and RGS5 are down-regulated after banding, but are highly overexpressed 28 days after injury. High RGS4 and RGS5 expression in aortas showed reduced contraction in response to $G\alpha_q$ and $G\alpha_i$- mediated vasoconstrictors[121]. RGS5 is highly expressed in vSMCs of the major arteries, with varied expression levels in cells derived from different embryonic origins[122] (Mahoney, unpublished data). RGS5 expression is related to the regulation of vascular tone, as multiple polymorphisms in RGS5 are strongly associated with hypertension[123,124]. In addition to its expression in vSMC of the large arteries, RGS5 is also a maker of pericytes[120] The expression of RGS5 by pericytes on new capillaries indicates maturity and stability, making RGS5 expressing pericyte coated capillaries resistant to pruning and regression[125].

RGS proteins are also regulated by selective degradation in response to $NO^{\bullet}$. Endothelial cells produce $NO^{\bullet}$ in response to shear stress, which signals to adjacent vSMCs[126]. $NO^{\bullet}$ signaling triggers the hyperpolarization of the cell, via cGMP and PKG, and allows relaxation of arterial SMCs. The vascular expressed RGS proteins (RGS4, RGS5 and RGS16) are negatively regulated by $NO^{\bullet}$ signaling via the proteasomal degradation (N-end rule[127,128]. These RGS proteins have an N-terminal cysteine, which in the presence of $NO^{\bullet}$, are oxidized and arginylated by arginyl-tRNA-protein transferase-1 (ATE1), ubiquitinated and degraded[128]. ATE1-null mice are embryonically lethal, and have impaired $G\alpha_q$-

mediated ERK1/2 signaling due to increased levels of RGS4 and RGS5[129]. $NO^{\bullet}$ regulated RGS protein degradation in the cardiovascular system may provide a feedback mechanism for tuning vascular contractile sensitivity to GPCR agonists.

Overexpression of RGS5 in cardiomyocytes has been shown to be cardioprotective in the thoracic aortic constriction model by inhibiting fibrosis and pathogenic remodeling[130]. RGS5 also serves as a marker for vascular remodeling[131] and for pericyte coverage of capillaries[125]. RGS5-null mice develop normally but are hypotensive[132]. A lower body weight compared to wild-type littermates has been observed[133]. Conversely, Deng et al. determined RGS5-null mice have increased bodyweight and are prone to metabolic disorder[134]. This may be related to mouse colony differences, as this phenotype has not been reported previously and we do not observe this phenotype in our colony (personal observations). RGS5-null mice have increased smooth muscle cell hypertrophy and fibrosis in a hypertension injury model[135].

1.10 The role of pericytes in fibrosis

Pericytes are perivascular cells located on the exterior surface of the microvasculature, with multiple fine projections allowing contact with multiple endothelial cells[136]. Markers such as PDGFRβ, SMA, desmin, and RGS5 commonly identify pericytes. The pericytes derive from the same developmental origin of the resident tissue. Brain and thymus pericytes are neural crest in origin, while pericytes of coelomic organs are mesothelium derived[137]. Despite having similar origins, their signaling behaviors may differ. Developmental studies of PDGF-BB/PDGFRβ signaling showed that PDGF-BB is important for pericyte localization and periendothelial recruitment in the heart, lungs, and gut, but the HSCs do not require PDGF-BB signaling and do not express PDGFRβ during development[138]. The control of vascular permeability is thought to be regulated by pericytes, as loss of pericyte encoatment results in increased endothelial transcytosis[137]. Pericytes in various organ systems differentiate into myofibroblasts, which create scar tissue in response to injury. Fate mapping studies in models of kidney fibrosis, including unilateral ureter ligation (UUO) injury model and ischemia reperfusion, confirmed that kidney myofibroblasts are pericyte-derived[139,140]. In the liver, fate mapping has shown that HSCs, the pericytes of the liver[141], give rise to between 82% and 96% of myofibroblasts in fibrotic liver injury[142].

In the skin, capillary rarefaction and fibrosis occurs in scleroderma. Scleroderma is characterized by the loss of skin capillaries and scar tissue deposition, resulting in skin thickening and necrosis. The role of RGS5 in scleroderma is not known, however skin fibrosis is associated with activated myofibroblasts expressing RGS5 and this RGS5 expression normalizes following the resolution of fibrosis [143,144].

1.11 Regulator of G-protein Signaling 5 in fibrosis

Models of fibrotic disease and injury with potential roles for RGS5 include kidney fibrosis, lung fibrosis, and liver fibrosis. In an experimental murine model of kidney fibrosis induced by UUO, the up-regulation of RGS5 expression coincides with progressive fibrosis (Mahoney unpublished data). Similarly, bleomycin–induced lung fibrosis causes inflammation, cell death, and fibrosis, and RGS5 expression is up-regulated as fibrosis progresses (Mahoney unpublished data). This phenomenon is also observed in the CCl_4–induced liver injury model, with RGS5 expression being up-regulated during the activation of HSCs and during chronic fibrosis (Chapter 2). In each of these injuries, a tissue-specific pericyte population is activated and differentiates into myofibroblasts. RGS5 expression in these pericytes and the pattern of RGS5 up-regulation during fibrotic remodeling across multiple organ systems suggests a central role in a common pathway regulating fibrosis. Pathways involved in multiple organs suggests a conserved and fundamental target for controlling fibrosis[145]. Taken together, we suggest that an RGS5-based therapy would be widely applicable to many forms of fibrotic injury.

1.12 Summary

Fibrosis is the common endpoint of numerous liver diseases, and ultimately leads to cirrhosis. The few therapeutic options are aimed at managing the symptoms of cirrhosis, and insufficient numbers of organs for transplant result in high mortality and morbidity. A lack of anti-fibrotic strategies leaves the primary mechanism of hepatic destruction un-addressed. Activated HSCs create the collagen that disrupts liver function. Inhibition of HSC activation via targeting GPCR signaling could provide a means of reducing fibrosis. RGS5 is an inhibitor of GPCR signaling expressed in pericytes throughout the body and regulated in response to fibrosis. This thesis explores the regulation and function of RGS5-mediated control of signaling in HSCs and liver fibrosis, identifying a novel target for anti-fibrotic therapy. We hypothesize that RGS5 is up-regulated during injury to control HSC activation and thus fibrosis. Our

major findings are that RGS5 is a marker of HSCs and expression is up-regulated in response to injury. CCl_4-induced injury in RGS5-null mice causes increased HSC activation and increased hepatocyte damage and fibrosis. Therefore we propose that RGS5 is a critical regulator of the HSC response to injury and fibrosis.

1.13 Figures

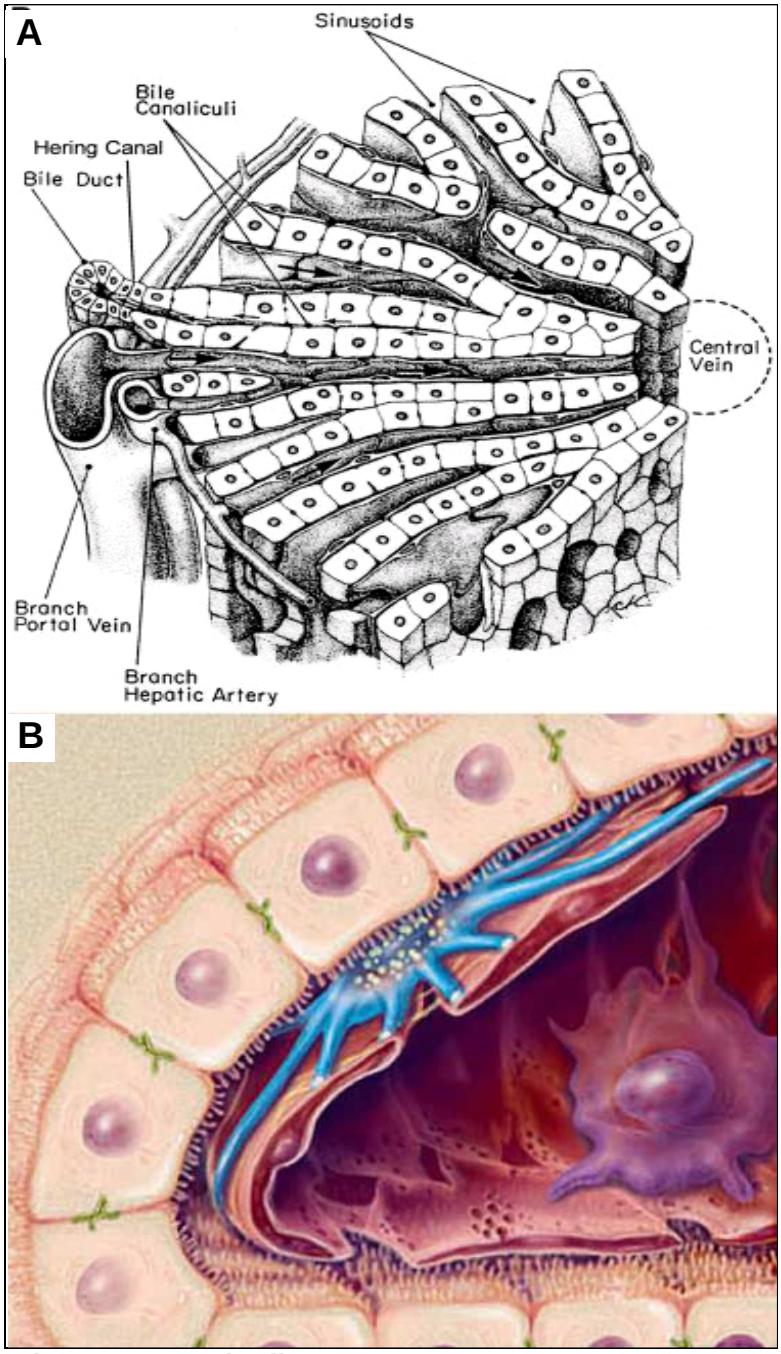

Figure 1.1 Hepatic structure and cell types

A. Hepatic lobules are the working unit of the liver. Blood flows in through the portal vein, down the sinusoids, and drains from the central vein. Figure adapted from Le Lay et al. 2010[146]. **B.** Cell types of the liver. The sinusoids are lined with fenestrated endothelial cells. Between the hepatocytes and endothelial cells is the space of Disse, which contains the HSC (in blue). Kupffer cells adhere to the lumen of the sinusoids (purple) Figure adapted from Friedman et al 2008[147].

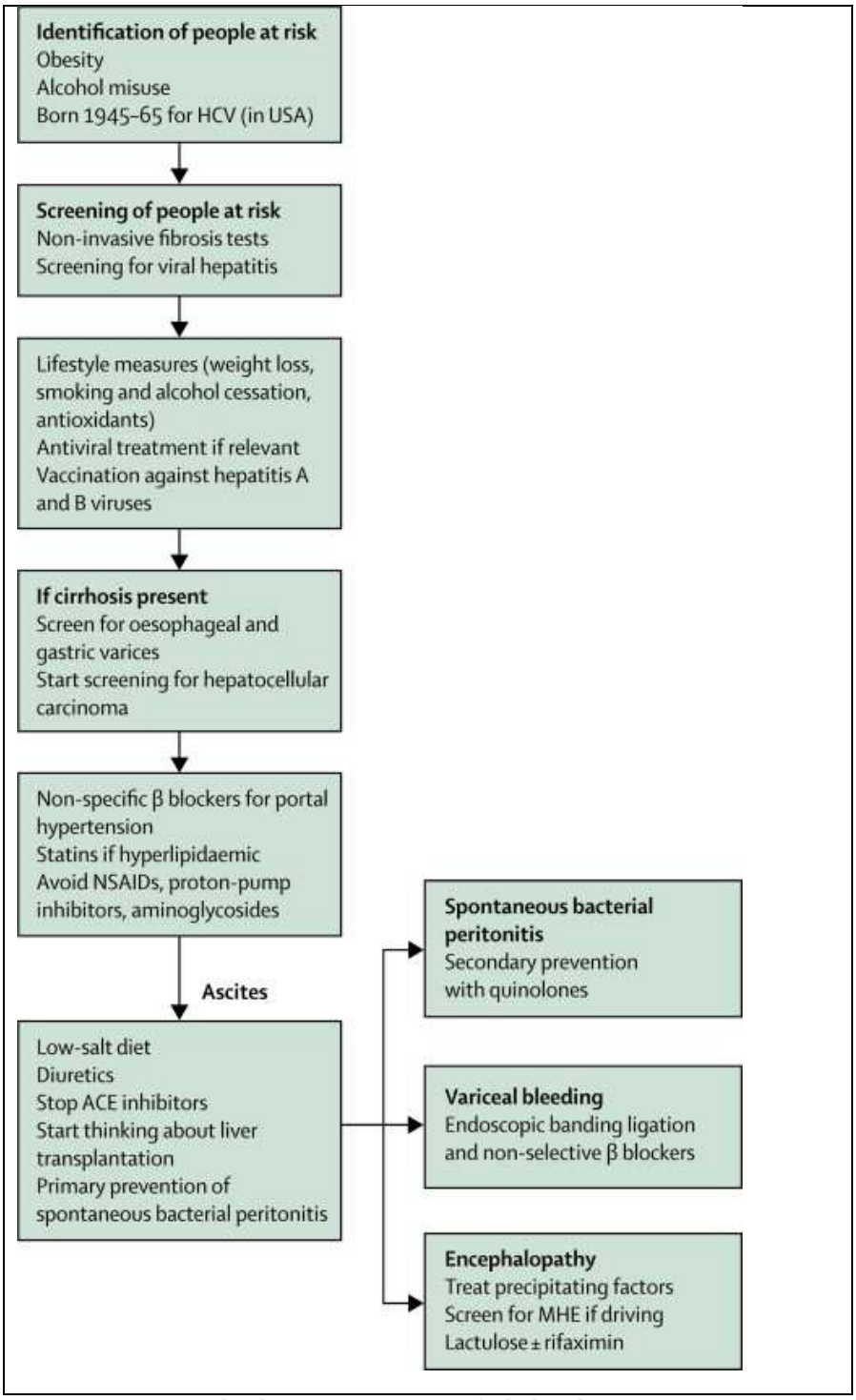

Figure 1.2 Current strategy in the management of cirrhosis.

Adapted from Tsochatzis et al. 2014 [4]

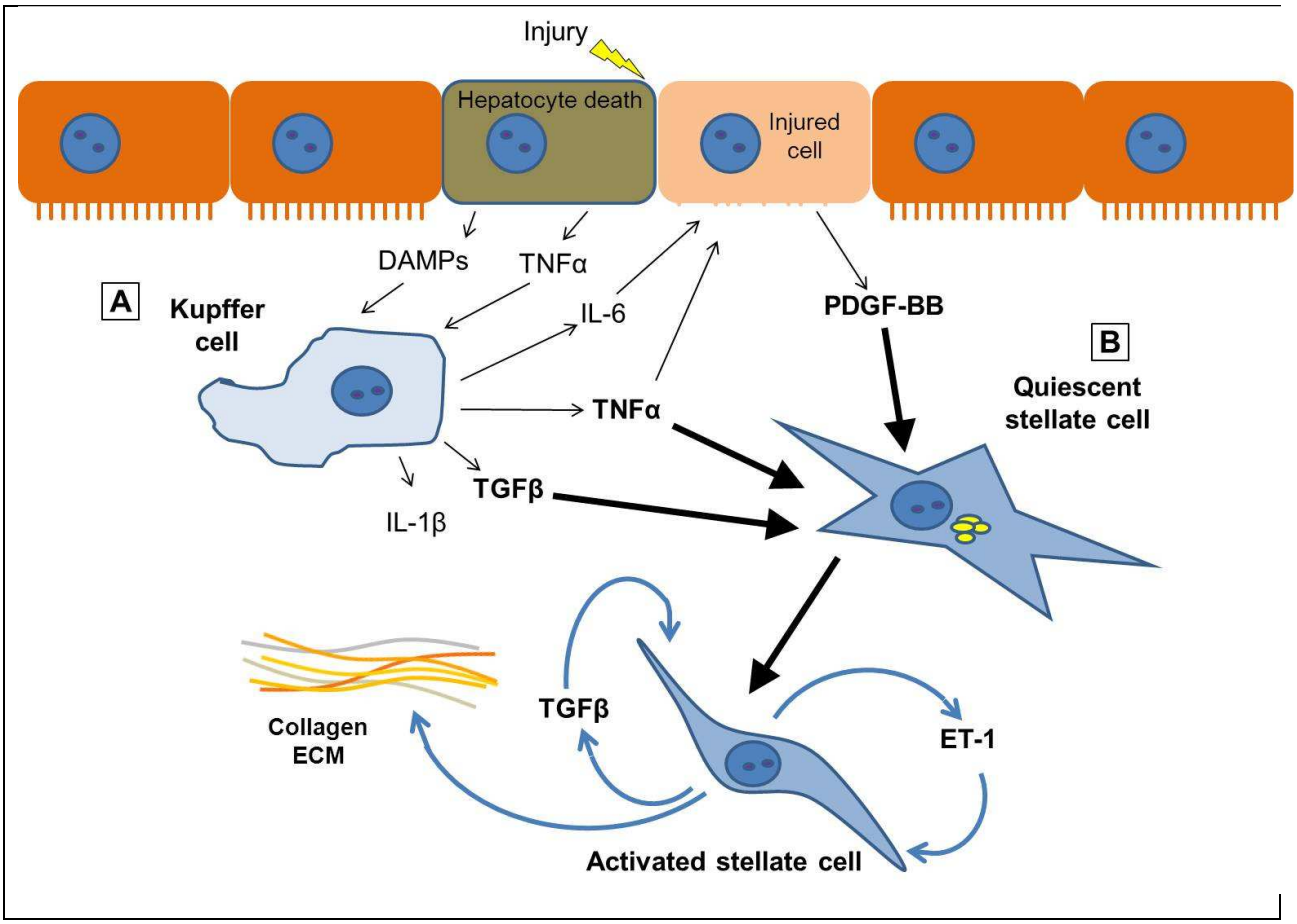

Figure 1.3 Hepatocyte injury and Kupffer cell mediated inflammation activate stellate cell fibrogenesis.

A. Hepatocyte death and damaged hepatocytes release Tumor Necrosis Factor-α (TNFα), which activates the Kupffer cells. Necrotic hepatocytes release damage-associated molecular patterns (DAMPs) which also stimulate the Kupffer cells to release an array of cytokines including TNFα, IL-1β, and IL-6. IL-1β provokes the infiltration of neutrophil and macrophages, which remove the necrotic tissue. IL-6 is anti-apoptotic in injured hepatocytes, balancing the pro-apoptotic signaling from TNFα. **B.** TNFα, TGFβ, and PDGF-BB activate HSCs. Activated HSCs become contractile, exocytose their lipid droplets and proliferate. Active HSC migrate to the injury, while secreting ET-1 and TGFβ, which maintaining activation and promote collagen expression and extracellular matrix (ECM) production.

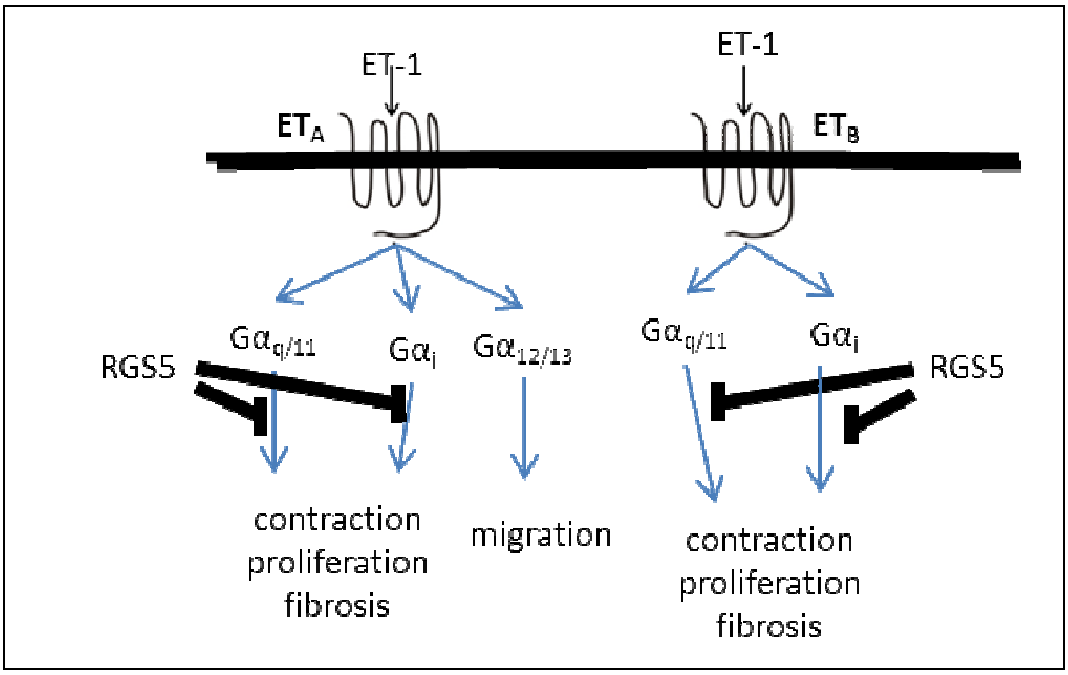

Figure 1.4 ETA and ETB receptors utilize different Gα subunits.

RGS5 inhibits $G\alpha_q$- and $G\alpha_i$-mediated signaling, completely blocking ET_B signaling, and restricting ET_A signaling to $G\alpha_{12/13}$ mediated pathways.

Chapter 2:

Regulator of G-Protein 5 is a marker of hepatic stellate cells and expression mediates response to liver injury.

ABSTRACT:

Liver fibrosis is mediated by hepatic stellate cells (HSCs), which respond to a variety of cytokine and growth factors to moderate the response to injury and create extracellular matrix at the site of injury. G-protein coupled receptor (GPCR)-mediated signaling, via endothelin-1 (ET-1) and angiotensin II (AngII), increases HSC contraction, migration and fibrogenesis. Regulator of G-protein signaling-5 (RGS5), an inhibitor of vasoactive GPCR agonists, functions to control GPCR-mediated contraction and hypertrophy in pericytes and smooth muscle cells (SMCs). Therefore we hypothesized that RGS5 controls GPCR signaling in activated HSCs in the context of liver injury. In this study, we localize RGS5 to the HSCs and demonstrate that *Rgs5* expression is regulated during carbon tetrachloride (CCl_4)-induced acute and chronic liver injury in $Rgs5^{LacZ/LacZ}$ reporter mice. Furthermore, CCl_4 treated RGS5-null mice develop increased hepatocyte damage and fibrosis in response to CCl_4 and have increased expression of markers of HSC activation. Knockdown of *Rgs5* enhances ET-1-mediated signaling in HSCs *in vitro*. Taken together, we demonstrate that RGS5 is a critical regulator of GPCR signaling in HSCs and regulates HSC activation and fibrogenesis in liver injury.

Submitted to *PLoS One* (06-2014)
Contributing authors: Arya J. Bahrami, Jagadambika J. Gunaje, Brian J. Hayes, Kimberly Riehle, Heidi L. Kenerson, Raymond S. Yeung, April S. Stempien-Otero, Jean S. Campbell, William M. Mahoney, Jr.

2.1 Introduction:

Liver fibrosis and its sequelea of cirrhosis and hepatocellular carcinoma (HCC) are responsible for 29,000 deaths a year in the United States, making it the 12th leading cause of death[148]. Injury to the liver results in a wave of cytokine mobilization[149], many of which are secreted by Kupffer cells, the liver's resident macrophages. These cytokines (*e.g.* tumor necrosis factor α (TNF- α)[150] and transforming growth factor-β1 (TGF- β) [62]) then activate HSCs, which deposit extracellular matrix (*e.g.* collagen) as part of the wound repair response. With chronic injury, ongoing inflammation and HSC activation results in accumulation of scar tissue and eventual decreased liver function[151].

In the uninjured liver, quiescent HSCs behave like pericytes[141], surrounding the endothelium of the sinusoids. However, upon injury-induced activation, HSCs become the primary collagen-producing cell in the fibrotic liver[10,152]. HSC activation, in response to platelet derived growth factor BB (PDGF-BB)[57–59] and TGFβ[61,62], is well characterized; however, G-protein coupled receptor (GPCR) signaling pathways also influence their behavior during fibrosis. AngII[69–71], ET-1[82–85,153], and norepinephrine (NE)[154–157] have been implicated in promoting HSC activation and thus fibrosis. Therefore, modulating signaling downstream of GPCRs may represent a novel therapeutic target in liver fibrosis, potentially preventing HCC.

RGS5 is a small GTPase activating protein that inhibits $G\alpha_q$ and $G\alpha_i$-mediated signaling downstream of GPCRs[158]. RGS5 is primarily expressed in vascular smooth muscle cells (SMCs) and pericytes[120,125,132,159], and inhibits AngII- and ET-1-mediated signaling[116,160] to regulate blood pressure[123,124,132,133] and vascular remodeling[121,161]. Moreover, RGS5 expression correlates with both cardiac[130] and skin[162] fibrosis, and expression is increased in multiple cancers (e.g., breast, ovarian, acute myeloid leukemia, and liver)[110–112,163–165].

We hypothesized that RGS5 controls liver injury via its ability to modulate GPCR-mediated signaling in activated HSCs. In this study, we localize expression of RGS5 to HSCs in the liver, and demonstrate that *Rgs5* expression is regulated in both acute and chronic liver injury. Furthermore, mice lacking RGS5 expression develop increased hepatocyte damage and fibrosis in response to carbon tetrachloride (CCl_4). *Rgs5* expression is regulated in cultured HSCs in response to fibrogenic agonists, and ET-1-mediated signaling is potentiated in the absence of *Rgs5* expression. Taken together, we demonstrate that RGS5 is

a critical regulator of GPCR signaling in HSCs, and controls HSC activation and fibrogenesis in response to liver injury.

2.2 Materials and methods:

2.2.1 Animals: *Rgs5*^{LacZ} mice, which have a nuclear localized β-galactosidase reporter gene knocked into exon 2 of the *Rgs5* locus and mice have been backcrossed to a C57BL/6 background , were purchased (Deltagen[166]). To induce acute liver injury, mice were injected (*i.p.*) with 10 µl/g body weight CCl_4 (Sigma-Aldrich) diluted 10% (v/v) in olive oil once. To induce chronic liver injury, mice were injected twice weekly for four weeks. Olive oil-injected animals served as controls for CCl_4-injected mice. At the indicated time-points, mice were sacrificed using CO_2 inhalation. The Institutional Animal Care and Use Committee of the University of Washington, which is certified by the Association for Assessment and Accreditation of Laboratory Animal Care International, approved all experiments.

2.2.2 X-gal labeling: To preserve β-galactosidase activity, liver tissue was fixed in PLP (4% paraformaldehyde (PFA), 75 mM L-lysine, 10 mM sodium periodate) for 2 hours at 4℃ , cryopreserved in 18% sucrose, frozen in optimum cutting temperature compound, and 5-µm cryosections were prepared for X-gal labeling or immunofluorescence (IF). LacZ activity was measured using a standard 5-bromo-4-chloro-3-indolyl-β-D-galactoside (X-gal) staining protocol[139] for 16 hours at 37℃. After washing, sections were post-fixed in 1% PFA for 5 minutes and immunolabeled for additional histologic analysis (see below).

2.2.3 Measurement of relative hepatocyte cytoplasmic clearing: Approximately twenty 10x fields of H&E stained 5 µm paraffin embedded sections liver were imaged, each representing a 1.19x.89 mm area. Using the ImageJ software package, the relative cleared hepatocyte cytoplasmic area was measured. Images were automatically adjusted for contrast, converted to grey scale, and sharpened to enhance borders. The threshold tool isolated the tissue from slide background. Particle analysis included sizes 49 μm^2 to 324 μm^2 and circularity value between 0.3 and 1.0, yielding total particle area measured as a percentage of slide area. Data was processed by macro to remove potential bias.

2.2.4 Quantification of collagen deposition: To label collagen deposition (indicative of fibrosis), 5 µm

paraffin embedded tissue sections were stained with picrosirius red (365548 and P6744, Sigma) and 0.1% Fast Green (F7258, Sigma) at room temperature for 30 minutes. The relative quantification of fibrosis was measured using ImageJ. Ten 4x fields were imaged for each liver, representing a 2.95x2.21mm area. Using the color threshold tool, red staining was isolated. The image is then converted to grey scale, and threshold is used to subtract remaining background. Measurement of the remaining area yielded the area of the slide with red staining. This was normalized to the area of the tissue (vessel lumen subtracted) for each slide to yield the percent of tissue with picrosirius red staining. Data was processed by macro to remove potential bias.

2.2.5 Immunofluorescence (IF): IF was performed using standard techniques, with liver sections incubated overnight with the following primary antibodies: rabbit anti-GFAP 1:1000 (Z0334, Dako), chicken anti-β-gal 1:1000 (ab9361, Abcam), rabbit anti-SMA1:200 (ab32575 Abcam), rabbit anti-CRBP1 1:200 (sc30106, Santa Cruz), rabbit anti-VWF 1:200 (A0082, Dako), Rat anti-CD-31 1:100 (553370, BD Pharmingen), and Rat anti-F4/80 1:200 (122603, Biolegend). Immune complexes were detected with the following secondary antibodies: Alexa 488 conjugated goat anti-Rabbit IgG (A11034, Life Technologies), Alexa 488 conjugated goat anti-rat IgG (A21208, Life Technologies), Alexa 647 conjugated donkey anti-rat IgG (A21247, Life Technologies), Alexa 594 conjugated donkey anti-chicken IgG (703-516-155, Jackson Immunoresearch), antibodies. Sections were mounted with VectaShield (H-1000, Vector Labs) and imaged with a Zeiss Axiovert 200 microscope. Confocal images generated using an Olympus FV1000 confocal microscope.

2.2.6 Cell Culture: The LX-2 HSC cell line was generously provided by Scott L. Friedman[167]. LX-2 cells were passaged in DMEM high glucose (Gibco/Life Technologies) supplemented with 2% FBS and penicillin-streptomycin and used between passages 10 and 20.

2.2.7 Hepatic stellate cell isolation: Mouse primary HSCs were prepared by perfusion with collagenase/pronase and density centrifugation using Optiprep (Sigma) as reported previously[168].

2.2.8 siRNA Knockdown of *Rgs5* Expression: *Rgs5* was knocked down in LX-2 cells using a specific small interfering RNA (siRNA) from Life Technologies (5′-AGGAGAUUAAGAUCAAGUUTT-3′). LX-2

HSCs were transfected with Lipofectamine RNAiMAX Transfection reagent (Life Technologies) following the manufacturer's specifications. Briefly, $5x10^5$ cells were transfected with either *Rgs5*-specific siRNA (12.5 nM) or siRNA negative control (12.5 nM; Life technologies) and plated at a final density of 10^5 cells/60 mm dish (for protein isolation) or 4×10^4 cells/6-well dish (for RNA isolation) and grown in 2% FBS growth media. After 24hr, the media were changed to serum-free media and cells were starved for 24 hr. Where indicated, cells were stimulated with endothelin-1 (ET-1; 100 nM; Sigma), TGFβ (5 ng/ml; R&D systems), TNFα (5 ng/ml; R&D systems), or PDGF-BB (10 ng/ml; R&D systems).

2.2.9 RNA isolation and quantitative RT-PCR (qPCR): RNA was isolated from LX-2 cells and mouse livers using the E.Z.N.A. Total RNA Kit I (Omega Bio Tek). For tissue lysates, 27 mm^3 were homogenized in TRK lysis buffer using a stator-rotor homogenizer, as per kit instructions. cDNA was prepared by reverse transcription using the High-Capacity cDNA Reverse Transcription Kit; (Applied Biosystems). 20ng cDNA was used in each qPCR reaction, using PerfeCTa SYBR Green FastMix (Quanta biosciences). Gene expression was calculated by the ΔΔCt method: Fold expression $= 2^{-\Delta\Delta Ct}$. Gene expression was normalized to Gapdh expression within each sample then normalized to individual control treatment conditions within each dataset.

2.2.10 Immunoblot: Lysates were prepared from LX-2 cells 0, 10, and 20, min after ET-1 treatment by resuspending scraped cell pellets in lysis buffer [50 mM Tris·HCl (pH 8.0), 120 mM NaCl, 0.5% Igepal, 1 mM EDTA, with protease inhibitors (Calbiochem)]. After protein quantitation, 10 µg of each protein extract was separated on 10% bis-Tris gels. Proteins were transferred to PVDF and blocked with 5% nonfat dry milk (NFDM) in TBS-T (0.1% Tween). Membranes were incubated with the following primary antibodies diluted in 5% NFDM in TBS-T overnight at 4℃: 1:1,0 00 phospho-p42/44 (Thr202/Tyr204; pERK) (Cell Signaling); 1:5,000 total p42/44 (ERK)[169]. After 3× washes with TBS-T, membranes were incubated with the following secondary antibodies diluted in 5% NFDM in TBS-T at room temperature for 1 h: 1:8,000 goat α-rabbit IgG HRP conjugate (Bio-Rad); 1:8,000 goat α-mouse IgG HRP (Bio-Rad). After 4× washes with TBS-T, blots were incubated in ECL reagent (Super Signal West Pico, Pierce) and exposed to autoradiographic film.

2.2.11 Statistics:

Quantitative data were analyzed by unpaired t-test in excel. A p-value of less than 0.05 was considered significant. Where indicated, significance was analyzed using a non-parametric Mann-Whitney U test.

2.2.12 Ethics statement: Mice were housed in a specific pathogen-free environment overseen by the Department of Comparative Medicine at the University of Washington with IACUC approval under protocol 4253-01.

2.3 Results:

Regulator of G-Protein 5 is expressed in HSCs. Using $RGS5^{LacZ}$ reporter mice, we localized the expression of RGS5 in the liver by X-gal staining (Figure 2.1A). β-gal$^+$ cells, and therefore RGS5$^+$ cells, are observed adjacent to liver sinusoids. As expected, a subset of vascular SMCs of large vessels (arrows, Figure 2.1A) express both RGS5 and smooth muscle α-actin (SMA) (Figure 2.1B) by IF, consistent with published findings[161]. Glial fibrillary acidic protein (GFAP) is expressed in HSCs[147,170], and co-labeling with the GFAP and the β-gal antibody demonstrates co-localization of the RGS5 reporter and GFAP in HSCs adjacent to sinusoids (Figure 2.1C). Another protein expressed in HSCs, cellular retinol-binding protein-1 (CRBP1[171]), also co-localizes with β-gal, confirming that these cells are HSCs (Figure 2.1D). Von Willebrand Factor (VWF) is expressed in endothelial cells, including those in the liver sinusoids (LSECs)[172]. IF for VWF and β-gal demonstrates that LSECs are distinct from β-gal$^+$ cells (Figure 2.1E); LSECs are VWF$^+$, whereas the β-gal$^+$ cells are sparse and evenly distributed, and do not overlap with VWF$^+$ cells. Similarly, F4/80$^+$ Kupffer cells and β-gal$^+$ cells are also distinct, with no co-localization observed (Figure 2.1F). Confocal imaging for GFAP and β-gal confirms that the nuclei of GFAP$^+$ HSC are β-gal$^+$ (Figure 2.1G). No co-localization is observed in confocal imaging for CD31$^+$, another endothelial cell marker, and β-gal$^+$ cells (Figure 2.1H). Finally, to verify that RGS5 expression is restricted to HSCs, we measured *Rgs5* expression in primary HSCs isolated from WT mice[168]. We found that primary HSCs express high levels of *Rgs5* relative to other non-parenchymal cell markers (Figure 2.11A, B). In summary, our co-localization analyses determined that RGS5 is specifically expressed in HSCs, but not in hepatocytes, LSECs, or Kupffer cells.

2.3.1 Increased Regulator of G-Protein 5 expression is associated with liver tumor and liver fibrosis.

Multiple studies have demonstrated RGS5 expression in liver tumors[163,164]. Because these tumors are associated with HSC activation, we examined RGS5 expression in two mouse models of HCC, mice with hepatocyte-specific deletion of either tuberous sclerosis complex 1 (*Tsc1*) or phosphatase and tensin homolog (*Pten*). The loss of either of these genes results in disruption of the (PI3K)/AKT/mTORC1 pathway, leading to HCC or cholangiocarcinoma[55]. First we performed trichrome staining on *Tsc1*$^{fl/fl}$*;Alb*^{Cre} and Pten$^{fl/fl}$*;Alb*^{Cre} liver sections spanning HCCs and adjacent non-tumor liver. *Tsc1*$^{fl/fl}$*;Alb*^{Cre} mice had collagen deposition in tumors (Figure 2.2C), but not in adjacent non-tumor liver (Figure 2.2A), while Pten$^{fl/fl}$*;Alb*^{Cre} mice had significant trichrome staining in both tumor and non-tumor liver (Figure 2.2B, D). When we macro-dissected tumors from these mice and performed qPCR for *Rgs5* expression (Figure 2.2E, F), we found that *Rgs5* expression mirrored collagen deposition: 1) *Rgs5* is elevated in fibrotic *Tsc1*$^{fl/fl}$*;Alb*^{Cre} tumors but not adjacent non-fibrotic liver; 2) *Rgs5* is elevated in both tumor and surrounding liver (both fibrotic) in Pten$^{fl/fl}$*;Alb*^{Cre} mice. The up-regulation of *Rgs5* expression in fibrotic liver tissue suggests that *Rgs5* expression may be associated with HSC activation, which occurs both in liver injury and in HCC[173].

2.3.2 Regulator of G-Protein 5 expression is up-regulated in acute Carbon tetrachloride injury.

Acute injection of CCl_4 leads to hepatocyte death and a subsequent injury response[36,49,174]. We found that acute CCl_4-induced injury induces a 4-fold up-regulation of *Rgs5* mRNA expression 48 hours after injection (Figure 2.3A). Elevated *Rgs5* expression correlates with the increased expression of additional markers of HSC activation and fibrosis in the murine liver, including *Sma* (Figure 2.3B), *Desmin* (Figure 2.3C), and *Pdgfrβ* (Figure 2.3D)[71,175], which also peak at 48 hours post injury. *Pdgfrα* (Fig 3E) and *Col1a* (Fig 3F) are up-regulated at 48 hours, but peak at 72 hours post injury. Taken together, these data support the hypothesis that RGS5 is associated with fibrosis and HSC activation in both tumor and non-tumor associated fibrosis, and that the observed up-regulation of RGS5 expression in fibrotic liver tumors[163,164] may be due to tumor associated activated HSCs.

2.3.3 Regulator of G-Protein 5 expression is regulated in response to inflammatory and profibrotic stimuli *in vitro*.

HSCs are activated in response to the growth factor and cytokine milieu released during the response to hepatocyte injury, including TNFα[9], TGFβ[63], PDGF-BB[176], and ET-1[44]. To determine whether

RGS5 expression is affected by any of these factors, we stimulated LX-2 cells and assayed the expression of *Rgs5* by qPCR. *Rgs5* expression was up-regulated by TNFα stimulation but inhibited by TGFβ stimulation. Interestingly, both of these agonists had a similar relative effect upon endothelin receptor B (ET_B) expression (Figure 2.4), a marker of HSC activation[177]. ET_B receptors are rapidly internalized after activation, serving as a sink for ET-1 agonists[96]. The simultaneous co-regulation of RGS5 and ET_B expression makes sense, as ET_B sequestering ET-1 agonist and RGS5 inhibiting $G\alpha_q$-mediated signaling results both result in the blockade of ET-1-mediated signal transduction. Regulation of RGS5 in response to cytokines released after hepatocyte injury could enable tunable control of ET-1-mediated signaling in HSCs.

2.3.4 Regulator of G-Protein 5^+ Hepatic stellate cells participate in the response to hepatic injury.

As stated above, RGS5 expression is up-regulated in both genetically-induced HCC (Figure 2.2) and acutely in response to CCl_4-induced liver injury (Figure 2.3). To investigate the role of RGS5 in mediating HSC activation and liver fibrosis, we induced liver injury (CCl_4 model, as above) in $Rgs5^{LacZ/LacZ}$ mice to assess the changes in RGS5 cellular expression over time during injury. To identify $RGS5^+$ HSCs during the injury response, we co-localized expression of GFAP and β-gal by IF. In uninjured liver tissue, HSCs are sparsely distributed throughout the liver of both $RGS5^{+/+}$ and $RGS5^{LacZ/LacZ}$ mice (Figure 2.5A,D). However, 48hr post CCl_4 injury, HSCs migrate to the necrotic foci (Figure 2.5B). β-gal^+ HSCs are clustered in the necrotic foci, and are scarce in the uninjured parenchyma (Figure 2.5E). At 96 hours, HSCs are tightly clustered at the foci of injury and are rare in the parenchyma (Figure 2.5C, F). Co-localization analysis (Figure 2.12) shows 75% of β-gal^+ cells are $GFAP^+$, and that this ratio does not significantly change over the course of injury. The expression of RGS5 remains localized to $GFAP^+$ HSCs before and during injury (Figure 2.5G-I), and its up-regulation correlates with expression of HSC activation markers (desmin and SMA)[71,175], peaking at 48hr post injury (Figure 2.3). Since RGS5 functions to inhibit GPCR signaling[158], the up-regulation of RGS5 mRNA in migrating HSC during the liver injury response suggests a role in controlling GPCR mediated HSC activation.

2.3.5 Regulator of G-Protein 5 deficient mice have increased hepatocyte damage in response to acute liver injury.

Given the induction of RGS5 expression after CCl_4 injection, we next used $RGS5^{LacZ/LacZ}$ mice to assess the functional consequences of loss of RGS5 expression. Uninjured liver appears histologically normal in *Rgs5*$^{LacZ/LacZ}$ mice (Figure 2.6A,D). At 48hr post injury, foci of necrosis are visible around the central veins (Figure 2.6B,E). At 96hr post injury, necrotic hepatocytes undergo clearance and infiltrating cells remain at the site of injury (denoted by arrow in Figure 2.6C&F). In *Rgs5*$^{LacZ/LacZ}$ mice, necrotic foci are similar to wild-type mice. At 96hr post injury, the foci of necrosis are diminished; however, hepatocytes throughout the liver have cleared cytoplasm and have a ballooned appearance (Figure 2.6F). To determine if $RGS5^{LacZ/LacZ}$ mice are more susceptible to CCl_4-induced liver damage than wild-type mice, we performed careful morphological analysis of H&E stained sections of liver tissue 96hr after injury. $RGS5^{+/+}$ mice have comparatively normal hepatocytes (Figure 2.7A, B). In contrast, $RGS5^{LacZ/LacZ}$ mice demonstrated widespread hepatocyte ballooning (Figure 2.7C, D). Furthermore, in $RGS5^{LacZ/LacZ}$ mice, the hepatocytes are characterized by cleared cytoplasm and central nuclei (Figure 2.7D). Quantification of cleared hepatocyte area, using ImageJ, confirms a significant increase in injured hepatocyte area in $RGS5^{LacZ/LacZ}$ mice (Figure 2.7E). Further, by analyzing the liver/body weight ratio in $RGS5^{+/+}$ compared to $RGS5^{LacZ/LacZ}$ mice, we observe injured $RGS5^{LacZ/LacZ}$ livers are larger than uninjured livers, while $RGS5^{+/+}$ liver/body weight ratios do not show an injury-induced increase in size (Figure 2.13). Oil red-O staining shows that the cleared hepatocytes do not contain lipids (Figure 2.14), nor accumulated glycogen (Figure 2.15). TUNEL staining shows no difference in apoptosis between the genotypes, and no association with cleared hepatocytes (Figure 2.16).

We propose that in the absence of RGS5 expression in HSCs, HSCs are increasingly sensitive to GPCR agonists, such as ET-1 and AngII, which contribute to HSC activation, portal hypertension, and the severity of fibrosis[70,71,82–85]. Excessive ET-1 or AngII signaling in $RGS5^{LacZ/LacZ}$ mice may induce inappropriate or excessive activation of HSCs, causing increased stress on hepatocytes during injury. Therefore, we compared the mRNA expression of HSC activation markers in $RGS5^{+/+}$ and $RGS5^{LacZ/LacZ}$ mice in acutely injured liver tissue. Expression of desmin, endothelin-1 receptor B (ET_B), and PDGFRβ[71,175] is increased in $RGS5^{LacZ/LacZ}$ mouse liver tissue relative to $RGS5^{+/+}$ littermates at 48hr post CCl_4 injury (Figure 2.7F). The observed increase in expression of HSC activation markers may be

attributed to an increase in HSC proliferation or an increase in HSC activation throughout the liver of $RGS5^{LacZ/LacZ}$ mice. Taken together these data suggest RGS5 controls HSC activation in acute liver injury.

2.3.6 Regulator of G-Protein 5 suppresses ET-1 signaling in HSCs. As stated above, the increased hepatocyte injury and fibrosis observed in the $RGS5^{LacZ/LacZ}$ mouse may be due to excessive signaling through GPCRs, since RGS5 inhibits $G\alpha_q$ signal transduction[158]. To elucidate the role of RGS5 in HSCs during activation and fibrosis, we utilized a human HSC cell line (LX-2 HSCs[167]) to investigate RGS5-mediated ET-1 signaling *in vitro*. LX-2 cells are transfected with RGS5 siRNA or non-specific siRNA, stimulated with ET-1, and the activation of MAPK signaling was determined. As shown in Figure 2.8A and 8B, knock-down of RGS5 expression significantly increases ERK1/2 phosphorylation in response to ET-1 in LX-2 HSCs. Therefore, in the context of increased ET-1-mediated signaling during liver injury, the absence of RGS5 expression could further exacerbate fibrogenic signaling.

2.3.7 RGS5 expression is up-regulated in chronic liver injury: While acute injury models provide insight to the HSC response to damage, HSCs produce detectable fibrosis and scarring during chronic liver injury. Chronic exposure to CCl_4 in mice recapitulates the fibrosis observed in human chronic liver disease[36]. $RGS5^{+/+}$ and $RGS5^{LacZ/LacZ}$ mice were repeatedly injected with CCl_4 over a period of 4 weeks. In damaged $RGS5^{LacZ/LacZ}$ liver tissue, SMA expression localizes activate HSCs in fibrotic septa (Figure 2.9A). HSCs ($GFAP^+$, βGAL^+) were associated with fibrotic septa bridging the portal veins, near the sites of collagen deposition (Figure 2.9B). Interestingly, the β-gal reporter is limited to these GFAP expressing cells in the chronically injured liver. RGS5 mRNA expression is increased 8-fold in the chronic CCl_4 injured liver (Figure 2.9C), while HSC activation markers desmin, SMA, PDGFRα, and PDGFRβ are elevated, yet below the levels observed in acute CCl_4 injury (Figure 2.3). Elevated expression of RGS5 in HSCs during the chronic CCl_4 injury indicates an ongoing role during fibrosis, while classic markers of HSC activation have subsided, suggesting RGS5's function may extend beyond controlling HSC activation.

2.3.8 Regulator of G-Protein 5 deficient mice have increased liver fibrosis during chronic Injury.

In the acute liver injury model, $RGS5^{LacZ/LacZ}$ mice were characterized by an increase in ballooning of hepatocytes (Figure 2.7E) and increased liver/body weight ratio (Figure 2.13), as compared to $RGS5^{+/+}$ mice. To determine whether this phenotype persists in the chronic liver injury setting, hepatic fibrosis was

visualized and quantified using picrosirius red. Fibular collagen is stained red, and the relative degree of fibrosis is quantitated by ImageJ (Figure 2.10 A-D). Chronic CCl_4-treated $RGS5^{+/+}$ mice develop scar tissue bridging between portal veins (Figure 2.10A), while oil-treated control mice are histologically normal, with minimal picrosirius red staining in $RGS5^{+/+}$ (Figure 2.10C) and $RGS5^{LacZ/LacZ}$ (Figure 2.10D). In contrast, chronic CCl_4-treated $RGS5^{LacZ/LacZ}$ mice develop severe fibrosis, as demonstrated by fibrotic septa bridging between portal veins and encircling hepatic lobules (Figure 2.10B). Quantification of picrosirius red staining reveals significantly increased fibrosis in $RGS5^{LacZ/LacZ}$ mice relative to $RGS5^{+/+}$ mice (Figure 2.10E). Taken together with the finding that RGS5 is up-regulated in chronic injury (Figure 2.9A), the increase in fibrosis in $RGS5^{LacZ/LacZ}$ mice suggests a RGS5-dependent role in controlling HSC-mediated collagen deposition.

2.4 Discussion:

In this study, we have identified RGS5 as a marker of HSCs and a regulator of GPCR-mediated signaling in the liver. Up-regulation of *Rgs5* expression correlates with HSC activation during liver injury, and *Rgs5* is highly expressed in the fibrotic liver. RGS5 deficient mice develop more severe liver injury following acute CCl_4 exposure, and increased fibrosis after chronic CCl_4 administration. *In vitro*, profibrotic and pro-inflammatory mediators regulate *Rgs5* expression in HSCs, and RGS5 knockdown in HSCs resulted in increased ERK1/2 signaling in response to ET-1, a possible mechanism for its effects in the liver. Taken together, these data suggest that the regulation of RGS5 in HSCs allows for tunable sensitivity to ET-1 signaling following hepatic injury. Loss of RGS5 disrupts this fine level of control, leading to increased HSC activation, hepatic injury, and fibrosis.

The $Rgs5^{LacZ}$ reporter mouse provides a robust and sensitive method to specifically localize RGS5 expression *in vivo*. Co-localization of β-galactosidase activity and traditional HSC markers (GFAP[147] and CRBP1[178]) in these mice establishes RGS5 as a marker of HSCs in the liver. RGS proteins have been implicated in the progression of HCC[164,179], and an earlier study localized hepatic *Rgs5* expression to endothelial cells in HCC[163] using *in situ* hybridization (ISH). However, the nature of ISH makes precise localization and discrimination between adjacent cells difficult. IF labeling of endothelial cells with an antibody to detect VWF confirms that $RGS5^{+}$ HSCs are distinct from endothelial

cells. A recent publication correlates RGS5 expression with increased vascular invasion, tumor recurrence, and decreased survival in patients with HCC[164]. However, HSCs are the major stromal cell in the tumor microenvironment, and promote HCC proliferation and invasion[180–182]. The correlation of increased RGS5 expression with decreased survival may reflect the level of HSC activation within the tumor, therefore predicting tumor metastasis and proliferation. High RGS5 expression has also been found in select patient-derived HCC cell lines, suggesting expression by transformed hepatocytes. These data should be interpreted with caution, however, as high passage number in culture conditions containing serum and associated growth factors may select for a phenotype that does not reflect *in vivo* expression. We therefore propose that the specific co-localization of β-gal expression (and therefore RGS5 expression) with markers of HSCs, and not with markers of other non-parenchymal cells, establishes RGS5 as a marker of HSCs.

We observed that RGS5 deficient mice had widespread hepatocyte clearing after a single CCl_4 injection, while this phenotype was not observed in *Rgs5*$^{+/+}$ mice (Figure 2.7). The hepatocyte cytoplasmic clearing observed after acute CCl_4 treated *Rgs5*$^{LacZ/LacZ}$ mice is similar to ballooning observed in human cases of non-alcoholic fatty liver disease (NAFLD). Conflicting evidence suggests RGS5 plays a role in maintaining body weight and steatosis, with one group reporting that *Rgs5*$^{-/-}$ mice exhibit spontaneous hepatic steatosis and obesity[134] while another study demonstrates RGS5$^{-/-}$ mice have low body weight[133]. Although RGS proteins have been implicated in the control of hepatic fatty acid oxidation[109] and homeostasis[107], we did not observe any differences in baseline mouse body weight or oil red-o staining (Figure 2.13,Figure 2.14) after CCl_4 injection, indicating that the ballooning is not due to lipid accumulation. The differences in our findings may be due to differences in mouse strains or housing conditions used in the different institutions, and the overall effects of RGS5 expression on body weight are unclear. Glycogen storage can also induce ballooning in hepatocytes, but periodic acid-schiff staining showed no difference between *Rgs5*$^{LacZ/LacZ}$ mice and wild type littermates (Figure 2.15). Hepatocyte swelling reflects reversible cell injury[7] in *Rgs5*$^{LacZ/LacZ}$ mice, and it has been suggested that ballooning is protective in hepatotoxicity[175,183]. To explore this possibility, TUNEL staining was conducted to determine whether ballooned hepatocytes were undergoing apoptosis. However, there was minimal staining in hepatocytes 96hrs after CCl_4 injection, and no difference was observed between

Rgs5$^{LacZ/LacZ}$ mice and wild type littermates (Figure 2.16). We similarly did not appreciate a difference in liver necrosis between the genotypes, and *Rgs5*$^{LacZ/LacZ}$ mice survive repeated doses of CCl_4 in the chronic liver injury model, suggesting that the hepatocyte swelling is reversible.

Feathery hepatocyte degeneration is commonly observed in cholestasis[28] and is characterized by enlarged periportal hepatocytes with a flocculent cytoplasm. Intrahepatic cholestasis due to endotoxemia or drug toxicity can induce feathery degeneration; however, we did not observe pigmented hepatocytes in *Rgs5*$^{LacZ/LacZ}$ mice, and the hepatocyte swelling was equally distributed throughout the liver lobule. Whether hepatocyte swelling enhances hepatocyte survival or is simply a surrogate for more severe injury, *Rgs5*$^{LacZ/LacZ}$ mice show extensive hepatocyte swelling after a single injection of CCl_4, while *Rgs5*$^{+/+}$ mice have normal histology.

Potential mechanisms for the increased injury observed in *Rgs5*$^{LacZ/LacZ}$ mice include portal hypertension or increased activation of HSCs. ET-1 and AngII-mediated sinusoidal constriction by HSCs induces portal hypertension[85,184,185]; loss of RGS5 expression enhances GPCR signaling[160] in response to these agonists, and may thus result in sinusoidal constriction. Loss of VEGF induces sinusoidal capillarization, portal hypertension and HSC activation[186] in mice. However no parenchymal injury was observed, invalidating portal hypertension as a potential mechanism.

The increased hepatocyte injury in *Rgs5*$^{LacZ/LacZ}$ mice may be due to enhanced HSC activation via GPCR signaling. ET-1-mediated control of HSC activation has been demonstrated in previous studies, in which pharmaceutical inhibition of AngII and ET-1 reduces HSC activation *in vitro*[69,83] and in rat models of cirrhosis[71,85]. Our findings of increased expression of HSC markers (desmin, ET_B, and PDGFRβ) in *Rgs5*$^{LacZ/LacZ}$ mice are consistent with this hypothesis, as removal of ET-1 inhibition would enhance expression of markers of HSC activation. ET-1 induced TGFβ secretion[89,91] would be expected to increase in the absence of RGS5 expression, further activating HSCs and contributing to enhanced fibrosis after chronic CCl_4 administration. This hypothesis could be further confirmed by rescue of the RGS5-null phenotype through ET-1 antagonism. For instance, the ET_A antagonist BQ-123 and the ET_B antagonist BQ-788 could be administered to *Rgs5*$^{LacZ/LacZ}$ mice during CCl_4 injury, and would be expected to mitigate the hepatocyte swelling and increased fibrosis that we found in these mice.

RGS5-deficient mice exhibit enhanced arterial hypertrophy and perivascular fibrosis in a hypertension-induced vascular injury model[135]. This pathogenic remodeling was attributed to enhanced MEK/ERK and Rho kinase (ROCK) signaling via increased AngII-induced $G\alpha_q$ signaling in RGS5-null mice. Enhanced ERK activity due to RGS5 knock-down has been previously reported in aortic SMCs[160], and we observed enhanced ERK signaling in LX-2 cells following RGS5 siRNA treatment (Figure 2.8A,B). ET-1 induced Rho activation in HSCs has been shown to enhance migration *in vitro*[187], and inhibition of ROCK improves fibrosis in choline deficient diet fed rats[188]. Loss of RGS5-mediated inhibition of ROCK could be one mechanism behind the enhanced HSC activation and fibrosis observed in $Rgs5^{LacZ/LacZ}$ mice.

RGS5 inhibition of ET-1 signaling has potential in the treatment of liver fibrosis and cirrhosis. While animal models of cirrhosis benefit from ET-1 antagonism, patients risk liver failure[98] due the hepatotoxic effects these drugs. RGS5 inhibition of ET-1 signaling specifically in HSCs provides a novel avenue for future therapies. Enhancing the expression of RGS5 in HSCs could reduce their activation and subsequent development of fibrosis and cirrhosis. The anti-fibrotic effects of RGS5 overexpression could be validated with studies of chronic CCl_4 administration to mice in which RGS5 expression is conditionally overexpressed in HSCs. High RGS5 expression would be expected to block ET-1 mediated signaling in HSCs, potentially reducing HSC activation, contraction, migration, and ultimately fibrosis.

2.5 Conclusions:

RGS5 is a marker of HSCs that is up-regulated as HSCs respond to injury. RGS5 controls HSC activation via inhibition of ET-1 signaling and reduction of ERK activation. The critical role of RGS5 in liver injury is demonstrated by enhanced HSC activation, hepatocyte ballooning, and fibrosis in CCl_4 treated RGS5-deficient mice. RGS5-mediated control of GPCR signaling in the liver is a novel mechanism by which HSC activation can be controlled, and a potential target of therapeutic intervention for liver fibrosis.

2.6 Figures

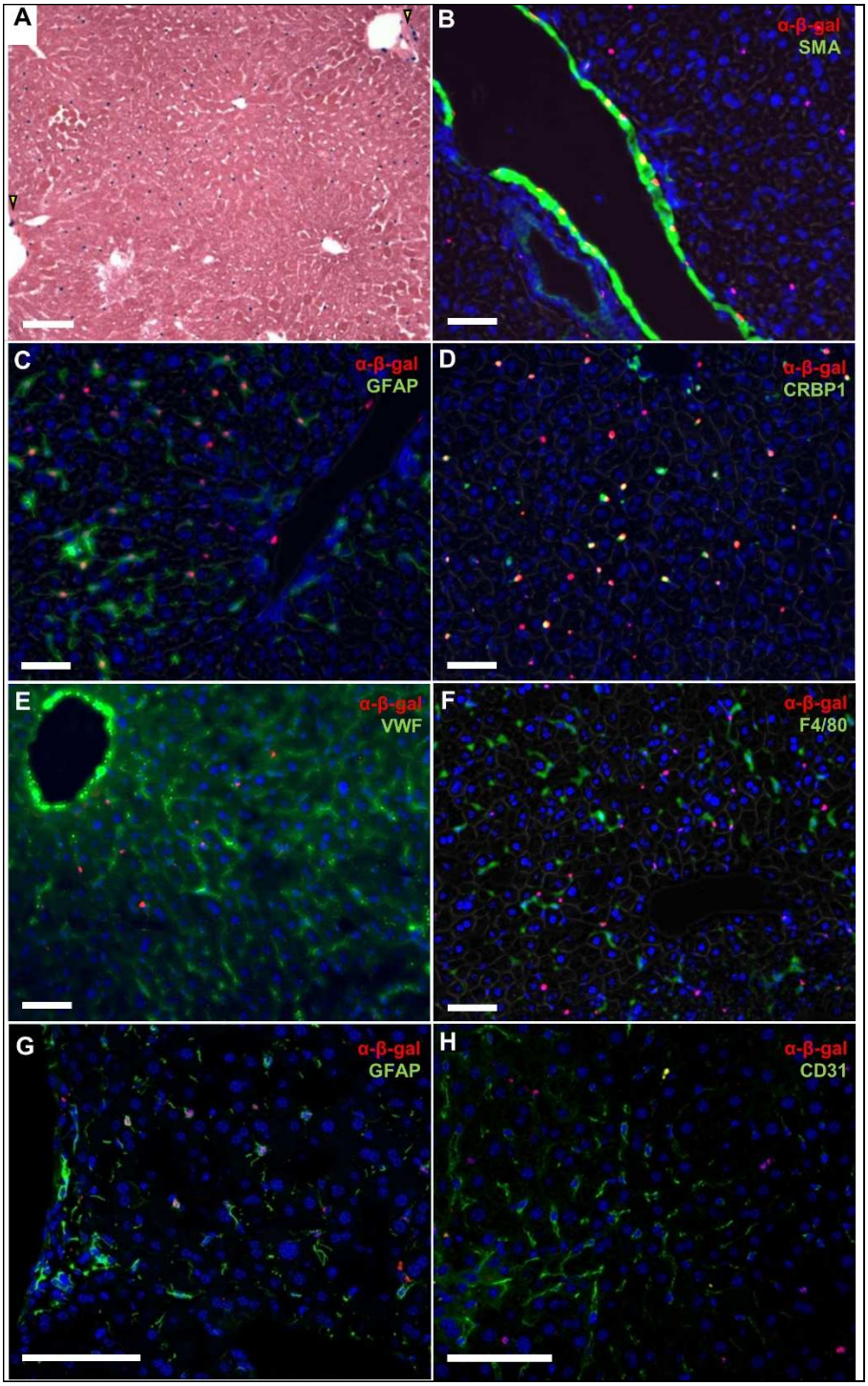

Figure 2.1 Hepatic Stellate Cells express RGS5.

A. Rgs5$^{LacZ/LacZ}$ mouse liver with X-gal labeling. RGS5+ peri-sinusoidal cells are distributed throughout the liver. RGS5 is also expressed in a subset of SMC of the portal vein (yellow arrows). B-G. Immunofluorescence (IF) for cell-specific markers in the RGS5$^{LacZ/LacZ}$ liver. B. SMA and α-β-gal show RGS5 expression in vascular SMCs, as expected. C. GFAP and α-β-gal IF in RGS5$^{LacZ/LacZ}$ mouse liver. β-gal+ nuclei are visible within GFAP+ astrocyte-like HSC cells, localizing RGS5 expression to HSCs. D. CRBP1 and α-β-gal IF are co-localized in HSC of RGS5$^{LacZ/LacZ}$ liver. E. VWF (a marker of endothelial

cells) and α-β-gal are not co-localized. VWF extends through all sinusoids, while β-gal+ cells are sparsely distributed. F. F4/80 (a maker of macrophage/Kupffer cells) and β-gal+ cells represent distinct cell populations. G. Confocal image of α-GFAP IF showing co-localization of the nuclear α-β-gal. H. Confocal image of CD31 (a marker of endothelial cells) and α-β-gal. CD31+ cells have β-gal- nuclei, while β-gal+ nuclei are not associated with CD31+ endothelial cells. All scale bars are 100µm.

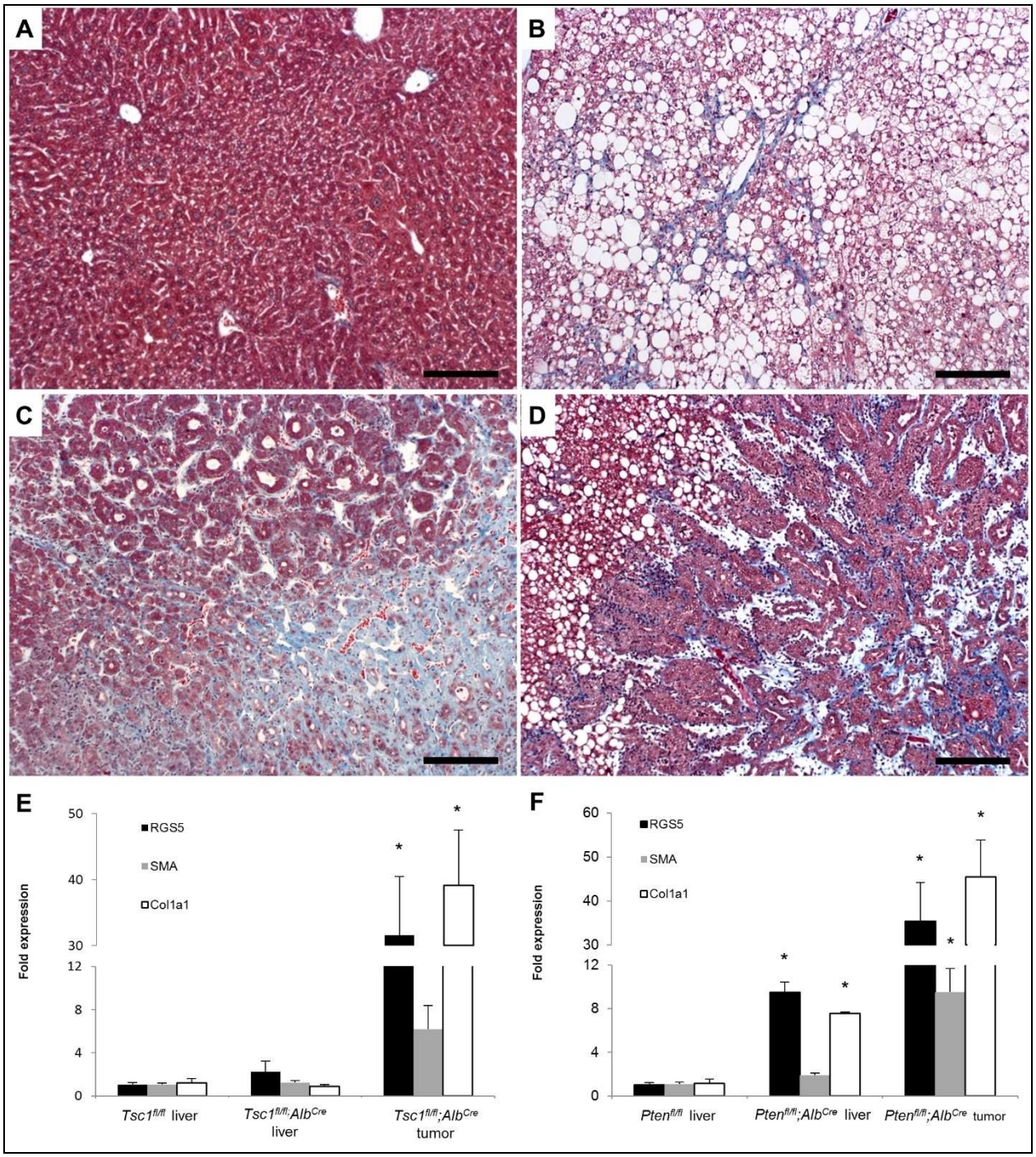

Figure 2.2 RGS5 expression is up-regulated in HCC and liver fibrosis

Sections of liver from Tsc1fl/fl;AlbCre (A,C) and Ptenfl/fl;AlbCre (B,D) mice were stained with Masson's trichrome. A. Tsc1fl/fl;AlbCre non-tumor liver is histologically normal. B. Ptenfl/fl;AlbCre non-tumor liver tissue is steatotic and shows collagen deposition in sinusoids (blue). C. Tsc1fl/fl;AlbCre tumor tissue shows disorganized architecture and high levels of collagen deposition. D. Ptenfl/fl;AlbCre tumor tissue is glandular in appearance, with robust collagen deposition. Scale bars are 100 µm. E-F. RNA was isolated from wild-type normal tissue and matched tumor and non-tumor tissues of $Tsc1^{fl/fl};Alb^{Cre}$ and $Pten^{fl/fl};Alb^{Cre}$ **E**. $Tsc1^{fl/fl};Alb^{Cre}$ mice have normal RGS5, SMA, and Collagen expression in non-tumor parenchyma, and elevated expression in tumor tissue. **F**. $Pten^{fl/fl};Alb^{Cre}$ mice have elevated expression of RGS5 and collagen in non-tumor parenchyma and in tumors. Data is normalized to expression in wild-type liver tissue. n= 5, error bars=SEM, *=p<0.05

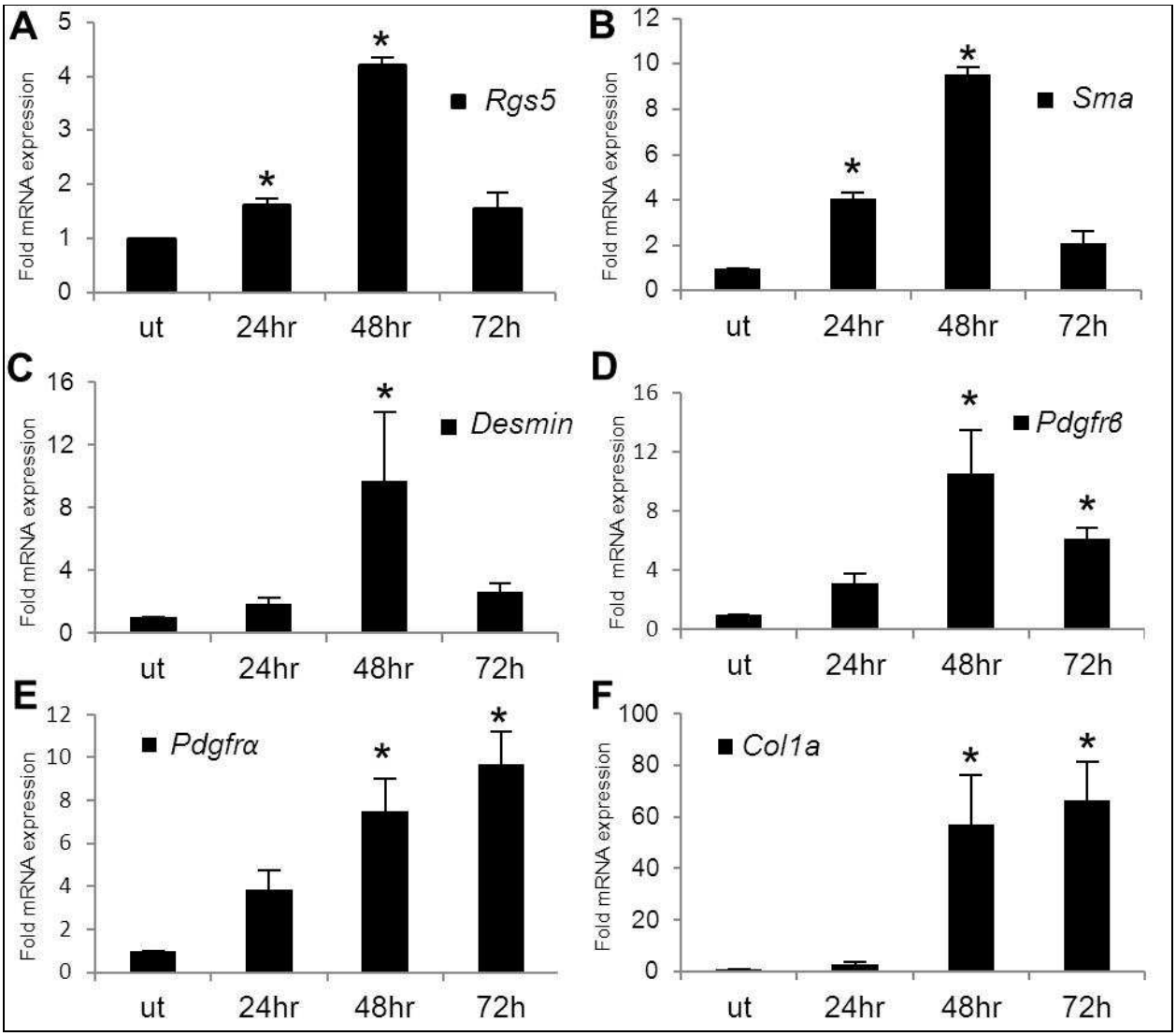

Figure 2.3 RGS5 expression is up-regulated in acute liver injury

C57BL/6 mice were injected i.p. with 10 µl/g body weight 10% CCl4 diluted in olive oil 10% (v/v). Livers were collected at 24, 48, 72hr post injection. RNA was isolated and expression of HSC activation markers was determined by qPCR. A. RGS5 expression is elevated from 24 to 72hr post injury, peaking at 48hr. Expression of B. SMA, C. Desmin, and D. PDGFRβ is up-regulated at 24 and 48 hours post injury. E. PDGFRα and F. Col 1a are up-regulated 48 hours post injury and remain high at 72 hr. Data is normalized to expression in untreated (ut) samples. n=3-5, error bars=SEM, *=p<0.05

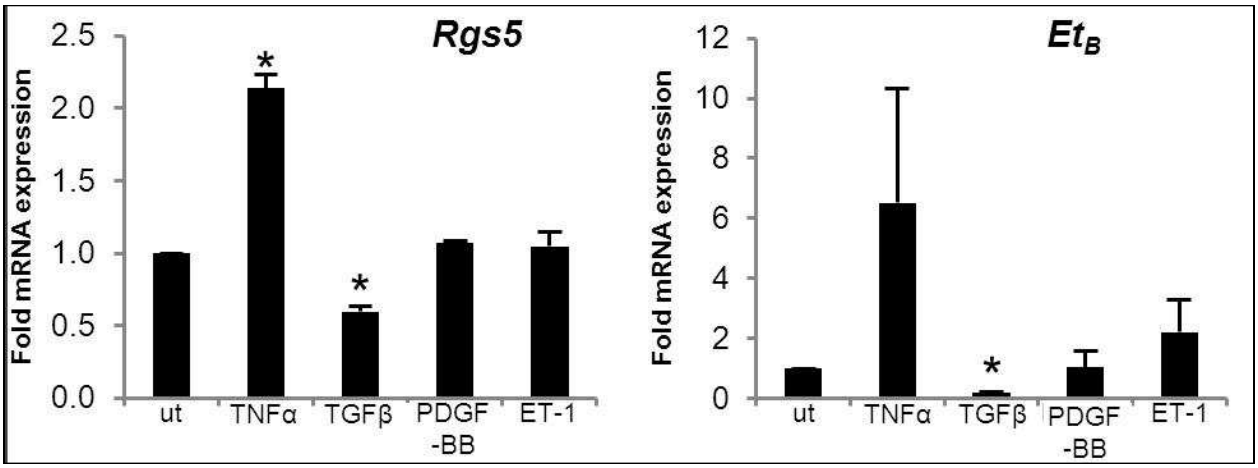

Figure 2.4 RGS5 expression is regulated by profibrotic cytokines in concert with ETB

LX2 HSCs were treated with TNFα (5ng/ml), TGFβ (5ng/ml), PDGF-BB (10 μM), and ET-1 (100 nm) for 24hr. RNA was collected for qPCR analysis of RGS5 and ET_B expression. Both RGS5 and ET_B are up-regulated by TNFα stimulation and down-regulated by TGFβ stimulation. RGS5 and ET_B expression are correlated, responding similarly to the same stimuli. n=3, error bars=SEM, *=$p<0.05$

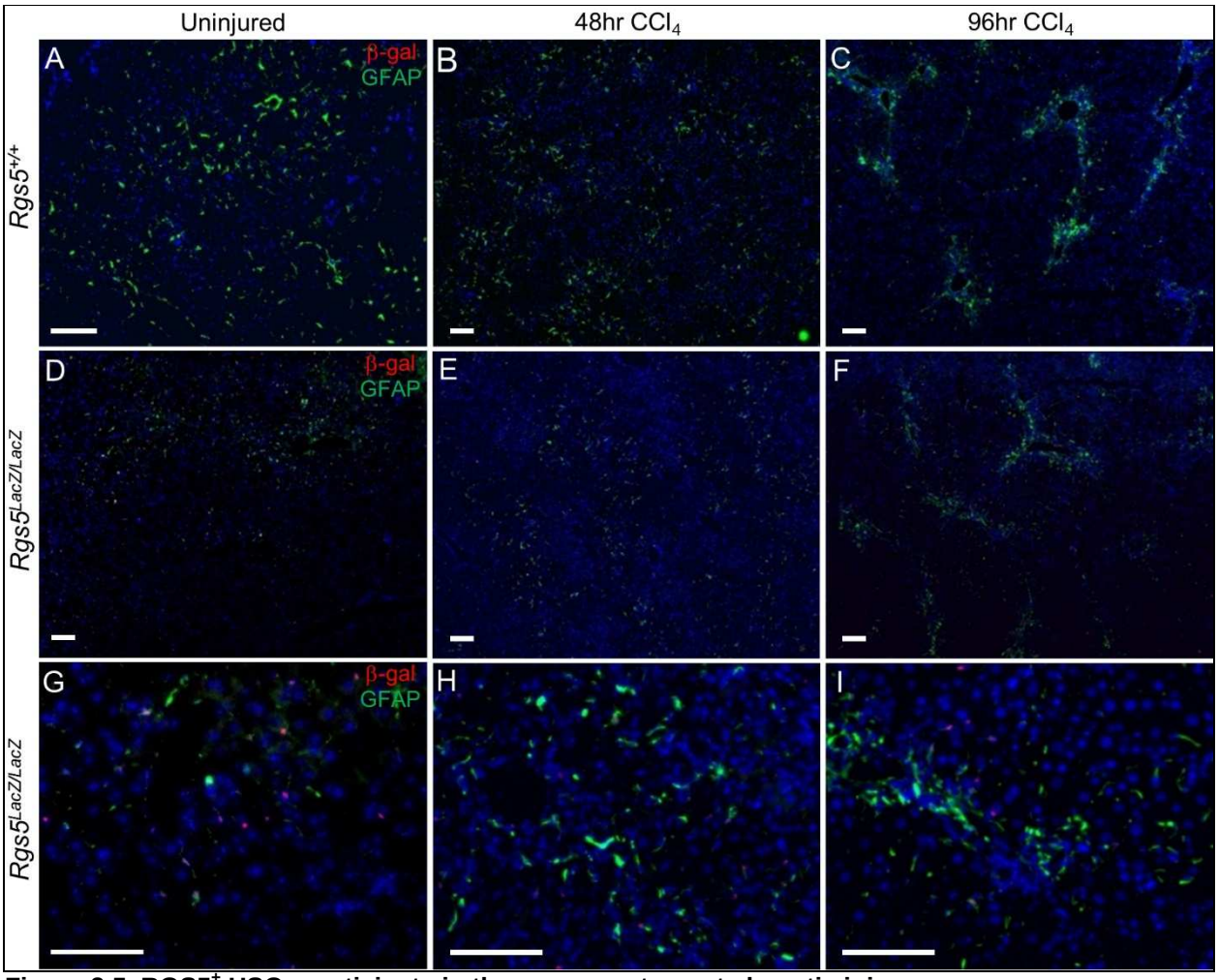

Figure 2.5 RGS5^{+} HSCs participate in the response to acute hepatic injury

Anti-GFAP and anti-β-gal immunofluorescence were used to localize HSCs in acutely injured liver tissue. **A-F.** Low magnification images. **G-I.** High magnification of *Rgs5*$^{LacZ/LacZ}$ **A,D** Uninjured liver tissue from *Rgs5*$^{+/+}$ and *Rgs5*$^{LacZ/LacZ}$ mice show sparse HSCs distributed throughout the liver. High magnification in uninjured *Rgs5*$^{LacZ/LacZ}$ shows HSCs are GFAP^{+} and β-gal^{+}. **B,E.** At 48 hours post injury, HSCs are concentrated in the necrotic foci surrounding the central veins. β-gal^{+} cells (**E,H)** are associated with GFAP^{+} cells. **C,F** At 96 hours post injury, HSCs are tightly clustered at the foci of injury. **I.** β-gal^{+} cells are GFAP^{+}. All scale bars are 100μm.

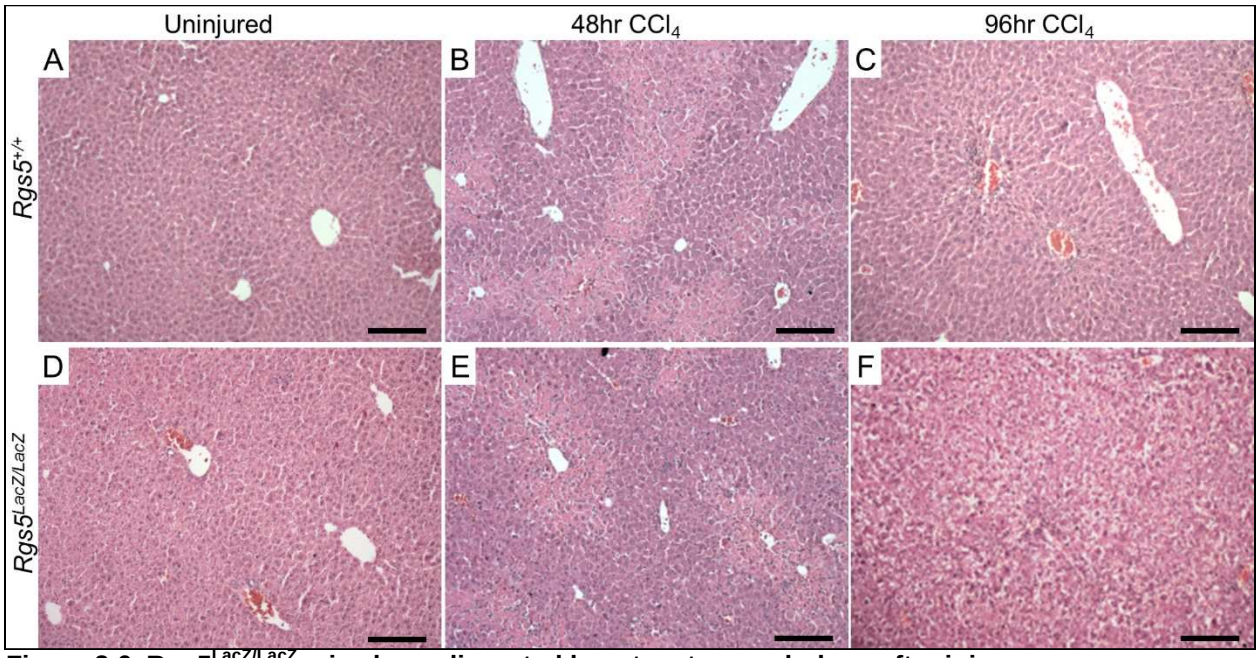

Figure 2.6 $Rgs5^{LacZ/LacZ}$ mice have disrupted hepatocyte morphology after injury

Acute CCl_4-induced injury in *Rgs5*$^{+/+}$ mice (**A-C**) and *Rgs5*$^{LacZ/LacZ}$ (**D-F**). **A,D.** Uninjured mice are histologically normal. **B**,**E** At 48hr post CCl_4 injection, foci of necrosis are visible central veins in both *Rgs5*$^{+/+}$ and *Rgs5*$^{LacZ/LacZ}$ mice. **C,F.** At 96hr post injury, clearance of necrotic hepatocytes is underway and infiltrating cells remain at the site of injury. **F.** In *Rgs5*$^{LacZ/LacZ}$ mice, hepatocytes throughout the liver have cleared cytoplasm. Scale bars are 100 µm.

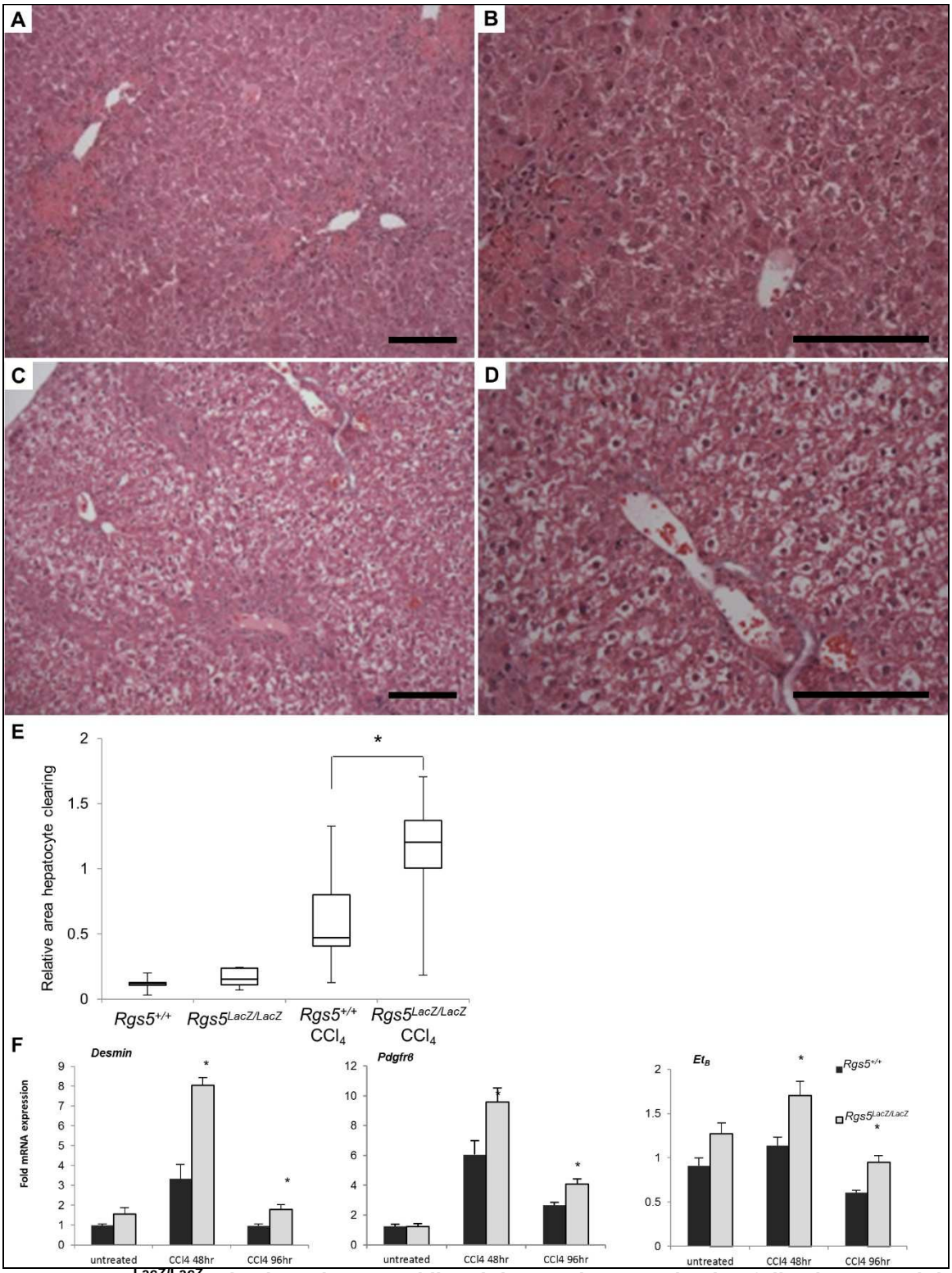

Figure 2.7 Rgs5$^{LacZ/LacZ}$ mice have increased liver injury and HSC activation following acute injury

Livers from *Rgs5*$^{+/+}$ and *Rgs5*$^{LacZ/LacZ}$ were collected at 96hr following a single CCl_4 injection. **A**. and **B**. H&E stain of *Rgs5*$^{+/+}$ mice recover normally from acute injury. Foci of necrosis are centered on the central veins. **B.** Hepatocytes appear normal. **C**. and **D**. *Rgs5*$^{LacZ/LacZ}$ livers have extensive ballooning of hepatocytes throughout the liver. Foci of necrosis are present. **D**. *Rgs5*$^{LacZ/LacZ}$ hepatocytes show cleared

cytoplasm and centralized nuclei in hepatocytes distant from necrotic foci. Scale bars are 100 µm. **E**. Quantification of damaged hepatocyte area reveals a significant increase in ballooning in *Rgs5*$^{LacZ/LacZ}$ mice compared to *Rgs5*$^{+/+}$ mice (n=8-10; error bars=SEM; *=p<0.05) **F**. mRNA expression of markers of HSC activation (Desmin, PDGFRβ, and ET_B) are elevated in *Rgs5*$^{LacZ/LacZ}$ mice compared to *Rgs5*$^{+/+}$ mice following acute CCl_4 injury. n= 4-6, *=p<0.05 by Mann-Whitney U test.

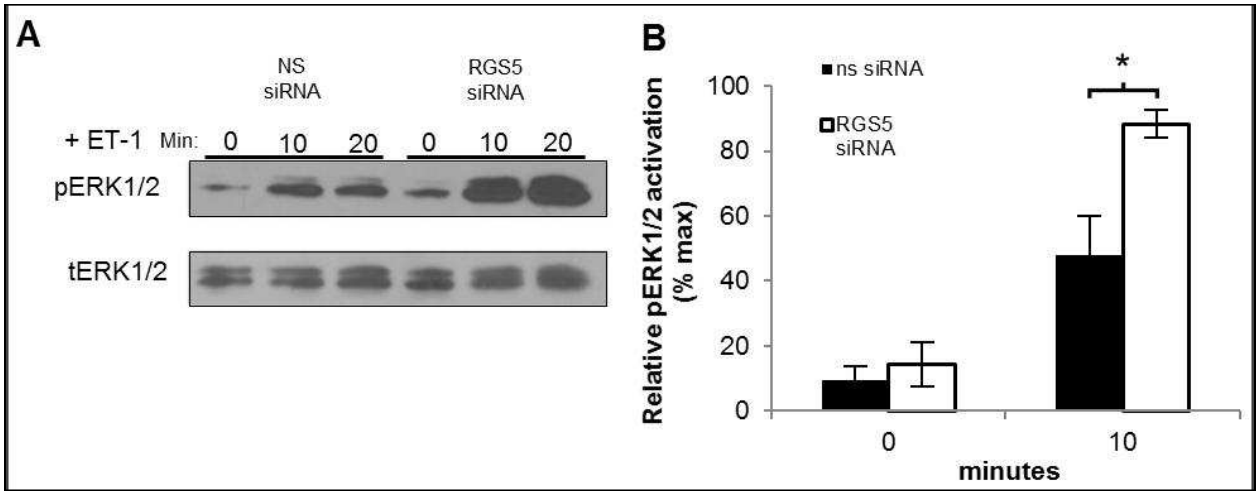

Figure 2.8 Knock-down of RGS5 expression enhances endothelin-1-mediated signaling in LX-2 HSCs

LX2 cells were treated with *Rgs5* siRNA or non-specific siRNA for 24 hours, then stimulated with 100nM ET-1 for the indicated times. Whole cell protein extracts were isolated and analyzed by Western blot. **A**. A representative immunoblot against pERK1/2 demonstrates increased ET-1-mediated signaling in the absence of RGS5 expression; tERK serves as loading control. **B**. Quantitation of densitometry of (**A)** n=7, error bars=SEM, *=p<0.05

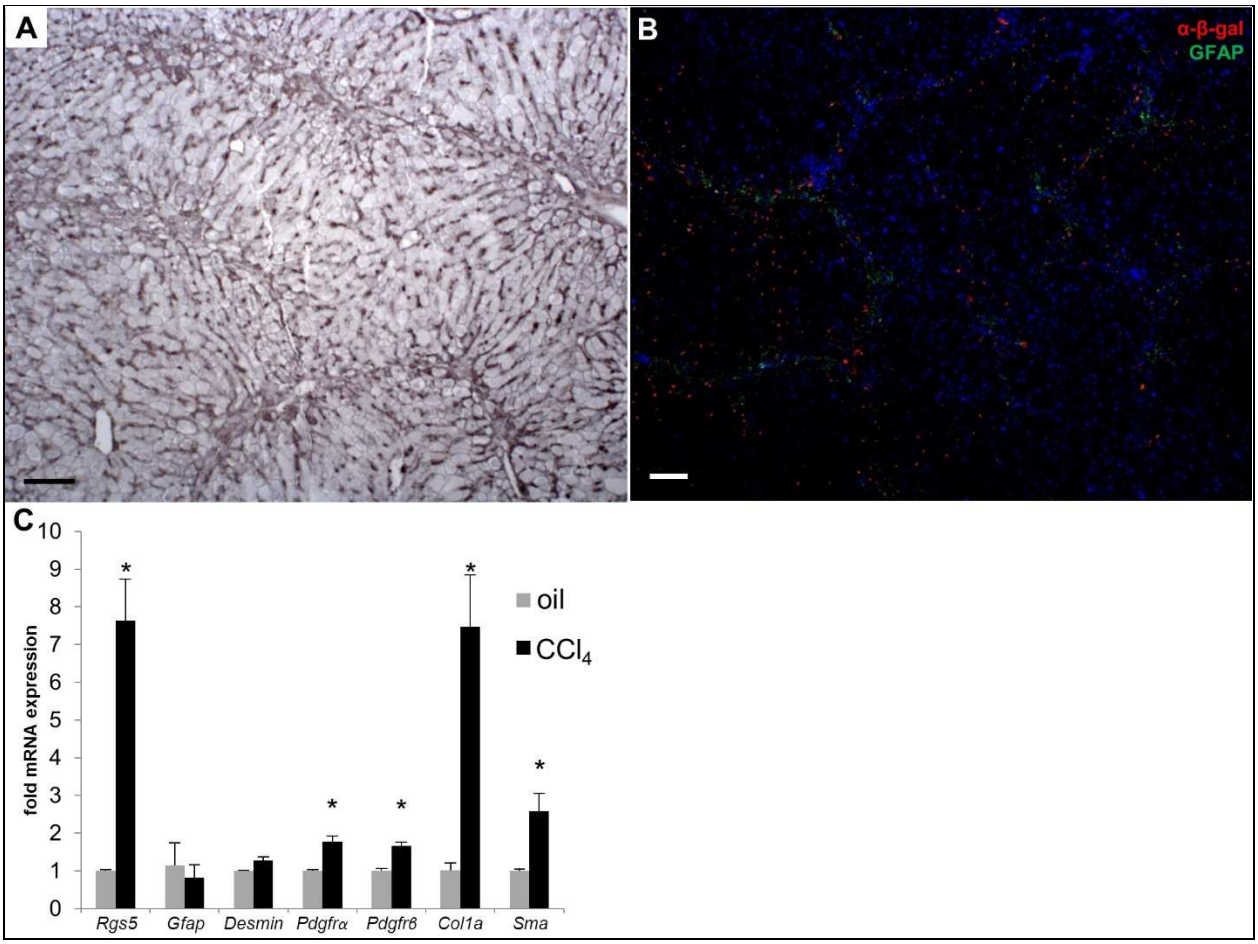

Figure 2.9 RGS5 expression is up-regulated with HSC activation in chronic liver injury

Rgs5$^{LacZ/LacZ}$ mice were chronically injected with CCl_4 (or oil), twice weekly for 4 weeks. RNA was isolated from whole liver and analyzed by qPCR for expression of Rgs5 and HSC activation markers. **A**. Chronic CCl_4 treated *Rgs5*$^{LacZ/LacZ}$ dab labeled with anti-SMA shows activated HSCs. **B**. Rgs5$^{LacZ/LacZ}$ liver immunolabeled with α-β-gal and α-GFAP antibodies. GFAP$^+$ HSCs are visible along fibrotic septa bridging the portal veins. β-gal$^+$ HSCs are visible *in Rgs5*$^{LacZ/LacZ}$ (**B**) around the fibrotic septa. Scale bars are 100 µm. **C.** qPCR of *Rgs5*$^{+/+}$ liver RNA shows Rgs5 is up-regulated in chronic CCl_4 injury. Collagen 1α expression is elevated and multiple HSC activation markers (PDGFRα, PDGFRβ, and SMA) are increased relative to oil-injected mice. Data is normalized to oil injected mice. n=6; error bars=SEM; *=p<.05

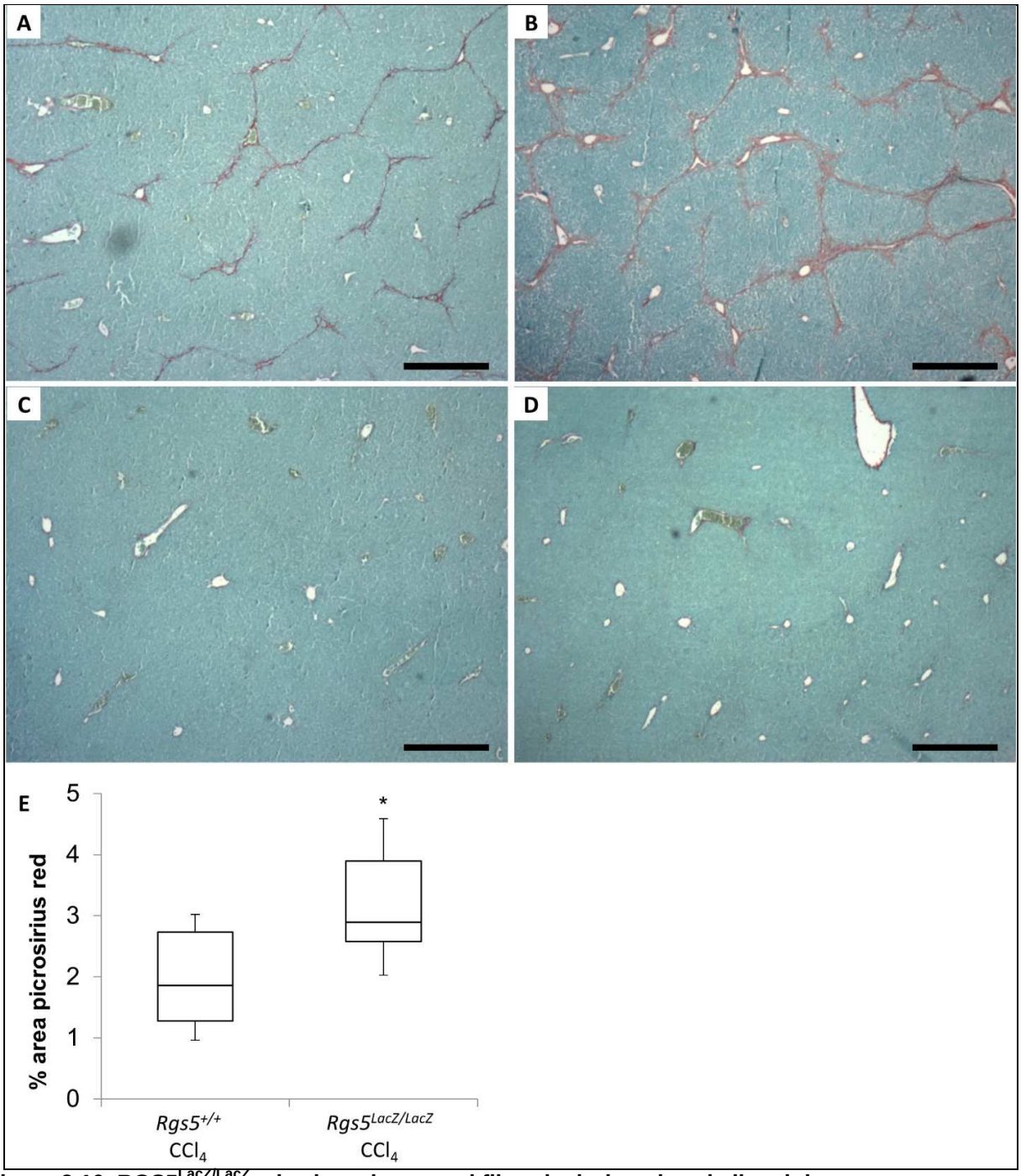

Figure 2.10 RGS5$^{LacZ/LacZ}$ mice have increased fibrosis during chronic liver injury
Mice were injected with CCl_4 (or oil), twice weekly for 4 weeks. Formalin fixed, paraffin embedded liver sections were stained with picrosirius red to assess fibrosis. **A**. *Rgs5*$^{+/+}$ mice show periportal fibrosis and bridging fibrosis between portal veins. **B**. *Rgs5*$^{LacZ/LacZ}$ mice show severe periportal fibrosis bridging between portal veins and surrounding lobules. **C**. *Rgs5*$^{+/+}$ and **D**. *Rgs5*$^{LacZ/LacZ}$ oil injected mice have minimal fibrosis. Scale bars are 500 µm. **E**. ImageJ quantitation of total picrosirius red staining in chronic CCl_4 injury shows significantly more fibrosis in *Rgs5*$^{LacZ/LacZ}$ mice, compared to *Rgs5*$^{+/+}$ mice. n=6, *=p<0.05 by Mann-Whitney U test.

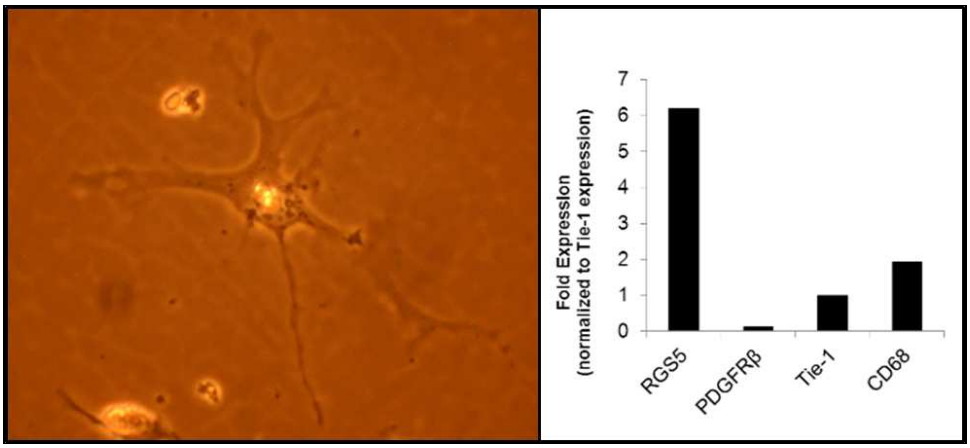

Figure 2.11 Supplemental 1: RGS5 is expressed in freshly isolated primary HSCs

1˚ HSC have astrocyte-like morphology. **A.** Isolated 1˚ HSCs have an astrocyte-like phenotype and store vitamin A in lipid droplets. **B.** Isolated 1˚ HSCs are characterized by high RGS5 expression and low Tie1 and CD68 expression, indicating there are few contaminating cells. Low PDGFRβ expression demonstrates the 1˚ HSCs are in a quiescent state.

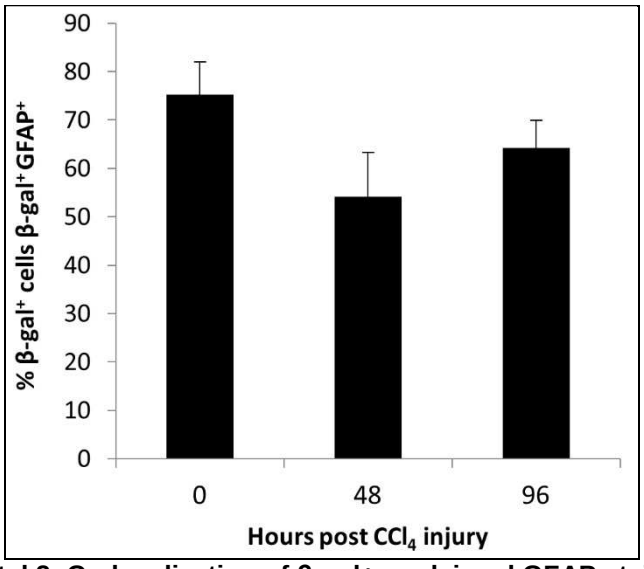

Figure 2.12 Supplemental 2: Co-localization of β-gal+ nuclei and GFAP staining does not change during injury

Frozen sections of CCl_4 injected mouse liver were immunofluorescently labeled with antibodies for β-gal and GFAP. Co-localization analysis using ImagePro showed that the fraction of β-gal$^+$ cells that are β-gal$^+$ and GFAP$^+$ does not significantly change during the course of injury. n=3 mice per group.

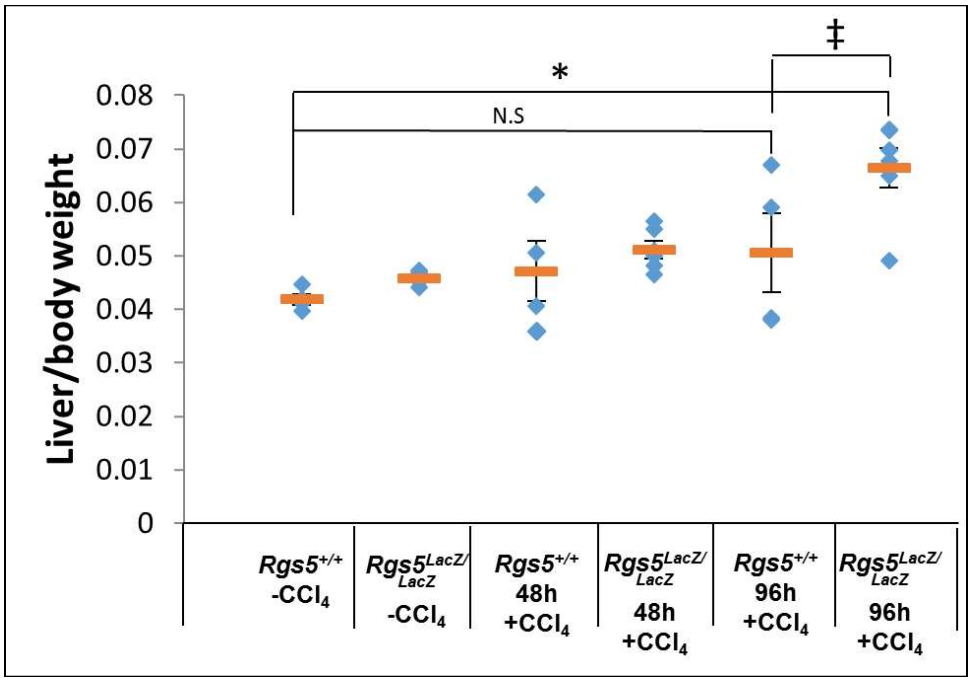

Figure 2.13 Supplemental 3. Liver weight to body weight ratio is moderately elevated in Rgs5$^{LacZ/LacZ}$ mice at 96hr post CCl4 injury

Body and liver weights of CCl_4 injected mice were measured at time of sacrifice. *Rgs5*$^{LacZ/LacZ}$ mice had elevated liver to body weight ratio 96h post injury. *Rgs5*$^{+/+}$ liver to body weight ratio was not significantly different from untreated mice. *p= .001, ‡ p= .06 n=4-6

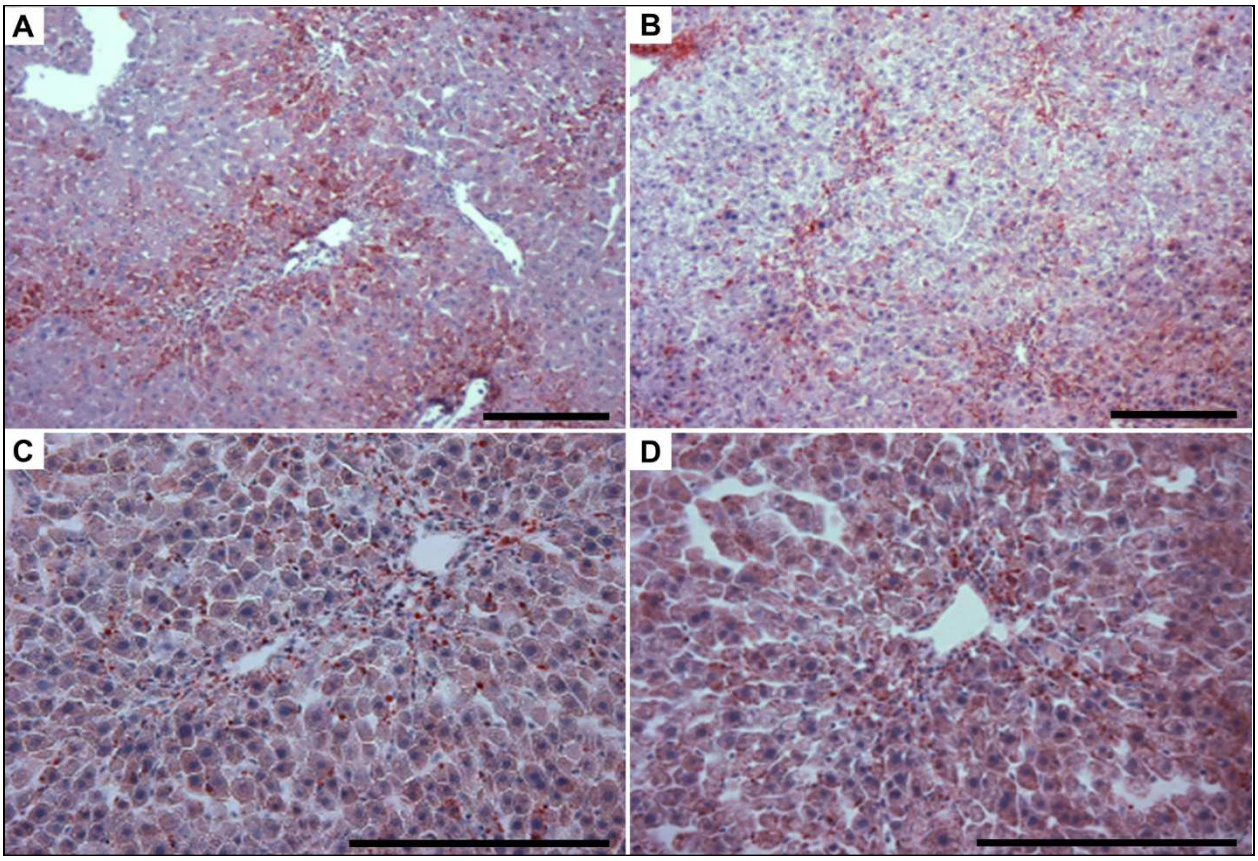

Figure 2.14 Supplemental 4: Hepatocyte clearing is not associated with lipid accumulation

Oil red O staining of mouse liver 96hr post CCl_4 injection was used to assess lipid accumulation. **A.** Lipid droplets are visible around the site of injury in both *Rgs5*$^{+/+}$ **A**,**C** and *Rgs5*$^{LacZ/LacZ}$ **B,D** mice. Cleared hepatocytes are visible in **B**, distant from the site of injury and droplets of lipid. **C,D.** Oil red O staining is present, but there is no accumulation of lipid in hepatocytes. Scale bar is 100 µm.

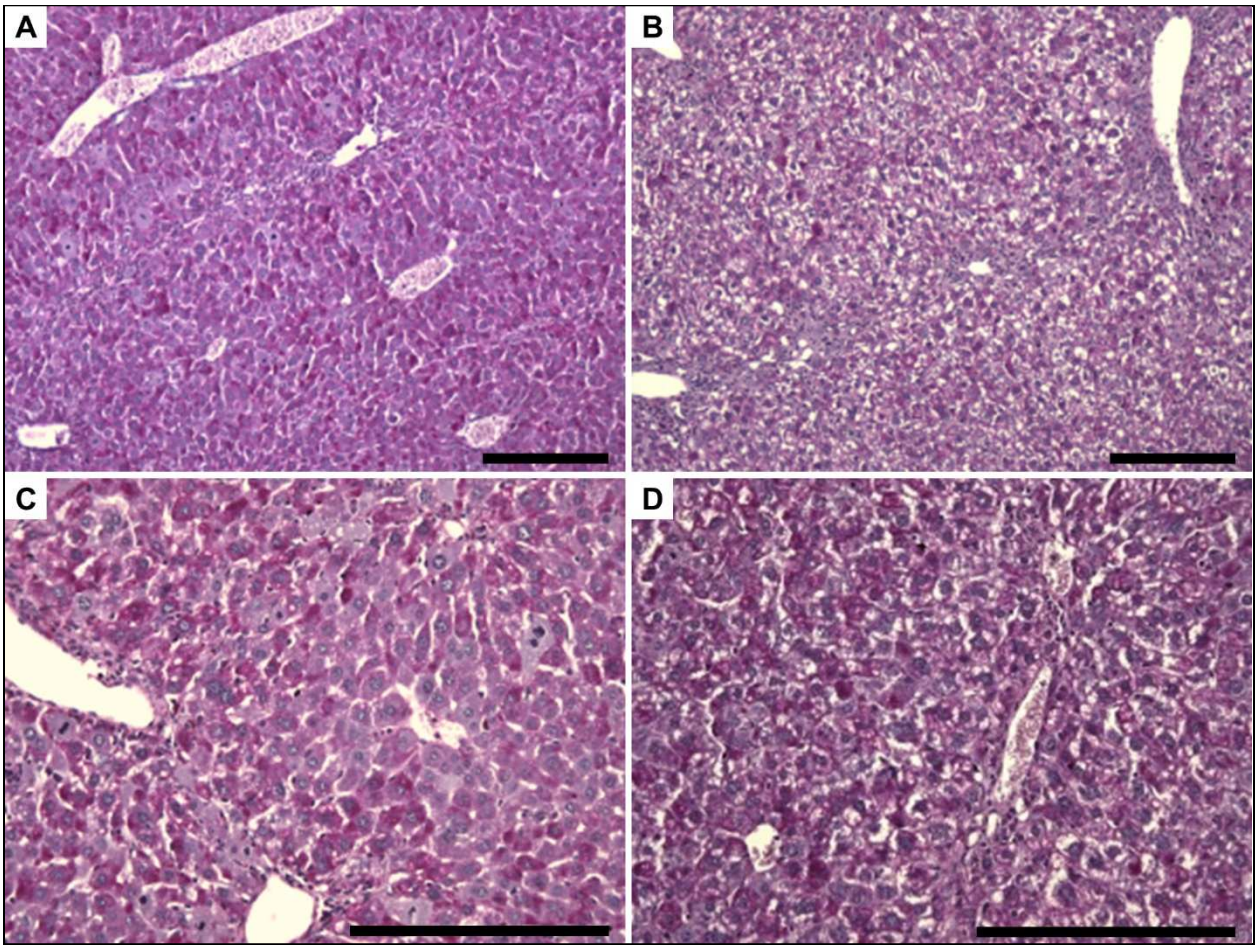

Figure 2.15 Supplemental 5: Hepatocyte clearing is not associated with glycogen accumulation

Periodic acid schiff stain of frozen mouse liver 96hr post CCl_4 injection was used to assess glycogen accumulation. **A.** Hepatocytes appear normal in *Rgs5*$^{+/+}$ liver. Intense magenta staining labels glycogen in the hepatocytes. **B.** Cleared hepatocytes are visible in *Rgs5*$^{LacZ/LacZ}$ and glycogen staining is present in hepatocytes. High magnification of **C** *Rgs5*$^{+/+}$ and **D** *Rgs5*$^{LacZ/LacZ}$ liver show RGS5 that cleared hepatocytes do not contain accumulated glycogen. Scale bar is 100 µm.

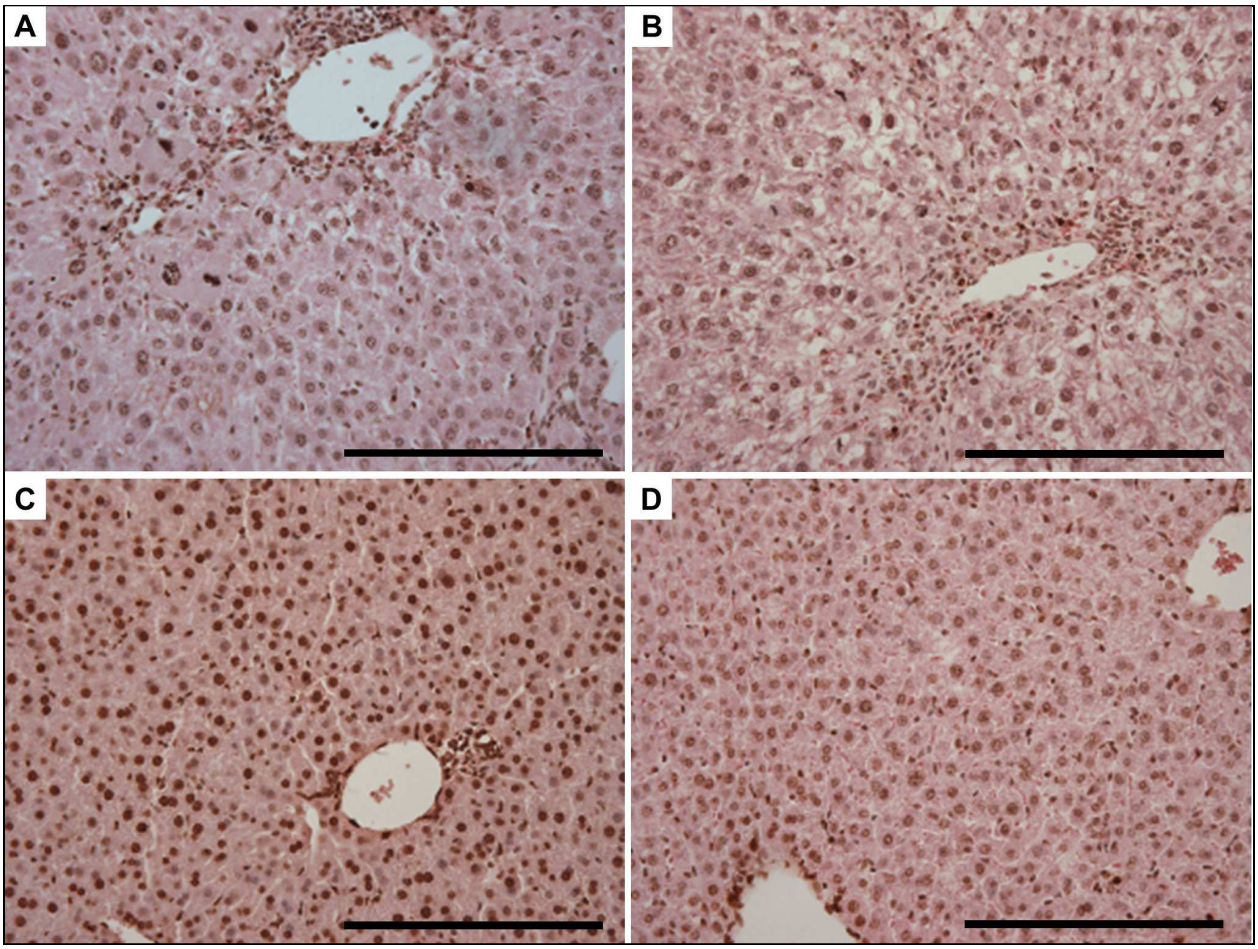

Figure 2.16 Supplemental 6: Cleared hepatocytes are not apoptotic

TUNEL staining of mouse liver 96hr post CCl_4 injection was used to assess apoptosis. **A.** *Rgs5*$^{+/+}$ liver shows TUNEL minimal staining 96hr post injection. **B.** Cleared hepatocytes are visible in *Rgs5*$^{LacZ/LacZ}$ liver 96hr post CCl_4. No difference in TUNEL staining is visible in cleared hepatocytes. **C.** DNAse I treated positive control shows intense staining. **D.** Uninjured *Rgs5*$^{LacZ/LacZ}$ has minimal TUNEL staining. Scale bar is 100 µm.

Chapter 3: Studies investigating the regulation of RGS5 expression

The expression of RGS5 alters GPCR signaling and modulates the cellular response to injury. As noted in Chapter 1, previous studies have shown that RGS5 is down-regulated in response to acute arterial injury and up-regulated with chronic arterial injury[121]. Additionally, the absence of RGS5 expression leads to increased SMC hypertrophy and perivascular fibrosis[135]. Combined with my findings that RGS5 moderates liver fibrosis (Chapter 2), these data suggest that RGS5 expression may control the cellular response to injury. Therefore, understanding of the signaling and growth factors that affect RGS5 regulation may provide a means of manipulating its expression therapeutically. In order to study the cell-specific regulation of Rgs5 expression, we used a reporter mouse to localize expression *in vivo*, experiments to study factors controlling its expression *in vitro*. This chapter is a summary of these descriptive studies I contributed to in the Mahoney laboratory, and provide a foundation for future exploration.

3.1 Developmental regulation of RGS5

In arterial injury, smooth muscle cells dedifferentiate and reactivate embryonic genes associated with development[189]. Understanding gene expression changes in the smooth muscle lineage may inform our understanding of their behavior during the response to injury. RGS5 is expressed in the SMCs of the great arteries of adult mice; however the onset and changes in RGS5 expression not known. Developmental studies were conducted using the $RGS5^{LacZ}$ reporter mouse (commercially available from Deltagen[166]), and expression of RGS was localized using the x-gal labeling procedure[139]. Timed matings of $RGS5^{LacZ/+}$ mice produced fetuses at 12,15,18,21 days post fertilization, and post natal day 2 (P2). Periodate-Lysine-paraformaldehyde (PLP) fixation and cryosectioning was used to generate x-gal stained sections at each stage of development. Sectioning through the aortic arch (Figure 3.1) shows that the expression of RGS5 is controlled by embryonic lineage. The different origins of the aorta are visible, the aortic root and arch are derived from neural crest, while the thoracic aorta is derived from the somites[190]. The boundary between the segments is visible due to high expression of RGS5 in the aortic arch and relatively low expression in the thoracic aorta at 15 days post fertilization. This is consistent with our observations that RGS5 expression is organized by vascular beds, which is determined during development. We observe that expression of RGS5 is high in the thoracic aorta and low in the vena cava

by sectioning through the thorax and below the heart at post natal day 2 (Figure 3.2). At this stage in development, RGS5 expression is now elevated throughout the aorta; however, it is still greatest in the abdominal aorta and aortic arch. The mechanical properties of the aorta develop with increased cardiac output and pressure. This is demonstrated in elastin deficient mice, which have normal aortic development until 18 days[191], despite having fragile, inelastic vessels. After day 18, increasing pressure requires mature, layered vessels. The onset of RGS5 expression in the thoracic aorta occurs between days 15 and birth, and is likely related to SMC maturation and hypertrophy. These developmental studies of RGS5 are still in progress, with ongoing work examining Shh signaling between arterial SMCs and the adventitia. The RGS5 mediated inhibition of Shh signaling during vessel maturation, remodeling and injury are being studied using a *Gli1*^{LacZ};*Rgs5*^{GFP} dual reporter mouse.

The developmental origins and expression patterns of RGS5 in vessels can inform our understanding of its regulation. Atherosclerotic lesions of the large vessels occur most commonly in the aortic arch, abdominal aorta, and iliac arteries[192]. These segments have distinct embryonic origins, and have very high expression of RGS5[122] (Mahoney, personal observations), suggesting a connection with pathogenic remodeling of the arteries.

3.2 Growth factor regulation of RGS5

Growth factors produced in arterial injury affect SMC proliferation and phenotype, and these factors may target or work in tandem with RGS5. PDGF-BB is involved in recruitment of pericytes to endothelial tubes during vascular development. RGS5 is an established marker of pericytes and is down-regulated in embryos lacking PDGF-BB[120,138,159], suggesting it may control the expression of RGS5 in in vSMCs. PDGF-BB is released from platelets in injury, and promotes the proliferation of SMCs in culture[193]. After arterial injury, neointimal SMCs express TGFβ[194], which promotes SMC proliferation via Smad3 and ERK signaling[195] and causes the de-differentiation of SMC to a developmental phenotype[196]. These findings are detailed[160] in the appendix.

Conversely, BMP4 inhibits the proliferation and migration of SMCs. Endothelial expression of BMP4 is up-regulated after carotid artery banding, with peak intensity 7 days post injury[197]. The anti-proliferative effects of BMP4 inhibit PDGF-BB driven migration and proliferation. The changes in

expression of RGS5 with arterial injury occur in sync with signaling via these growth factors, suggesting they may control its expression. Therefore, we measured the effects of these agonists on the expression of RGS5 in rat aortic SMCs and the mesenchymal stem cell line, C3H10T1/2, which differentiate into SMCs. Analysis of mRNA expression by qPCR (Figure 3.3) demonstrated that RGS5 is up-regulated by BMP4, and down-regulated by PDGF-BB, while TGFβ did not alter RGS5 expression. Interestingly, the effects of BMP4 stimulation were different in C3H10T1/2 and aortic SMCs. BMP4 induced a modest increase in RGS5 expression in aortic SMC, and a large increase in RGS5 expression in C3H10T1/2 cells. Because BMP4 is associated with promoting the differentiated state of vascular SMCs[198], a greater effect in an undifferentiated mesenchymal stem cell is expected as compared to the differentiated aortic SMCs. BMP4-mediated up-regulation of RGS5 expression is consistent with its role as an anti-proliferative factor, promoting the differentiated state of SMCs. PDGF-BB down-regulated RGS5 in aortic SMCs[160]. This may be the mechanism by which RGS5 is down-regulated in arterial injury models. PDGF-BB signaling from platelets at the time of injury may down-regulate RGS5 expression in medial SMCs, when SMCs de-differentiate and proliferate[199]. Seven days post injury, endothelial cells express BMP4, which inhibits SMC proliferation and promotes the differentiated SMC phenotype[197] and up-regulates RGS5, restoring the vessel to the normal, quiescent state. My work identified BMP4 as a modulator of RGS5 expression, and as the potential factor that induces RGS5 expression post-injury. This hypothesis is the focus of a R01 currently under review.

These growth factor-induced changes in RGS5 expression have dramatic effects on GPCR signaling. Down regulation of RGS5 enhances $G\alpha_q$ mediated signaling in response to GPCR agonists, increasing the sensitivity to AngII and ET-1. AngII induced ERK1/2 phosphorylation is enhanced in the absence of RGS5, increasing migration and hypertrophy[160]. The expression of RGS5 may be a ‘switch’ that renders a cell resistant to pathogenic remodeling. With growth factor modulation of RGS5, we have identified a mechanism linking injury and repair to GPCR signaling in SMC.

While growth factor-mediated changes in the expression of RGS5 are likely due to significant changes in the cell’s behavior, GPCR-mediated changes in RGS protein expression would be likely due a negative feedback loop to moderate GPCR signaling. In this scenario, decreases in arterial expression of

RGS5 would result in increased signaling by AngII. To examine this possibility, cultured rat aortic smooth muscle cells were stimulated with an array vasoactive GPCR agonists. In response to these agonists, RGS5 expression was unchanged, indicating its regulation is not solely a negative feedback mechanism[160].

These data suggest RGS5 expression is a marker of the differentiated/quiescent SMCs. We hypothesize PDGF-BB signaling in response to an arterial injury down-regulates RGS5 and promotes proliferation of de-differentiated cells to repair the injury. As the vessel is repaired, endothelial-derived BMP4 signaling promotes the differentiation of the SMCs, and the up-regulation of RGS5 expression. This dynamic regulation of RGS5 modulates $G\alpha_q$ signaling in the SMCs, providing a mechanism for enhanced GPCR agonist sensitivity in the injured arteries. As stated above, this is the central hypothesis to a grant currently under review.

3.3 Figures

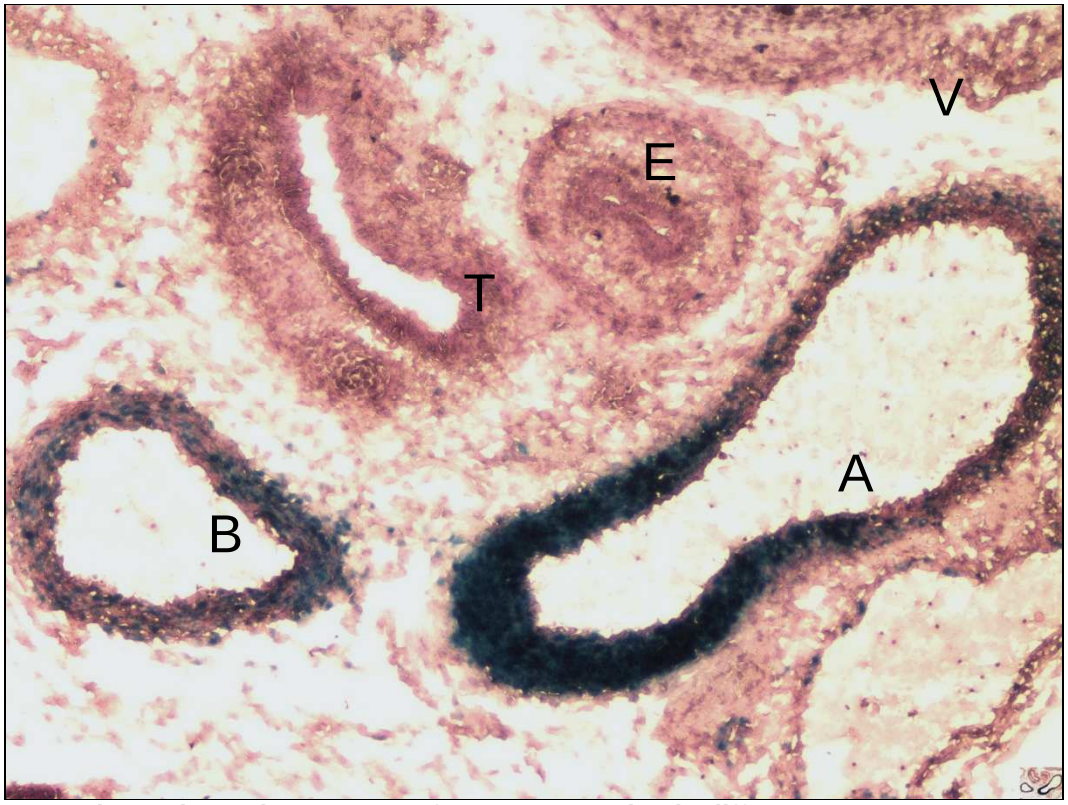

Figure 3.1 15 day embryo shows onset of RGS5 expression in different structures.

$Rgs5^{LacZ}$ 15 day mouse embryo stained with LacZ, Cryosection through the aortic arch. **A.** Aortic Arch. **B.** Brachiocephalic artery E. Esophagus. T. Trachea. **V.** Vertebra. 15 days post fertilization, Strong x-gal labeling indicates high expression of RGS5 in the root of the aortic arch and brachiocephalic artery. Section is through the aortic arch and highlights the neural crest derived aortic root and the somite derived descending thoracic aorta. RGS5 expression and thus X-gal staining of the thoracic aorta (right) is weaker, and staining of esophageal smooth muscle is absent.

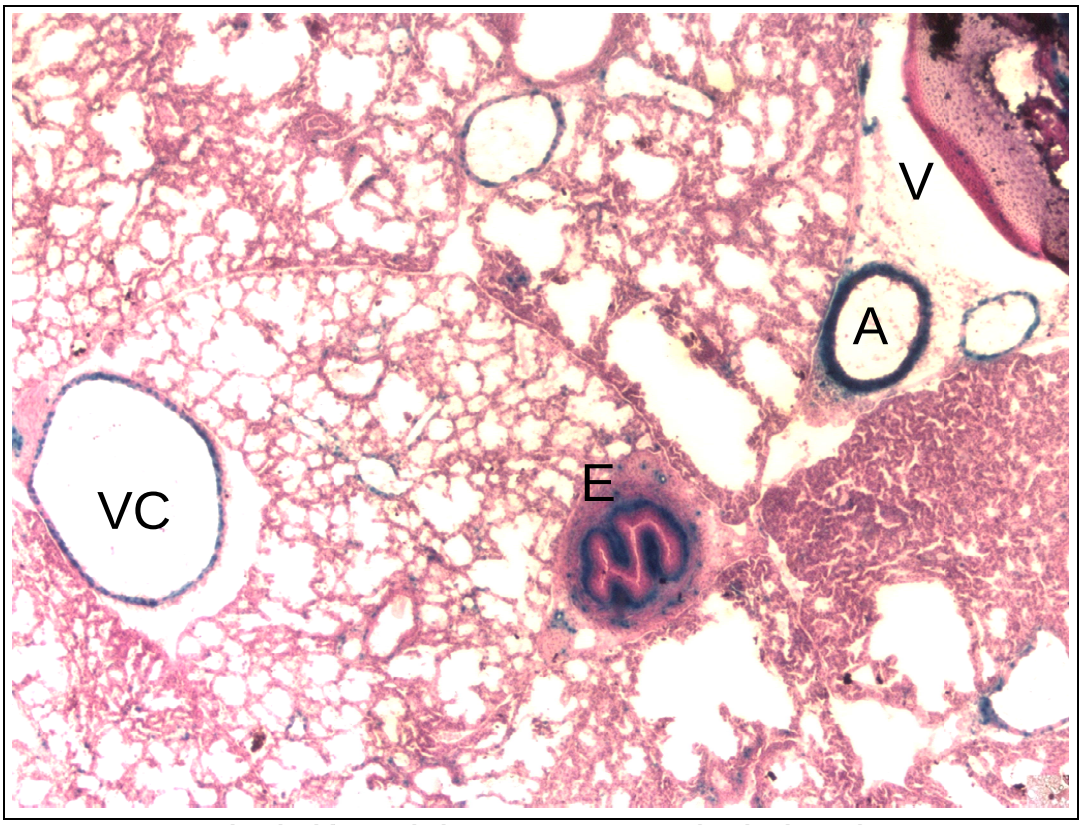

Figure 3.2 P2 mouse stained with X-gal shows RGS5 expression in thoracic aorta.

$Rgs5^{LacZ}$ 2 day old mouse stained with LacZ, Cryosections through the thorax. **A.** Descending thoracic Aorta. **E.** Esophagus. **VC.** Vena cava. **V.** Vertebra. In Day old mice strong x-gal labeling indicates high expression of RGS5 in the thoracic aortic. X-gal staining of the vena cava and esophageal smooth muscle is visible.

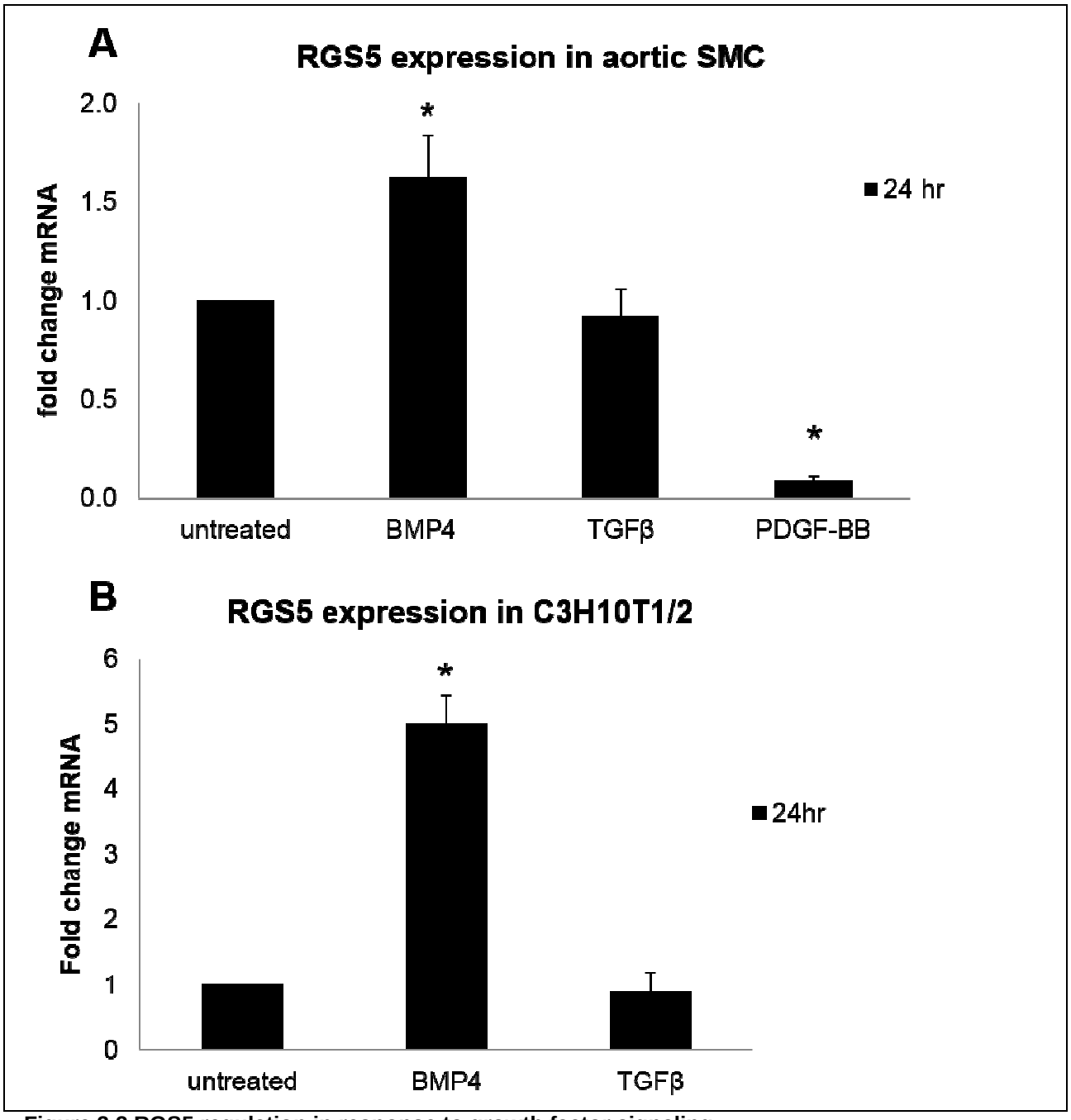

Figure 3.3 RGS5 regulation in response to growth factor signaling.

RGS5 regulation in response to growth factor signaling. A. Rat aortic smooth muscle cells and B. C3H10T1/2 cells were treated with BMP4, TGFβ, and PDGF-BB for 24 hours. RNA was isolated, and qPCR measured RGS5 expression relative to GAPDH. **A.** BMP4 induced a moderate increase in RGS5 expression in aortic smooth muscle cells, while PDGF-bb induced a 10 fold reduction in RGS5 expression. n=4 *= $p < 0.05$ **B.** BMP4 induced a 5 fold increase in RGS5 expression. n=3 *= $p < 0.05$

Chapter 4: Conclusions and future directions

Understanding the processes that lead to fibrosis is critical to reducing the mortality and morbidity associated with liver cirrhosis and failure. No therapies today target the deposition of collagen that disrupts liver function. Chronic disease of many etiologies inflicts liver injury and inflammation, promoting the activation of HSCs. The active HSCs proliferate, migrate, and generate scar tissue, disrupting hepatic perfusion and reducing functional capacity and eventually inducing liver failure. The sources of liver injury are often difficult to treat and are typically undetected until significant damage has occurred. Treatment of cirrhosis and liver failure are mainly palliative measures to prolong remaining function. Therefore, the activation of HSCs and the deposition of matrix represent the best targets for therapeutic intervention in treating liver disease. RGS5 expression moderates the fibrotic response to injury, and reduces HSC activation. As a marker and moderator of HSC activation and fibrosis, RGS5 is a valuable target necessitating further study as a therapeutic target.

4.1 Major findings

The primary findings of my dissertation are presented in Chapter 2, demonstrating that HSCs are the RGS5 expressing cell in the liver and that RGS5 expression is up-regulated with HSC activation during injury. This up-regulation occurs in acute and chronic CCl_4-induced necrosis and repair. *In vitro* experiments using the LX-2 cell line show that RGS5 inhibits normal $G\alpha_q$-mediated GPCR signaling in HSCs. These data suggest that RGS5 is a critical component of GPCR signaling in activated HSCs. The observed increase of RGS5 expression occurred in sync with acute HSC activation, suggesting a role in GPCR signaling during cell activation. In the chronic injury model, RGS5 is elevated in active HSCs as they generate scar tissue. This signifies a role of altered GPCR signaling in the fibrogenic HSC.

RGS5-null mice were found to have increased liver injury, as measured by hepatocyte cytoplasmic clearing in an acute CCl_4–induced injury. Additionally, they develop increased fibrosis with chronic CCl_4–induced injury. The absence of RGS5 results in unregulated GPCR-mediated signaling via $G\alpha_q$ with chronic injury and HSC activation, thereby increasing the deposition of collagen. Therefore RGS5 controls the HSC response to injury and is a regulator of hepatic fibrosis.

4.2 Future studies:

To determine if RGS5-null mice have altered HSC proliferation, these studies would require more stringent quantification of HSCs. GFAP is expressed in the majority, but not by not all HSCs. Additionally, we observed that GFAP expression is regulated with injury, making it less useful as a marker for cell number quantification. If there is a population of HSCs that are $GFAP^-$ and $RGS5^-$, they would not be detected by the methods used in the studies presented here. Approximately 70% of HSCs in the liver express GFAP and 70% express desmin; however if used together, these markers cover 90% of HSCs[200], making quantification and RGS5/β-gal co-localization more accurate. In future studies, double-labeling HSCs with desmin and GFAP would allow more precise quantification. Alternatively, the HSC marker lecithin-retinol acyltransferase (*Lrat*), which identifies 99% of HSCs[142], could be used. The tracing of HSCs in RGS5-null livers could be determined unambiguously by crossing the LRAT-Cre;GFP mice with the $RGS5^{lacZ}$ mouse.

A recent publication characterizes RGS5 as a switch that blocks $G\alpha_q$ signaling and promotes $G\alpha_{12/13}$ signaling in vascular smooth muscle cells[201]. They report that SMC GPCR stimulation promotes $G\alpha_q$-mediated contraction with low RGS5, and $G\alpha_{12/13}$ mediated RhoA activation and stress fiber formation needed for vascular remodeling. This is consistent with findings that RGS5 regulates vascular remodeling via a RhoA mediated pathway[135]. Future work could test these findings in LX-2 HSCs or primary HSCs treated with RGS5 siRNA and stimulated with ET-1. We expect immunofluorescent labeling for F-actin would reveal increased stress fiber staining in ET-1 treated cells. RGS5-knockdown cells would have reduced or no change in F-actin staining with ET-1 treatment. Addition of a RhoA inhibitor would block this effect. If RGS5 is indeed shifting GPCR signaling from $G\alpha_q$ to $G\alpha_{12/13}$, then the RGS5-null mice would have reduced RhoA signaling compared to wild-type mice. Numerous studies have linked ET-1 induced, $G\alpha_{12/13}$ mediated, contraction and migration in HSCs[187,188,202,203]. This is predicted to reduce HSC contraction and migration and would likely be beneficial in controlling fibrosis. In the RGS5-null animals, the benefits of reduced RhoA activation may be undetectable against the effects of unregulated $G\alpha_q$ signaling.

The observed increase in hepatocyte cytoplasmic clearing in the RGS5-null mice is unexpected, as hepatocytes do not express RGS5. As stated before, this organ-wide clearance is not associated with

lipid or glycogen accumulation; only a decrease in cytoplasmic eosin staining is observed. This suggests a systemic effect, such as a change in a soluble factor produced by HSCs, is able to induce this damage. One potential mechanism is via increased oxidative stress in RGS5-null mice. As stated before, RGS5-null mice are more sensitive to vasoactive agonists, producing changes in blood pressure regulation. In the injured RGS5-null liver, increased ET-1 and AngII signaling may cause excessive vasoconstriction in HSCs. To compensate for the resulting increased shear stress, endothelial cells produce $NO^{\bullet}$ to signal for vasodilation, and this increased $NO^{\bullet}$ by sinusoidal endothelial cells can diffuse into adjacent hepatocytes. Oxidative stress due to injury, inflammation, and CCl_4 can produce superoxide (O_2^-) in hepatocytes[204]. The reaction of superoxide and $NO^{\bullet}$ yields peroxynitrite ($ONOO^-$), a potent oxidant that generates lipid radicals, protein oxidation, and nitration. The presence of peroxynitrite increases hepatocyte injury and can induce hepatocyte apoptosis[205]; however, we did not observe an increase in hepatocyte apoptosis in the RGS5-null mice (Figure 2.16). To test for increased oxidative stress, the level of lipid peroxidation can be measured via liver tissue levels of F2-isoprostanes, a byproduct of the lipid peroxidation of arachidonic acid[206,207]. The relative levels of peroxynitrite formation between RGS5-null and wild-type mice can be measured using a plasma protein nitration assay[208]. Increased markers of oxidation and nitration would support the $NO^{\bullet}$-mediated compensation hypothesis. Confirmation of $NO^{\bullet}$-mediated oxidative damage could be tested by the administration of the nitric oxide synthase inhibitor L-NAME[209]. If the inhibition of $NO^{\bullet}$ production restores hepatocyte lipid peroxidation and protein nitration to wild-type levels, it may reduce the hepatocyte ballooning as well.

Confirmation of the $Rgs5^{LacZ/LacZ}$ phenotype and validation of its potential therapeutic potential could be demonstrated using an RGS5 overexpression mouse model. A future study using a tamoxifen inducible Cre recombinase driven by a HSC-specific promoter, such as GFAP, would provide a model to analyze RGS5-mediated protection against fibrosis. Pretreatment of the mouse with tamoxifen would induce the overexpression of RGS5 in HSCs. With acute CCl_4 treatment, HSC activation and hepatocyte clearance could be measured. Increased RGS5 expression is expected to block $G\alpha_q$ signaling and prevent GPCR mediated HSC signaling and activation. We anticipate that this would be beneficial in a chronic CCl_4 model as well, and would further validate RGS5 as a therapeutic target. The ET-1 inhibition provided by overexpression of RGS5 could be combined with existing ET-1 antagonists, allowing a lower

dose that improves fibrosis and avoids hepatotoxic effects that limit their use. Validating this approach in mice would support the need for therapies that enhance RGS5 expression.

RGS5 interacts with a number of GPCRs that have significant roles in stellate cells including S1P, Shh, and AngII. Consequently, our understanding of the mechanisms of RGS5-mediated HSC activation and fibrosis is complicated. Dosing of mice with an ET-1 receptor antagonist could mitigate the effects of excessive to $G\alpha_q$ signaling. However, the phenotype observed may be due to the combinatorial effect of unregulated $G\alpha_q$ signaling through a combination of GPCR pathways, complicating the identification of the dominant pathway.

Progressive chronic disease is rarely detected before the liver is significantly compromised. With the development of a therapeutic a strategy that targets HSC activation and fibrosis, the progression of disease can be halted and resolution of accumulated fibrosis can begin. Future therapies could inhibit RGS5 degradation via targeting the N-end rule of proteasomal degradation. Interruption of the activity of ATE-1 would block the arginylation and ubiquitination of RGS5. In cells where RGS5 is highly expressed, such as HSCs, RGS5 protein levels would be increased, or at a minimum, maintained at steady-state levels. The increased levels of RGS5 protein would inhibit GPCR signaling, reduce HSC activation, and consequently, reduce collagen deposition. Such a therapy could be combined with ET-1 antagonists at reduced doses to avoid the hepatotoxic complications that have precluded their use previously.

4.3 Conclusion

RGS5 is a HSC specific modulator of GPCR signaling that is up-regulated in response to liver injury. The increased expression limits $G\alpha_q$ mediated signaling, reducing the activating stimuli, and thus the activation of HSCs. Mice lacking RGS5 have increased HSC activation in response to injury and increased hepatocyte damage. During chronic liver injury, aberrant HSC activation results in increased collagen deposition. Our studies identify RGS5 as a novel regulator of fibrosis in the liver and a potential target for future anti-fibrotic therapies. RGS5 is associated with the injury response and pathogenic remodeling of smooth muscle and pericyte-like cells. Further studies are warranted, as understanding of the function of RGS5 may provide insight to the general pathways that control injury induced myofibroblast activation and fibrotic diseases.

References

1. Heron M (2013) Deaths: leading causes for 2010. Natl Vital Stat Rep 62: 1–96.

2. Muddu AK, Guha IN, Elsharkawy AM, Mann DA (2007) Resolving fibrosis in the diseased liver: translating the scientific promise to the clinic. Int J Biochem Cell Biol 39: 695–714. doi:S1357-2725(06)00280-9 [pii] 10.1016/j.biocel.2006.10.006.

3. Felipo V (2013) Hepatic encephalopathy: effects of liver failure on brain function. Nat Rev Neurosci 14: 851–858. doi:10.1038/nrn3587.

4. Tsochatzis EA, Bosch J, Burroughs AK (2014) Liver cirrhosis. Lancet 383: 1749–1761. doi:10.1016/S0140-6736(14)60121-5.

5. Ellis EL, Mann DA (2012) Clinical evidence for the regression of liver fibrosis. J Hepatol 56: 1171–1180. doi:S0168-8278(12)00044-X [pii] 10.1016/j.jhep.2011.09.024.

6. Anthony PP, Ishak KG, Nayak NC, Poulsen HE, Scheuer PJ, et al. (1977) The morphology of cirrhosis: definition, nomenclature, and classification. Bull World Heal Organ 55: 521–540.

7. Abbas AK, Fausto N, Robbins SL, Cotran RS, Kumar SUPPLS disc Health Books QZ 4 R6354 2005 text AVAILABLE Health Books QZ 4 R6354 2005 disc DUE 10-02-12 Health Books QZ 4 R6354 2005 disc AVAILABLE VCN-HBQZ 4 R 2005 text (2005) Robbins and Cotran pathologic basis of disease. 7th ed. Philadelphia: Elsevier Saunders.

8. Braet F, Riches J, Geerts W, Jahn KA, Wisse E, et al. (2009) Three-dimensional organization of fenestrae labyrinths in liver sinusoidal endothelial cells. Liver Int 29: 603–613. doi:LIV1836 [pii] 10.1111/j.1478-3231.2008.01836.x.

9. Zimmermann HW, Trautwein C, Tacke F (2012) Functional role of monocytes and macrophages for the inflammatory response in acute liver injury. Front Physiol 3: 56. doi:10.3389/fphys.2012.00056.

10. Sato M, Suzuki S, Senoo H (2003) Hepatic stellate cells: unique characteristics in cell biology and phenotype. Cell Struct Funct 28: 105–112.

11. Fukazawa K, Lee HT (2013) Updates on Hepato-Renal Syndrome. J Anesth Clin Res 4: 352. doi:10.4172/2155-6148.1000352.

12. Ginès P, Cárdenas A, Arroyo V, Rodés J (2004) Management of cirrhosis and ascites. N Engl J Med 350: 1646–1654. doi:10.1056/NEJMra035021.

13. Tumgor G (2014) Cirrhosis and hepatopulmonary syndrome. World J Gastroenterol 20: 2586–2594. doi:10.3748/wjg.v20.i10.2586.

14. Leise MD, Poterucha JJ, Kamath PS, Kim WR (2014) Management of hepatic encephalopathy in the hospital. Mayo Clin Proc 89: 241–253. doi:10.1016/j.mayocp.2013.11.009.

15. Forner A, Llovet JM, Bruix J (2012) Hepatocellular carcinoma. Lancet 379: 1245–1255. doi:10.1016/S0140-6736(11)61347-0.

16. Aravalli RN, Cressman ENK, Steer CJ (2013) Cellular and molecular mechanisms of hepatocellular carcinoma: an update. Arch Toxicol 87: 227–247. doi:10.1007/s00204-012-0931-2.

17. Neff GW, Kemmer N, Duncan C, Alsina A (2013) Update on the management of cirrhosis - focus on cost-effective preventative strategies. Clinicoecon Outcomes Res 5: 143–152. doi:10.2147/CEOR.S30675.

18. Schlegel A, Dutkowski P (2014) Role of hypothermic machine perfusion in liver transplantation. Transpl Int. doi:10.1111/tri.12354.

19. Chayanupatkul M, Liangpunsakul S (2014) Alcoholic hepatitis: A comprehensive review of pathogenesis and treatment. World J Gastroenterol 20: 6279–6286. doi:10.3748/wjg.v20.i20.6279.

20. Galli A, Pinaire J, Fischer M, Dorris R, Crabb DW (2001) The transcriptional and DNA binding activity of peroxisome proliferator-activated receptor alpha is inhibited by ethanol metabolism. A novel mechanism for the development of ethanol-induced fatty liver. J Biol Chem 276: 68–75. doi:10.1074/jbc.M008791200.

21. Gao B, Bataller R (2011) Alcoholic liver disease: pathogenesis and new therapeutic targets. Gastroenterology 141: 1572–1585. doi:10.1053/j.gastro.2011.09.002.

22. Dureja P, Lucey MR (2010) The place of liver transplantation in the treatment of severe alcoholic hepatitis. J Hepatol 52: 759–764. doi:10.1016/j.jhep.2009.12.021.

23. Lee WM (2012) Acute liver failure. Semin Respir Crit Care Med 33: 36–45. doi:10.1055/s-0032-1301733.

24. Larson AM, Polson J, Fontana RJ, Davern TJ, Lalani E, et al. (2005) Acetaminophen-induced acute liver failure: results of a United States multicenter, prospective study. Hepatology 42: 1364–1372. doi:10.1002/hep.20948.

25. Lin J, Wu J-F, Zhang Q, Zhang H-W, Cao G-W (2014) Virus-related liver cirrhosis: Molecular basis and therapeutic options. World J Gastroenterol 20: 6457–6469. doi:10.3748/wjg.v20.i21.6457.

26. Chang M-H (2014) Prevention of hepatitis B virus infection and liver cancer. Recent Results Cancer Res 193: 75–95. doi:10.1007/978-3-642-38965-8_5.

27. Papatheodoridis G V, Lampertico P, Manolakopoulos S, Lok A (2010) Incidence of hepatocellular carcinoma in chronic hepatitis B patients receiving nucleos(t)ide therapy: a systematic review. J Hepatol 53: 348–356. doi:10.1016/j.jhep.2010.02.035.

28. Li MK, Crawford JM (2004) The pathology of cholestasis. Semin Liver Dis 24: 21–42. doi:10.1055/s-2004-823099.

29. Hirschfield GM, Heathcote EJ, Gershwin ME (2010) Pathogenesis of cholestatic liver disease and therapeutic approaches. Gastroenterology 139: 1481–1496. doi:10.1053/j.gastro.2010.09.004.

30. Blais P, Husain N, Kramer JR, Kowalkowski M, El-Serag H, et al. (2014) Nonalcoholic Fatty Liver Disease is Underrecognized in the Primary Care Setting. Am J Gastroenterol. doi:10.1038/ajg.2014.134.

31. Brunt EM (2010) Pathology of nonalcoholic fatty liver disease. Nat Rev Gastroenterol Hepatol 7: 195–203. doi:nrgastro.2010.21 [pii] 10.1038/nrgastro.2010.21.

32. Schwenger KJP, Allard JP (2014) Clinical approaches to non-alcoholic fatty liver disease. World J Gastroenterol 20: 1712–1723. doi:10.3748/wjg.v20.i7.1712.

33. Kanuri G, Bergheim I (2013) In Vitro and in Vivo Models of Non-Alcoholic Fatty Liver Disease (NAFLD). Int J Mol Sci 14: 11963–11980. doi:10.3390/ijms140611963.

34. Aron-Wisnewsky J, Gaborit B, Dutour A, Clement K (2013) Gut microbiota and non-alcoholic fatty liver disease: new insights. Clin Microbiol Infect 19: 338–348. doi:10.1111/1469-0691.12140.

35. Weber LW, Boll M, Stampfl A (2003) Hepatotoxicity and mechanism of action of haloalkanes: carbon tetrachloride as a toxicological model. Crit Rev Toxicol 33: 105–136. doi:10.1080/713611034.

36. Weiler-Normann C, Herkel J, Lohse AW (2007) Mouse models of liver fibrosis. Z Gastroenterol 45: 43–50. doi:10.1055/s-2006-927387.

37. Marques TG, Chaib E, da Fonseca JH, Lourenço AC, Silva FD, et al. (2012) Review of experimental models for inducing hepatic cirrhosis by bile duct ligation and carbon tetrachloride injection. Acta Cir Bras 27: 589–594. doi:S0102-86502012000800013 [pii].

38. Narotsky MG, Pegram RA, Kavlock RJ (1997) Effect of dosing vehicle on the developmental toxicity of bromodichloromethane and carbon tetrachloride in rats. Fundam Appl Toxicol 40: 30–36.

39. Irie H, Asano-Hoshino A, Sekino Y, Nogami M, Kitagawa T, et al. (2010) Striking LD50 variation associated with fluctuations of CYP2E1-positive cells in hepatic lobule during chronic CCl4 exposure in mice. Virchows Arch 456: 423–431. doi:10.1007/s00428-009-0872-1.

40. Ghafoory S, Breitkopf-Heinlein K, Li Q, Scholl C, Dooley S, et al. (2013) Zonation of nitrogen and glucose metabolism gene expression upon acute liver damage in mouse. PLoS One 8: e78262. doi:10.1371/journal.pone.0078262.

41. Brenner C, Galluzzi L, Kepp O, Kroemer G (2013) Decoding cell death signals in liver inflammation. J Hepatol 59: 583–594. doi:10.1016/j.jhep.2013.03.033.

42. Bataller R, Brenner DA (2001) Hepatic stellate cells as a target for the treatment of liver fibrosis. Semin Liver Dis 21: 437–451. doi:10.1055/s-2001-17558.

43. Marra F, Romanelli RG, Giannini C, Failli P, Pastacaldi S, et al. (1999) Monocyte chemotactic protein-1 as a chemoattractant for human hepatic stellate cells. Hepatology 29: 140–148. doi:S0270913999000191 [pii] 10.1002/hep.510290107.

44. Khimji AK, Rockey DC (2011) Endothelin and hepatic wound healing. Pharmacol Res. doi:S1043-6618(11)00069-7 [pii] 10.1016/j.phrs.2011.03.005.

45. Kisseleva T, Cong M, Paik Y, Scholten D, Jiang C, et al. (2012) Myofibroblasts revert to an inactive phenotype during regression of liver fibrosis. Proc Natl Acad Sci U S A 109: 9448–9453. doi:1201840109 [pii] 10.1073/pnas.1201840109.

46. Krizhanovsky V, Yon M, Dickins RA, Hearn S, Simon J, et al. (2008) Senescence of activated stellate cells limits liver fibrosis. Cell 134: 657–667. doi:S0092-8674(08)00836-2 [pii] 10.1016/j.cell.2008.06.049.

47. Schrader J, Fallowfield J, Iredale JP (2009) Senescence of activated stellate cells: not just early retirement. Hepatology 49: 1045–1047. doi:10.1002/hep.22832.

48. Shanmukhappa K, Sabla GE, Degen JL, Bezerra JA (2006) Urokinase-type plasminogen activator supports liver repair independent of its cellular receptor. BMC Gastroenterol 6: 40. doi:1471-230X-6-40 [pii] 10.1186/1471-230X-6-40.

49. Starkel P, Leclercq IA (2011) Animal models for the study of hepatic fibrosis. Best Pract Res Clin Gastroenterol 25: 319–333. doi:10.1016/j.bpg.2011.02.004.

50. Reinehr R, Becker S, Keitel V, Eberle A, Grether-Beck S, et al. (2005) Bile salt-induced apoptosis involves NADPH oxidase isoform activation. Gastroenterology 129: 2009–2031. doi:S0016-5085(05)01849-4 [pii] 10.1053/j.gastro.2005.09.023.

51. Canbay A, Feldstein AE, Higuchi H, Werneburg N, Grambihler A, et al. (2003) Kupffer cell engulfment of apoptotic bodies stimulates death ligand and cytokine expression. Hepatology 38: 1188–1198. doi:S0270913903008760 [pii] 10.1053/jhep.2003.50472.

52. Liu Y, Wen XM, Lui ELH, Friedman SL, Cui W, et al. (2009) Therapeutic targeting of the PDGF and TGF-beta-signaling pathways in hepatic stellate cells by PTK787/ZK22258. Lab Invest 89: 1152–1160. doi:10.1038/labinvest.2009.77.

53. Sanderson N, Factor V, Nagy P, Kopp J, Kondaiah P, et al. (1995) Hepatic expression of mature transforming growth factor beta 1 in transgenic mice results in multiple tissue lesions. Proc Natl Acad Sci U S A 92: 2572–2576.

54. Campbell JS, Hughes SD, Gilbertson DG, Palmer TE, Holdren MS, et al. (2005) Platelet-derived growth factor C induces liver fibrosis, steatosis, and hepatocellular carcinoma. Proc Natl Acad Sci U S A 102: 3389–3394. doi:0409722102 [pii] 10.1073/pnas.0409722102.

55. Kenerson HL, Yeh MM, Kazami M, Jiang X, Riehle KJ, et al. (2013) Akt and mTORC1 have different roles during liver tumorigenesis in mice. Gastroenterology 144: 1055–1065. doi:10.1053/j.gastro.2013.01.053.

56. Lee UE, Friedman SL (2011) Mechanisms of hepatic fibrogenesis. Best Pr Res Clin Gastroenterol 25: 195–206. doi:S1521-6918(11)00031-X [pii] 10.1016/j.bpg.2011.02.005.

57. Reichenbach V, Fernández-Varo G, Casals G, Oró D, Ros J, et al. (2012) Adenoviral dominant-negative soluble PDGFRβ improves hepatic collagen, systemic hemodynamics, and portal pressure in fibrotic rats. J Hepatol 57: 967–973. doi:S0168-8278(12)00570-3 [pii] 10.1016/j.jhep.2012.07.012.

58. Breitkopf K, Roeyen C, Sawitza I, Wickert L, Floege J, et al. (2005) Expression patterns of PDGF-A, -B, -C and -D and the PDGF-receptors alpha and beta in activated rat hepatic stellate cells (HSC). Cytokine 31: 349–357. doi:S1043-4666(05)00193-6 [pii] 10.1016/j.cyto.2005.06.005.

59. Friedman SL (2008) Mechanisms of hepatic fibrogenesis. Gastroenterology 134: 1655–1669. doi:S0016-5085(08)00429-0 [pii] 10.1053/j.gastro.2008.03.003.

60. Wang Y, Gao J, Zhang D, Zhang J, Ma J, et al. (2010) New insights into the antifibrotic effects of sorafenib on hepatic stellate cells and liver fibrosis. J Hepatol 53: 132–144. doi:S0168-8278(10)00201-1 [pii] 10.1016/j.jhep.2010.02.027.

61. Inagaki Y, Okazaki I (2007) Emerging insights into Transforming growth factor beta Smad signal in hepatic fibrogenesis. Gut 56: 284–292. doi:56/2/284 [pii] 10.1136/gut.2005.088690.

62. Breitkopf K, Godoy P, Ciuclan L, Singer M V, Dooley S (2006) TGF-beta/Smad signaling in the injured liver. Z Gastroenterol 44: 57–66. doi:10.1055/s-2005-858989.

63. Dooley S, ten Dijke P (2012) TGF-β in progression of liver disease. Cell Tissue Res 347: 245–256. doi:10.1007/s00441-011-1246-y.

64. Khimji AK, Shao R, Rockey DC (2008) Divergent transforming growth factor-beta signaling in hepatic stellate cells after liver injury: functional effects on ECE-1 regulation. Am J Pathol 173: 716–727. doi:S0002-9440(10)61644-6 [pii] 10.2353/ajpath.2008.071121.

65. Tacke F, Luedde T, Trautwein C (2009) Inflammatory pathways in liver homeostasis and liver injury. Clin Rev Allergy Immunol 36: 4–12. doi:10.1007/s12016-008-8091-0.

66. Sudo K, Yamada Y, Moriwaki H, Saito K, Seishima M (2005) Lack of tumor necrosis factor receptor type 1 inhibits liver fibrosis induced by carbon tetrachloride in mice. Cytokine 29: 236–244. doi:S1043-4666(05)00008-6 [pii] 10.1016/j.cyto.2004.11.001.

67. Guo D, Hillger JM, IJzerman AP, Heitman LH (2014) Drug-target residence time-a case for G protein-coupled receptors. Med Res Rev 34: 856–892. doi:10.1002/med.21307.

68. Brasier AR, Recinos A, Eledrisi MS (2002) Vascular inflammation and the renin-angiotensin system. Arter Thromb Vasc Biol 22: 1257–1266.

69. Bataller R, Sancho-Bru P, Ginès P, Lora JM, Al-Garawi A, et al. (2003) Activated human hepatic stellate cells express the renin-angiotensin system and synthesize angiotensin II. Gastroenterology 125: 117–125. doi:S0016508503006954 [pii].

70. Bataller R, Gäbele E, Parsons CJ, Morris T, Yang L, et al. (2005) Systemic infusion of angiotensin II exacerbates liver fibrosis in bile duct-ligated rats. Hepatology 41: 1046–1055. doi:10.1002/hep.20665.

71. Bahde R, Kebschull L, Stöppeler S, Zibert A, Siaj R, et al. (2011) Role of angiotensin-1 receptor blockade in cirrhotic liver resection. Liver Int 31: 642–655. doi:10.1111/j.1478-3231.2011.02493.x.

72. Schwalm S, Pfeilschifter J, Huwiler A (2012) Sphingosine-1-phosphate: A Janus-faced mediator of fibrotic diseases. Biochim Biophys Acta. doi:S1388-1981(12)00157-6 [pii] 10.1016/j.bbalip.2012.07.022.

73. Shea BS, Tager AM (2012) Sphingolipid regulation of tissue fibrosis. Open Rheumatol J 6: 123–129. doi:TORJ-6-123 [pii] 10.2174/1874312901206010123.

74. Ikeda H, Watanabe N, Ishii I, Shimosawa T, Kume Y, et al. (2009) Sphingosine 1-phosphate regulates regeneration and fibrosis after liver injury via sphingosine 1-phosphate receptor 2. J Lipid Res 50: 556–564. doi:M800496-JLR200 [pii] 10.1194/jlr.M800496-JLR200.

75. Ikeda H, Yatomi Y, Yanase M, Satoh H, Maekawa H, et al. (2000) Biological activities of novel lipid mediator sphingosine 1-phosphate in rat hepatic stellate cells. Am J Physiol Gastrointest Liver Physiol 279: G304–10.

76. Liu X, Yue S, Li C, Yang L, You H, et al. (2011) Essential roles of sphingosine 1-phosphate receptor types 1 and 3 in human hepatic stellate cells motility and activation. J Cell Physiol 226: 2370–2377. doi:10.1002/jcp.22572.

77. Yang L, Wang Y, Mao H, Fleig S, Omenetti A, et al. (2008) Sonic hedgehog is an autocrine viability factor for myofibroblastic hepatic stellate cells. J Hepatol 48: 98–106. doi:S0168-8278(07)00528-4 [pii] 10.1016/j.jhep.2007.07.032.

78. Sicklick JK, Li YX, Choi SS, Qi Y, Chen W, et al. (2005) Role for hedgehog signaling in hepatic stellate cell activation and viability. Lab Invest 85: 1368–1380. doi:3700349 [pii] 10.1038/labinvest.3700349.

79. Rangwala F, Guy CD, Lu J, Suzuki A, Burchette JL, et al. (2011) Increased production of sonic hedgehog by ballooned hepatocytes. J Pathol 224: 401–410. doi:10.1002/path.2888.

80. Michelotti GA, Xie G, Swiderska M, Choi SS, Karaca G, et al. (2013) Smoothened is a master regulator of adult liver repair. J Clin Invest 123: 2380–2394. doi:10.1172/JCI66904.

81. Swiderska-Syn M, Syn WK, Xie G, Krüger L, Machado M V, et al. (2013) Myofibroblastic cells function as progenitors to regenerate murine livers after partial hepatectomy. Gut. doi:10.1136/gutjnl-2013-305962.

82. Rockey DC, Fouassier L, Chung JJ, Carayon A, Vallee P, et al. (1998) Cellular localization of endothelin-1 and increased production in liver injury in the rat: potential for autocrine and paracrine effects on stellate cells. Hepatology 27: 472–480. doi:S027091399800069X [pii] 10.1002/hep.510270222.

83. Rockey DC, Chung JJ (1996) Endothelin antagonism in experimental hepatic fibrosis. Implications for endothelin in the pathogenesis of wound healing. J Clin Invest 98: 1381–1388. doi:10.1172/JCI118925.

84. Cho JJ, Hocher B, Herbst H, Jia JD, Ruehl M, et al. (2000) An oral endothelin-A receptor antagonist blocks collagen synthesis and deposition in advanced rat liver fibrosis. Gastroenterology 118: 1169–1178. doi:S0016508500421190 [pii].

85. Anselmi K, Subbotin VM, Nemoto E, Gandhi CR (2002) Accelerated reversal of carbon tetrachloride-induced cirrhosis in rats by the endothelin receptor antagonist TAK-044. J Gastroenterol Hepatol 17: 589–597. doi:2705 [pii].

86. Housset C, Rockey DC, Bissell DM (1993) Endothelin receptors in rat liver: lipocytes as a contractile target for endothelin 1. Proc Natl Acad Sci U S A 90: 9266–9270.

87. Mallat A, Fouassier L, Préaux AM, Gal CS, Raufaste D, et al. (1995) Growth inhibitory properties of endothelin-1 in human hepatic myofibroblastic Ito cells. An endothelin B receptor-mediated pathway. J Clin Invest 96: 42–49. doi:10.1172/JCI118052.

88. Chi X, Anselmi K, Watkins S, Gandhi CR (2003) Prevention of cultured rat stellate cell transformation and endothelin-B receptor upregulation by retinoic acid. Br J Pharmacol 139: 765–774. doi:10.1038/sj.bjp.0705303.

89. Koda M, Bauer M, Krebs A, Hahn EG, Schuppan D, et al. (2006) Endothelin-1 enhances fibrogenic gene expression, but does not promote DNA synthesis or apoptosis in hepatic stellate cells. Comp Hepatol 5: 5. doi:1476-5926-5-5 [pii] 10.1186/1476-5926-5-5.

90. Shao R, Shi Z, Gotwals PJ, Koteliansky VE, George J, et al. (2003) Cell and molecular regulation of endothelin-1 production during hepatic wound healing. Mol Biol Cell 14: 2327–2341. doi:02-06-0093 [pii] 10.1091/mbc.02-06-0093.

91. Gandhi CR, Kuddus RH, Uemura T, Rao AS (2000) Endothelin stimulates transforming growth factor-beta1 and collagen synthesis in stellate cells from control but not cirrhotic rat liver. Eur J Pharmacol 406: 311–318. doi:S001429990000683X [pii].

92. Gabriel A, Kuddus RH, Rao AS, Gandhi CR (1999) Down-regulation of endothelin receptors by transforming growth factor beta1 in hepatic stellate cells. J Hepatol 30: 440–450. doi:S0168-8278(99)80103-2 [pii].

93. Hafizi S, Allen SP, Goodwin AT, Chester AH, Yacoub MH (1999) Endothelin-1 stimulates proliferation of human coronary smooth muscle cells via the ET(A) receptor and is co-mitogenic with growth factors. Atherosclerosis 146: 351–359. doi:S0021915099001781 [pii].

94. Kitada K, Ohkita M, Matsumura Y (2012) Pathological Importance of the Endothelin-1/ET(B) Receptor System on Vascular Diseases. Cardiol Res Pr 2012: 731970. doi:10.1155/2012/731970.

95. Horstmeyer A, Licht C, Scherr G, Eckes B, Krieg T (2005) Signalling and regulation of collagen I synthesis by ET-1 and TGF-beta1. FEBS J 272: 6297–6309. doi:EJB5016 [pii] 10.1111/j.1742-4658.2005.05016.x.

96. Boyd R, Rätsep MT, Ding LL, Wang HD (2011) ETA and ETB receptors are expressed in vascular adventitial fibroblasts. Am J Physiol Hear Circ Physiol 301: H2271–8. doi:ajpheart.00869.2010 [pii] 10.1152/ajpheart.00869.2010.

97. Rubin LJ, Badesch DB, Barst RJ, Galie N, Black CM, et al. (2002) Bosentan therapy for pulmonary arterial hypertension. N Engl J Med 346: 896–903. doi:346/12/896 [pii] 10.1056/NEJMoa012212.

98. Lavelle A, Sugrue R, Lawler G, Mulligan N, Kelleher B, et al. (2009) Sitaxentan-induced hepatic failure in two patients with pulmonary arterial hypertension. Eur Respir J 34: 770–771. doi:34/3/770 [pii] 10.1183/09031936.00058409.

99. Bansal G, Druey KM, Xie Z (2007) R4 RGS proteins: regulation of G-protein signaling and beyond. Pharmacol Ther 116: 473–495. doi:S0163-7258(07)00203-3 [pii] 10.1016/j.pharmthera.2007.09.005.

100. Tsang SH, Burns ME, Calvert PD, Gouras P, Baylor DA, et al. (1998) Role for the target enzyme in deactivation of photoreceptor G protein in vivo. Science (80-) 282: 117–121.

101. Dohlman HG, Song J, Apanovitch DM, DiBello PR, Gillen KM (1998) Regulation of G protein signalling in yeast. Semin Cell Dev Biol 9: 135–141. doi:S1084-9521(98)90218-X [pii] 10.1006/scdb.1998.0218.

102. Druey KM, Blumer KJ, Kang VH, Kehrl JH (1996) Inhibition of G-protein-mediated MAP kinase activation by a new mammalian gene family. Nature 379: 742–746. doi:10.1038/379742a0.

103. Matsuzaki N, Nishiyama M, Song D, Moroi K, Kimura S (2011) Potent and selective inhibition of angiotensin AT1 receptor signaling by RGS2: roles of its N-terminal domain. Cell Signal 23: 1041–1049. doi:S0898-6568(11)00036-2 [pii] 10.1016/j.cellsig.2011.01.023.

104. Heximer SP, Knutsen RH, Sun X, Kaltenbronn KM, Rhee MH, et al. (2003) Hypertension and prolonged vasoconstrictor signaling in RGS2-deficient mice. J Clin Invest 111: 1259.

105. Gurley SB, Griffiths RC, Mendelsohn ME, Karas RH, Coffman TM (2010) Renal actions of RGS2 control blood pressure. J Am Soc Nephrol 21: 1847–1851. doi:ASN.2009121306 [pii] 10.1681/ASN.2009121306.

106. Cifelli C, Rose RA, Zhang H, Voigtlaender-Bolz J, Bolz SS, et al. (2008) RGS4 regulates parasympathetic signaling and heart rate control in the sinoatrial node. Circ Res 103: 527–535. doi:CIRCRESAHA.108.180984 [pii] 10.1161/CIRCRESAHA.108.180984.

107. Iankova I, Chavey C, Clapé C, Colomer C, Guérineau NC, et al. (2008) Regulator of G protein signaling-4 controls fatty acid and glucose homeostasis. Endocrinology 149: 5706–5712. doi:10.1210/en.2008-0717.

108. Huang J, Pashkov V, Kurrasch DM, Yu K, Gold SJ, et al. (2006) Feeding and fasting controls liver expression of a regulator of G protein signaling (Rgs16) in periportal hepatocytes. Comp Hepatol 5: 8. doi:10.1186/1476-5926-5-8.

109. Pashkov V, Huang J, Parameswara VK, Kedzierski W, Kurrasch DM, et al. (2011) Regulator of G protein signaling (RGS16) inhibits hepatic fatty acid oxidation in a carbohydrate response element-binding protein (ChREBP)-dependent manner. J Biol Chem 286: 15116–15125. doi:M110.216234 [pii] 10.1074/jbc.M110.216234.

110. Bilger A, Bennett LM, Carabeo RA, Chiaverotti TA, Dvorak C, et al. (2004) A potent modifier of liver cancer risk on distal mouse chromosome 1: linkage analysis and characterization of congenic lines. Genetics 167: 859–866. doi:10.1534/genetics.103.024521.

111. Boss CN, Grünebach F, Brauer K, Häntschel M, Mirakaj V, et al. (2007) Identification and characterization of T-cell epitopes deduced from RGS5, a novel broadly expressed tumor antigen. Clin Cancer Res 13: 3347–3355. doi:10.1158/1078-0432.CCR-06-2156.

112. Hurst JH, Mendpara N, Hooks SB (2009) Regulator of G-protein signalling expression and function in ovarian cancer cell lines. Cell Mol Biol Lett 14: 153–174. doi:10.2478/s11658-008-0040-7.

113. Prokopiou EM, Ryder SA, Walsh JJ (2013) Tumour vasculature targeting agents in hybrid/conjugate drugs. Angiogenesis 16: 503–524. doi:10.1007/s10456-013-9347-8.

114. Silini A, Ghilardi C, Figini S, Sangalli F, Fruscio R, et al. (2012) Regulator of G-protein signaling 5 (RGS5) protein: a novel marker of cancer vasculature elicited and sustained by the tumor's proangiogenic microenvironment. Cell Mol Life Sci 69: 1167–1178. doi:10.1007/s00018-011-0862-8.

115. Manzur M, Hamzah J, Ganss R (2009) Modulation of g protein signaling normalizes tumor vessels. Cancer Res 69: 396–399. doi:10.1158/0008-5472.CAN-08-2842.

116. Anger T, Klintworth N, Stumpf C, Daniel WG, Mende U, et al. (2007) RGS protein specificity towards Gq- and Gi/o-mediated ERK 1/2 and Akt activation, in vitro. J Biochem Mol Biol 40: 899–910.

117. Yang Z, Balenga N, Cooper PR, Damera G, Edwards R, et al. (2012) Regulator of G-protein signaling-5 inhibits bronchial smooth muscle contraction in severe asthma. Am J Respir Cell Mol Biol 46: 823–832. doi:rcmb.2011-0110OC [pii] 10.1165/rcmb.2011-0110OC.

118. Yang Z, Cooper PR, Damera G, Mukhopadhyay I, Cho H, et al. (2011) Beta-agonist-associated reduction in RGS5 expression promotes airway smooth muscle hyper-responsiveness. J Biol Chem 286: 11444–11455. doi:M110.212480 [pii] 10.1074/jbc.M110.212480.

119. Mahoney WM, Gunaje J, Daum G, Dong XR, Majesky MW (2013) Regulator of G-protein signaling - 5 (RGS5) is a novel repressor of hedgehog signaling. PLoS One 8: e61421. doi:10.1371/journal.pone.0061421.

120. Cho H, Kozasa T, Bondjers C, Betsholtz C, Kehrl JH (2003) Pericyte-specific expression of Rgs5: implications for PDGF and EDG receptor signaling during vascular maturation. FASEB J 17: 440–442. doi:10.1096/fj.02-0340fje.

121. Wang X, Adams LD, Pabón LM, Mahoney WM, Beaudry D, et al. (2008) RGS5, RGS4, and RGS2 expression and aortic contractibility are dynamically co-regulated during aortic banding-induced hypertrophy. J Mol Cell Cardiol 44: 539–550. doi:S0022-2828(07)01323-5 [pii] 10.1016/j.yjmcc.2007.11.019.

122. Zhang H, Gu S, Al-Sabeq B, Wang S, He J, et al. (2012) Origin-specific epigenetic program correlates with vascular bed-specific differences in Rgs5 expression. FASEB J 26: 181–191. doi:fj.11-185454 [pii] 10.1096/fj.11-185454.

123. Chang YP, Liu X, Kim JD, Ikeda MA, Layton MR, et al. (2007) Multiple genes for essential-hypertension susceptibility on chromosome 1q. Am J Hum Genet 80: 253–264. doi:S0002-9297(07)62683-4 [pii] 10.1086/510918.

124. Faruque MU, Chen G, Doumatey A, Huang H, Zhou J, et al. (2011) Association of ATP1B1, RGS5 and SELE polymorphisms with hypertension and blood pressure in African-Americans. J Hypertens 29: 1906–1912. doi:10.1097/HJH.0b013e32834b000d.

125. Mitchell TS, Bradley J, Robinson GS, Shima DT, Ng YS (2008) RGS5 expression is a quantitative measure of pericyte coverage of blood vessels. Angiogenesis 11: 141–151. doi:10.1007/s10456-007-9085-x.

126. Lu D, Kassab GS (2011) Role of shear stress and stretch in vascular mechanobiology. J R Soc Interface 8: 1379–1385. doi:10.1098/rsif.2011.0177.

127. Bodenstein J, Sunahara RK, Neubig RR (2007) N-terminal residues control proteasomal degradation of RGS2, RGS4, and RGS5 in human embryonic kidney 293 cells. Mol Pharmacol 71: 1040–1050. doi:mol.106.029397 [pii] 10.1124/mol.106.029397.

128. Hu RG, Sheng J, Qi X, Xu Z, Takahashi TT, et al. (2005) The N-end rule pathway as a nitric oxide sensor controlling the levels of multiple regulators. Nature 437: 981–986. doi:nature04027 [pii] 10.1038/nature04027.

129. Lee MJ, Tasaki T, Moroi K, An JY, Kimura S, et al. (2005) RGS4 and RGS5 are in vivo substrates of the N-end rule pathway. Proc Natl Acad Sci U S A 102: 15030–15035. doi:0507533102 [pii] 10.1073/pnas.0507533102.

130. Li H, He C, Feng J, Zhang Y, Tang Q, et al. (2010) Regulator of G protein signaling 5 protects against cardiac hypertrophy and fibrosis during biomechanical stress of pressure overload. Proc Natl Acad Sci U S A 107: 13818–13823. doi:1008397107 [pii] 10.1073/pnas.1008397107.

131. Berger M, Bergers G, Arnold B, Hämmerling GJ, Ganss R (2005) Regulator of G-protein signaling-5 induction in pericytes coincides with active vessel remodeling during neovascularization. Blood 105: 1094–1101. doi:2004-06-2315 [pii] 10.1182/blood-2004-06-2315.

132. Nisancioglu MH, Mahoney WM, Kimmel DD, Schwartz SM, Betsholtz C, et al. (2008) Generation and characterization of rgs5 mutant mice. Mol Cell Biol 28: 2324–2331. doi:MCB.01252-07 [pii] 10.1128/MCB.01252-07.

133. Cho H, Park C, Hwang IY, Han SB, Schimel D, et al. (2008) Rgs5 targeting leads to chronic low blood pressure and a lean body habitus. Mol Cell Biol 28: 2590–2597. doi:MCB.01889-07 [pii] 10.1128/MCB.01889-07.

134. Deng W, Wang X, Xiao J, Chen K, Zhou H, et al. (2012) Loss of regulator of G protein signaling 5 exacerbates obesity, hepatic steatosis, inflammation and insulin resistance. PLoS One 7: e30256. doi:PONE-D-11-21348 [pii] 10.1371/journal.pone.0030256.

135. Holobotovskyy V, Manzur M, Tare M, Burchell J, Bolitho E, et al. (2013) Regulator of G-protein signaling 5 controls blood pressure homeostasis and vessel wall remodeling. Circ Res 112: 781–791. doi:10.1161/CIRCRESAHA.111.300142.

136. Greenhalgh SN, Conroy KP, Henderson NC (2014) Healing scars: targeting pericytes to treat fibrosis. QJM. doi:10.1093/qjmed/hcu067.

137. Armulik A, Genové G, Betsholtz C (2011) Pericytes: developmental, physiological, and pathological perspectives, problems, and promises. Dev Cell 21: 193–215. doi:10.1016/j.devcel.2011.07.001.

138. Hellström M, Kalén M, Lindahl P, Abramsson A, Betsholtz C (1999) Role of PDGF-B and PDGFR-beta in recruitment of vascular smooth muscle cells and pericytes during embryonic blood vessel formation in the mouse. Development 126: 3047–3055.

139. Humphreys BD, Lin S-L, Kobayashi A, Hudson TE, Nowlin BT, et al. (2010) Fate tracing reveals the pericyte and not epithelial origin of myofibroblasts in kidney fibrosis. Am J Pathol 176: 85–97. doi:10.2353/ajpath.2010.090517.

140. Schrimpf C, Duffield JS (2011) Mechanisms of fibrosis: the role of the pericyte. Curr Opin Nephrol Hypertens 20: 297–305. doi:10.1097/MNH.0b013e328344c3d4.

141. Hellerbrand C (2013) Hepatic stellate cells--the pericytes in the liver. Pflugers Arch 465: 775–778. doi:10.1007/s00424-012-1209-5.

142. Mederacke I, Hsu CC, Troeger JS, Huebener P, Mu X, et al. (2013) Fate tracing reveals hepatic stellate cells as dominant contributors to liver fibrosis independent of its aetiology. Nat Commun 4: 2823. doi:10.1038/ncomms3823.

143. Fleming JN, Nash RA, Mahoney WM, Schwartz SM (2009) Is scleroderma a vasculopathy? Curr Rheumatol Rep 11: 103–110.

144. Mahoney WM, Fleming JN, Schwartz SM (2011) A unifying hypothesis for scleroderma: identifying a target cell for scleroderma. Curr Rheumatol Rep 13: 28–36. doi:10.1007/s11926-010-0152-8.

145. Mehal WZ, Iredale J, Friedman SL (2011) Scraping fibrosis: expressway to the core of fibrosis. Nat Med 17: 552–553. doi:nm0511-552 [pii] 10.1038/nm0511-552.

146. Le Lay J, Kaestner KH (2010) The Fox genes in the liver: from organogenesis to functional integration. Physiol Rev 90: 1–22. doi:90/1/1 [pii] 10.1152/physrev.00018.2009.

147. Friedman SL (2008) Hepatic stellate cells: protean, multifunctional, and enigmatic cells of the liver. Physiol Rev 88: 125–172. doi:88/1/125 [pii] 10.1152/physrev.00013.2007.

148. Heron M (2011) Deaths: leading causes for 2007. Natl Vital Stat Rep 59: 1–95.

149. Hernandez-Gea V, Friedman SL (2011) Pathogenesis of liver fibrosis. Annu Rev Pathol 6: 425–456. doi:10.1146/annurev-pathol-011110-130246.

150. Tarrats N, Moles A, Morales A, García-Ruiz C, Fernández-Checa JC, et al. (2011) Critical role of TNF-receptor 1 but not 2 in hepatic stellate cell proliferation, extracellular matrix remodeling and liver fibrogenesis. Hepatology. doi:10.1002/hep.24388.

151. Bataller R, Brenner DA (2005) Liver fibrosis. J Clin Invest 115: 209–218. doi:10.1172/JCI24282.

152. Ankoma-Sey V, Wang Y, Dai Z (2000) Hypoxic stimulation of vascular endothelial growth factor expression in activated rat hepatic stellate cells. Hepatology 31: 141–148. doi:10.1002/hep.510310122.

153. Li T, Shi Z, Rockey DC (2012) Preproendothelin-1 expression is negatively regulated by IFNγ during hepatic stellate cell activation. Am J Physiol Gastrointest Liver Physiol 302: G948–57. doi:ajpgi.00359.2011 [pii] 10.1152/ajpgi.00359.2011.

154. Oben JA, Roskams T, Yang S, Lin H, Sinelli N, et al. (2003) Norepinephrine induces hepatic fibrogenesis in leptin deficient ob/ob mice. Biochem Biophys Res Commun 308: 284–292.

155. Oben JA, Yang S, Lin H, Ono M, Diehl AM (2003) Norepinephrine and neuropeptide Y promote proliferation and collagen gene expression of hepatic myofibroblastic stellate cells. Biochem Biophys Res Commun 302: 685–690.

156. Oben JA, Yang S, Lin H, Ono M, Diehl AM (2003) Acetylcholine promotes the proliferation and collagen gene expression of myofibroblastic hepatic stellate cells. Biochem Biophys Res Commun 300: 172–177.

157. Hsu CT (1992) The role of the sympathetic nervous system in promoting liver cirrhosis induced by carbon tetrachloride, using the essential hypertensive animal (SHR). J Auton Nerv Syst 37: 163–173.

158. Zhou J, Moroi K, Nishiyama M, Usui H, Seki N, et al. (2001) Characterization of RGS5 in regulation of G protein-coupled receptor signaling. Life Sci 68: 1457–1469. doi:S0024320501009390 [pii].

159. Bondjers C, Kalén M, Hellström M, Scheidl SJ, Abramsson A, et al. (2003) Transcription profiling of platelet-derived growth factor-B-deficient mouse embryos identifies RGS5 as a novel marker for pericytes and vascular smooth muscle cells. Am J Pathol 162: 721–729. doi:10.1016/S0002-9440(10)63868-0.

160. Gunaje JJ, Bahrami AJ, Schwartz SM, Daum G, Mahoney WM (2011) PDGF-dependent regulation of regulator of G protein signaling-5 expression and vascular smooth muscle cell functionality. Am J Physiol Cell Physiol 301: C478–89. doi:ajpcell.00348.2010 [pii] 10.1152/ajpcell.00348.2010.

161. Li J, Adams LD, Wang X, Pabon L, Schwartz SM, et al. (2004) Regulator of G protein signaling 5 marks peripheral arterial smooth muscle cells and is downregulated in atherosclerotic plaque. J Vasc Surg 40: 519–528. doi:10.1016/j.jvs.2004.06.021.

162. Fleming JN, Nash RA, McLeod DO, Fiorentino DF, Shulman HM, et al. (2008) Capillary regeneration in scleroderma: stem cell therapy reverses phenotype? PLoS One 3: e1452. doi:10.1371/journal.pone.0001452.

163. Chen X, Higgins J, Cheung S-T, Li R, Mason V, et al. (2004) Novel endothelial cell markers in hepatocellular carcinoma. Mod Pathol 17: 1198–1210. doi:10.1038/modpathol.3800167.

164. Hu M, Chen X, Zhang J, Wang D, Fang X, et al. (2013) Over-expression of regulator of G protein signaling 5 promotes tumor metastasis by inducing epithelial-mesenchymal transition in hepatocellular carcinoma cells. J Surg Oncol 108: 192–196. doi:10.1002/jso.23367.

165. Chen X, Cheung ST, So S, Fan ST, Barry C, et al. (2002) Gene expression patterns in human liver cancers. Mol Biol Cell 13: 1929–1939. doi:10.1091/mbc.02-02-0023.

166. Eppig JT, Bult CJ, Kadin JA, Richardson JE, Blake JA, et al. (2005) The Mouse Genome Database (MGD): from genes to mice--a community resource for mouse biology. Nucleic Acids Res 33: D471–5. doi:10.1093/nar/gki113.

167. Xu L, Hui AY, Albanis E, Arthur MJ, O'Byrne SM, et al. (2005) Human hepatic stellate cell lines, LX-1 and LX-2: new tools for analysis of hepatic fibrosis. Gut 54: 142–151. doi:54/1/142 [pii] 10.1136/gut.2004.042127.

168. Maschmeyer P, Flach M, Winau F (2011) Seven steps to stellate cells. J Vis Exp pii: 2710. doi:10.3791/2710.

169. Seger R, Seger D, Reszka AA, Munar ES, Eldar-Finkelman H, et al. (1994) Overexpression of mitogen-activated protein kinase kinase (MAPKK) and its mutants in NIH 3T3 cells. Evidence that MAPKK involvement in cellular proliferation is regulated by phosphorylation of serine residues in its kinase subdomains VII and VIII. J Biol Chem 269: 25699–25709.

170. Baratta JL, Ngo A, Lopez B, Kasabwalla N, Longmuir KJ, et al. (2009) Cellular organization of normal mouse liver: a histological, quantitative immunocytochemical, and fine structural analysis. Histochem Cell Biol 131: 713–726. doi:10.1007/s00418-009-0577-1.

171. Lepreux S, Bioulac-Sage P, Gabbiani G, Sapin V, Housset C, et al. (2004) Cellular retinol-binding protein-1 expression in normal and fibrotic/cirrhotic human liver: different patterns of expression in hepatic stellate cells and (myo)fibroblast subpopulations. J Hepatol 40: 774–780. doi:10.1016/j.jhep.2004.01.008.

172. Ning H, Lin G, Lue TF, Lin C-S (2011) Mesenchymal stem cell marker Stro-1 is a 75 kd endothelial antigen. Biochem Biophys Res Commun 413: 353–357. doi:10.1016/j.bbrc.2011.08.104.

173. Faouzi S, Lepreux S, Bedin C, Dubuisson L, Balabaud C, et al. (1999) Activation of cultured rat hepatic stellate cells by tumoral hepatocytes. Lab Invest 79: 485–493.

174. Liu Y, Meyer C, Xu C, Weng H, Hellerbrand C, et al. (2013) Animal models of chronic liver diseases. Am J Physiol Gastrointest Liver Physiol 304: G449–68. doi:10.1152/ajpgi.00199.2012.

175. Puche JE, Lee YA, Jiao J, Aloman C, Fiel MI, et al. (2012) A novel murine model to deplete hepatic stellate cells uncovers their role in amplifying liver damage. Hepatology. doi:10.1002/hep.26053.

176. Mallat A, Gallois C, Tao J, Habib A, Maclouf J, et al. (1998) Platelet-derived growth factor-BB and thrombin generate positive and negative signals for human hepatic stellate cell proliferation. Role of a prostaglandin/cyclic AMP pathway and cross-talk with endothelin receptors. J Biol Chem 273: 27300–27305.

177. Pinzani M, Milani S, De Franco R, Grappone C, Caligiuri A, et al. (1996) Endothelin 1 is overexpressed in human cirrhotic liver and exerts multiple effects on activated hepatic stellate cells. Gastroenterology 110: 534–548.

178. Van Rossen E, Vander Borght S, van Grunsven LA, Reynaert H, Bruggeman V, et al. (2009) Vinculin and cellular retinol-binding protein-1 are markers for quiescent and activated hepatic stellate cells in formalin-fixed paraffin embedded human liver. Histochem Cell Biol 131: 313–325. doi:10.1007/s00418-008-0544-2.

179. Sokolov E, Iannitti DA, Schrum LW, McKillop IH (2011) Altered expression and function of regulator of G-protein signaling-17 (RGS17) in hepatocellular carcinoma. Cell Signal 23: 1603–1610. doi:10.1016/j.cellsig.2011.05.012.

180. Yang JD, Nakamura I, Roberts LR (2011) The tumor microenvironment in hepatocellular carcinoma: current status and therapeutic targets. Semin Cancer Biol 21: 35–43. doi:10.1016/j.semcancer.2010.10.007.

181. Han S, Han L, Yao Y, Sun H, Zan X, et al. (2014) Activated hepatic stellate cells promote hepatocellular carcinoma cell migration and invasion via the activation of FAK-MMP9 signaling. Oncol Rep 31: 641–648. doi:10.3892/or.2013.2872.

182. Amann T, Bataille F, Spruss T, Mühlbauer M, Gäbele E, et al. (2009) Activated hepatic stellate cells promote tumorigenicity of hepatocellular carcinoma. Cancer Sci 100: 646–653. doi:10.1111/j.1349-7006.2009.01087.x.

183. Bergasa N V, Borque MJ, Wahl LM, Rabin L, Jones EA (1992) Modulation of thioacetamide-induced hepatocellular necrosis by prostaglandins is associated with novel histologic changes. Liver 12: 168–174.

184. Cavasin MA, Semus H, Pitts K, Peng Y, Sandoval J, et al. (2010) Acute effects of endothelin receptor antagonists on hepatic hemodynamics of cirrhotic and noncirrhotic rats. Can J Physiol Pharmacol 88: 636–643. doi:y10-038 [pii] 10.1139/Y10-038.

185. Watanabe N, Takashimizu S, Nishizaki Y, Kojima S, Kagawa T, et al. (2007) An endothelin A receptor antagonist induces dilatation of sinusoidal endothelial fenestrae: implications for endothelin-1 in hepatic microcirculation. J Gastroenterol 42: 775–782. doi:10.1007/s00535-007-2093-1.

186. May D, Djonov V, Zamir G, Bala M, Safadi R, et al. (2011) A transgenic model for conditional induction and rescue of portal hypertension reveals a role of VEGF-mediated regulation of sinusoidal fenestrations. PLoS One 6: e21478. doi:10.1371/journal.pone.0021478.

187. Shafiei MS, Rockey DC (2012) The function of integrin-linked kinase in normal and activated stellate cells: implications for fibrogenesis in wound healing. Lab Invest 92: 305–316. doi:labinvest2011155 [pii] 10.1038/labinvest.2011.155.

188. Kitamura K, Tada S, Nakamoto N, Toda K, Horikawa H, et al. (2007) Rho/Rho kinase is a key enzyme system involved in the angiotensin II signaling pathway of liver fibrosis and steatosis. J Gastroenterol Hepatol 22: 2022–2033. doi:JGH4735 [pii] 10.1111/j.1440-1746.2006.04735.x.

189. Alexander MR, Owens GK (2012) Epigenetic control of smooth muscle cell differentiation and phenotypic switching in vascular development and disease. Annu Rev Physiol 74: 13–40. doi:10.1146/annurev-physiol-012110-142315.

190. Majesky MW (2007) Developmental basis of vascular smooth muscle diversity. Arterioscler Thromb Vasc Biol 27: 1248–1258. doi:10.1161/ATVBAHA.107.141069.

191. Wagenseil JE, Ciliberto CH, Knutsen RH, Levy MA, Kovacs A, et al. (2010) The importance of elastin to aortic development in mice. Am J Physiol Heart Circ Physiol 299: H257–64. doi:10.1152/ajpheart.00194.2010.

192. VanderLaan PA, Reardon CA, Getz GS (2004) Site specificity of atherosclerosis: site-selective responses to atherosclerotic modulators. Arterioscler Thromb Vasc Biol 24: 12–22. doi:10.1161/01.ATV.0000105054.43931.f0.

193. Li L, Blumenthal DK, Terry CM, He Y, Carlson ML, et al. (2011) PDGF-induced proliferation in human arterial and venous smooth muscle cells: molecular basis for differential effects of PDGF isoforms. J Cell Biochem 112: 289–298. doi:10.1002/jcb.22924.

194. Majesky MW, Lindner V, Twardzik DR, Schwartz SM, Reidy MA (1991) Production of transforming growth factor beta 1 during repair of arterial injury. J Clin Invest 88: 904–910. doi:10.1172/JCI115393.

195. Suwanabol PA, Seedial SM, Shi X, Zhang F, Yamanouchi D, et al. (2012) Transforming growth factor-β increases vascular smooth muscle cell proliferation through the Smad3 and extracellular signal-regulated kinase mitogen-activated protein kinases pathways. J Vasc Surg 56: 446–454. doi:10.1016/j.jvs.2011.12.038.

196. Shi X, Direnzo D, Guo L-W, Franco SR, Wang B, et al. (2014) TGF-β/Smad3 Stimulates Stem Cell/Developmental Gene Expression and Vascular Smooth Muscle Cell De-Differentiation. PLoS One 9: e93995. doi:10.1371/journal.pone.0093995.

197. Corriere MA, Rogers CM, Eliason JL, Faulk J, Kume T, et al. (2008) Endothelial Bmp4 is induced during arterial remodeling: effects on smooth muscle cell migration and proliferation. J Surg Res 145: 142–149. doi:S0022-4804(07)00232-6 [pii] 10.1016/j.jss.2007.03.077.

198. King KE, Iyemere VP, Weissberg PL, Shanahan CM (2003) Krüppel-like factor 4 (KLF4/GKLF) is a target of bone morphogenetic proteins and transforming growth factor beta 1 in the regulation of vascular smooth muscle cell phenotype. J Biol Chem 278: 11661–11669. doi:M211337200 [pii] 10.1074/jbc.M211337200.

199. Mack CP (2011) Signaling mechanisms that regulate smooth muscle cell differentiation. Arterioscler Thromb Vasc Biol 31: 1495–1505. doi:10.1161/ATVBAHA.110.221135.

200. Geerts A (2001) History, heterogeneity, developmental biology, and functions of quiescent hepatic stellate cells. Semin Liver Dis 21: 311–335. doi:10.1055/s-2001-17550.

201. Arnold C, Feldner A, Pfisterer L, Hödebeck M, Troidl K, et al. (2014) RGS5 promotes arterial growth during arteriogenesis. EMBO Mol Med. doi:10.15252/emmm.201403864.

202. Sohail MA, Hashmi AZ, Hakim W, Watanabe A, Zipprich A, et al. (2009) Adenosine induces loss of actin stress fibers and inhibits contraction in hepatic stellate cells via Rho inhibition. Hepatology 49: 185–194. doi:10.1002/hep.22589.

203. Tangkijvanich P, Tam SP, Yee HF (2001) Wound-induced migration of rat hepatic stellate cells is modulated by endothelin-1 through rho-kinase-mediated alterations in the acto-myosin cytoskeleton. Hepatology 33: 74–80. doi:S0270-9139(01)75407-9 [pii] 10.1053/jhep.2001.20677.

204. Laskin JD, Heck DE, Gardner CR, Laskin DL (2001) Prooxidant and antioxidant functions of nitric oxide in liver toxicity. Antioxid Redox Signal 3: 261–271. doi:10.1089/152308601300185214.

205. Muriel P (2009) Role of free radicals in liver diseases. Hepatol Int 3: 526–536. doi:10.1007/s12072-009-9158-6.

206. Haque JA, McMahan RS, Campbell JS, Shimizu-Albergine M, Wilson AM, et al. (2010) Attenuated progression of diet-induced steatohepatitis in glutathione-deficient mice. Lab Invest 90: 1704–1717. doi:10.1038/labinvest.2010.112.

207. Montuschi P, Barnes PJ, Roberts LJ (2004) Isoprostanes: markers and mediators of oxidative stress. FASEB J 18: 1791–1800. doi:10.1096/fj.04-2330rev.

208. Lin C-L, Hsu Y-T, Lin T-K, Morrow JD, Hsu J-C, et al. (2006) Increased levels of F2-isoprostanes following aneurysmal subarachnoid hemorrhage in humans. Free Radic Biol Med 40: 1466–1473. doi:10.1016/j.freeradbiomed.2005.12.019.

209. Talas ZS, Gogebakan A, Orun I (2013) Effects of propolis on blood biochemical and hematological parameters in nitric oxide synthase inhibited rats by Nω-Nitro-L-arginine methyl ester. Pak J Pharm Sci 26: 915–919.

Appendix:

1.1 PDGF-DEPENDENT REGULATION OF REGULATOR OF G-PROTEIN SIGNALING-5 EXPRESSION AND VASCULAR SMOOTH MUSCLE CELL FUNCTIONALITY.

AUTHORS: Jagadambika J. Gunaje[1], Arya J. Bahrami[1], Stephen M. Schwartz[1], Guenter Daum[2], William M. Mahoney, Jr. [1,3]

Departments of [1]Pathology and Center for Cardiovascular Biology, and [2]Surgery, University of Washington, Seattle

CITATION: *PLoS One* **2013**, 8(4):e61421

ABSTRACT:

Regulator of G-protein signaling (RGS) proteins, and notably members of the RGS-R4 subfamily, control vasocontractility by accelerating the inactivation of Gα-dependent signaling. RGS5 is the most highly and differently expressed RGS-R4 subfamily member in arterial smooth muscle. Expression of RGS5 first appears in pericytes during development of the afferent vascular tree, suggesting that RGS5 is a good candidate for a regulator of arterial contractility and, perhaps, for determining the mass of the smooth muscle coats required to regulate blood flow in the branches of the arterial tree. Consistent with this hypothesis, using cultured vascular smooth muscle cells (SMCs), we demonstrate RGS5 over-expression inhibits G-protein coupled receptor (GPCR)-mediated hypertrophic responses. The next objective was to determine which physiologic agonists directly control RGS5 expression in vascular SMCs. GPCR agonists failed to directly regulate RGS5 mRNA expression, however platelet derived growth factor (PDGF) acutely represses expression. Down-regulation of RGS5 results in the induction of migration and the activation of the GPCR-mediated signaling pathways. This stimulation leads to the activation of mitogen-activated protein kinases (MAPKs) directly down-stream of receptor stimulation, and ultimately vSMC hypertrophy. These results demonstrate that RGS5 expression is a critical mediator of both vSMC contraction and potentially, arterial remodeling.

KEY WORDS: RGS5, PDGF, GPCR, vasoactive agonists, cardiovascular signaling

INTRODUCTION:

Angiotensin, endothelin, thrombin, acetylcholine, and catcholamines are major regulators of both smooth muscle contraction and arterial wall mass. All of these agonists transmit their signals through G-protein coupled receptors (GPCRs), a family of genes that comprise ~1% of the mammalian genome (11). GPCR-mediated signaling has many implications for vascular disease. The characterization of the receptor-agonist interaction should be and has been an important therapeutic target for both systemic and pulmonary hypertension. An equally important target may be the complex of regulatory molecules that determine the extent and duration of GPCR signaling within the vascular smooth muscle cell (vSMC). Expression of different regulators may determine very different functions for the same GPCR in different cells. One such group of regulatory protein, the regulator of G-protein signaling (RGS) proteins has been implicated in controlling the function of vasoactive GPCRs.

Members of the RGS protein family determine the signaling pathways downstream of activation of G proteins (5, 20, 32, 37, 58, 82, 83). Modulation of GPCR signaling by RGS proteins depends on the function of RGS proteins as activators of GTPase activity for GTP-bound G□ large G-proteins (9, 25). Due to this activity, members of the RGS-R4 subfamily appear to be critical to cardiovascular function and pathology (5, 62). For example, cardiac-directed over-expression of RGS5 and RGS4 results in the failure to efficiently remodel in response to pressure overload (41, 59, 60). RGS2 has been linked to blood pressure regulation, presumably via modulation of vasocontractility (31, 38, 56, 66, 70). We have demonstrated RGS5 is preferentially expressed in aortic SMCs, relative to venous SMCs (1, 2). Developmental studies and studies of tumor angiogenesis suggest RGS5 may be critical to vascular stability in newly formed vascular beds (7, 34, 51). Finally, we (55) and others (18, 22, 30) determined that RGS5 is also linked to blood pressure regulation.

The present study is aimed at determining which physiologic agonists control RGS5 expression in vascular SMCs. Very little is known about regulation of expression in this gene family other than the

observation that angiotensin II (AngII) up-regulates RGS2 expression *in vitro*, both at the transcript and protein level (43, 61), while sphingosine-1-phosphate (S1P) up-regulates RGS2 and RGS16 expression (36). In contrast, we found that RGS5 expression is not directly regulated by any of the 7 candidate GPCR agonists assayed following either 2, 6, or 24 hours of stimulation. We previously demonstrated RGS5 expression is down-regulated in response to aortic constriction (79). Perhaps explaining this *in vivo* response, RGS5 expression is down-regulated in response to platelet derived growth factor (PDGF) treatment. This results in increased migration and hypertrophic signaling in vSMCs. These results suggest that the role of PDGF in the vascular response to injury may be mediated by cross-talk between the growth factor and GPCR signaling pathways.

MATERIALS and METHODS:

Cell culture. All cells lines were derived from the rat aorta. The $RGS5^-$ vSMC line is described in Wang *et al*. (79) and was cultured in DMEM (Gibco), supplemented with 10% FBS (Hyclone) and penicillin/streptomycin. The $RGS5^+$ vSMC line was kindly provided by Dr. Gary Owens (University of Virginia (68)) and was cultured in DMEM/F12 (Gibco), supplemented with 10% FBS (Hyclone) and penicillin/streptomycin. All cells are grown at 37°C and 5%CO_2. Importantly, $RGS5^+$ vSMCs express members of the RGS-R4 subfamily at endogenous levels (see below).

Viral over-expression of RGS5. The construction and production of RGS5 retrovirus are described in Wang *et al* (79).

siRNA knock-down of RGS5 expression. RGS5 was knocked-down in $RGS5^+$ vSMCs using a specific siRNA from Invitrogen (5'-AAUUCUCACAGGCAACCCAGAACUC-3'). vSMCs were transfected by electroporation with the human AoSMC nuclefector kit (Amaxa Biosystems) following manufacturers specifications. Briefly, $6x10^6$ cells were transfected with either RGS5-specific siRNA (40nM) or non-specific siRNA (40nM; Invitrogen) and plated at a final density of $1x10^6$ cells/100mm dish (for protein isolation) or $1x10^5$ cells/6-well dish (for RNA isolation) and grown in complete growth media. After 24 hours, the cells were changed to serum-free media and starved for 24 hours. Cells were subsequently treated with the following agonists for 24 hours: angiotensin II (AngII; 100nM; Sigma), endothelin-1 (ET-1; 100nM; Sigma), phenylepherine (PE; 10□M; Sigma), isoproterenol (Iso; 10□M; Sigma), serotonin (5-HT; 5□M; Sigma), norepinephrine (NE; 10□M; Sigma), sphingosine-1-phosphate (S1P, 1□M; Cayman), platelet-derived growth factor (PDGF; 10ng/mL; R&D systems), vascular endothelial growth factor (VEGF; 10ng/mL; R&D systems), and epidermal growth factor (EGF; 10ng/mL; R&D systems).

Quantitative real-time RT-PCR (qPCR). RNA was isolated from vSMCs with or without agonist treatment using the RNAEasy RNA isolation mini kit (Qiagen). Following determination of RNA quantity and quality, cDNA was prepared by reverse transcription (Reverse Transcription cDNA Synthesis kit; Applied Biosystems), using random hexamer primers. Real-time PCR was performed by mixing 20ng cDNA with 20X primer-probe mixes and 2X Taqman PCR Master Mix (Applied Biosystems), and the quantity of each product was determined on the 7900HT Real Time PCR machine (Applied Biosystems). Thermal cycling for PCR was as follows: 2 min. at 50ºC, 10 min. at 95ºC, followed by 40 cycles of 15 sec. at 95ºC for denaturation and 1 min. at 60ºC for annealing and extension. The amount of each target molecule mRNA was calculated using a comparative C_T method (2^-□□C_T; Applied Biosystems, *Relative Quantitation Of Gene Expression, ABI PRISM 7700 Sequence Detection System: User Bulletin #2*), after normalized to glyceraldehyde-3-phosphate dehydrogenase (GAPDH) (48). The rat genes assayed were: RGS2 (Rn00584932_m1; Applied Biosystems), RGS4 (Rn00568067_m1; Applied Biosystems), RGS5 (Rn00571047_m1; Applied Biosystems), and GAPDH (Rn99999916_s1; Applied Biosystems).

Immunoblot. Protein cell lysates were prepared from vSMCs following 0 minute, 2 minutes, 5 minutes, 10 minutes, 30 minutes, and 60 minutes of agonist treatment. Briefly, cells were washed and scraped into 1xPBS. Whole cell extracts were prepared by resuspending the cell pellet in lysis buffer (50mM Tris-HCl (pH 8.0), 120mM NaCl, 0.5% Igepal, 1mM EDTA, and protease inhibitor cocktail (Calbiochem)). Following protein quantitation, 16□g of each protein extract was separated on 10% Bis-Tris gels. Proteins were transferred to PVDF and blocked with 5% non-fat dry milk (NFDM) in TBS-T (0.1% Tween). Membranes were incubated with the following primary antibodies overnight at 4°C, diluted in 5% NFDM in TBS-T : 1:1000 phospho-p42/44 (Thr202/Tyr204; pERK) (Cell Signaling); 1:5000 total p42/44 (ERK) (kindly provided by Dr. Jean Campbell (65)); 1:1000 phospho-Akt (Ser437) (Cell Signaling), 1:1000 phospho-SAPK/JNK (Thr183/Tyr185) (Cell Signaling), 1:1000 phospho-JNK2/3 (Cell Signaling); and 1:20,000 □Actin (Abcam). Following 4X washes with TBS-T, membranes were incubated with the following secondary antibodies at room temperature for 1 hour, diluted in 5% NFDM in TBS-T: 1:8000 goat □-rabbit IgG HRP conjugate (Bio-Rad); 1:8000 goat □-mouse IgG HRP (Bio-Rad). Following 4X washes with TBS-

T, blots were incubated in ECL reagent (Super Signal West Pico, Pierce) and exposed to autoradiographic film.

Hypertrophy assay. Following agonist stimulation for 24 hours, cells were incubated with 1□Ci [^{3}H]-leucine for 5 hours. Cells were washed 2X with cold PBS, followed by washing 2X with 10% TCA. To precipitate proteins, the cells were incubated with 1mL 0.5N NaOH for 15 minutes at room temperature. Cell lysates were transferred to scintillation vials, mixed with scintillation fluid, and the radioactivity was quantified with a scintillation counter.

Migration assay. Transwell plates (Costar) were pre-treated with 0.1% collagen (type 1) (Sigma) overnight at 4°C. RGS5^{+} vSMCs were trypsinized, counted, and re-suspended in migration media (DMEM/F12 supplemented with 0.2% BSA (Sigma)) at a final concentration of 1x10^{6} cells/mL. Following removal of collagen and washing with serum-free media, 1x10^{5} cells were plated in upper chamber of each well each well. Migration media containing PDGF (0ng/mL, 0.3ng/mL, 1ng/mL, or 3ng/mL) or VEGF (0ng/mL or 1ng/mL) was added to the lower chamber after incubation of the cells for 30 minutes at 37°C. Following incubation for 7 hours, the cells are fixed (MeOH for 15 minutes, 70% EtOH overnight at 4°C). The migrated cells are stained with hematoxylin and Scotts blue. The membrane was excised, mounted on glass slides, and the number of cells/40X field was counted.

RESULTS:

Over-expression of RGS5 inhibits the hypertrophic response in rat aortic vSMCs.

Multiple studies have implicated members of the RGS-R4 subfamily in the control of cardiovascular function (reviewed in Wieland and Mittman (83) , Bansal *et al*. (5), Riddle *et al*. (58), and Gu *et al*. (32)). RGS-R4 subfamily proteins interact specifically with the Gα_q and Gα_i large G-proteins (9, 25, 69). Therefore, it is expected that RGS-R4 subfamily members will regulate signals of common vasoactive agonists, which signal through Gα_q- and Gα_i-dependent GPCRs. Among others, RGS2 has been shown to interact with the α_{1A}-adrenergic receptor (33, 80), while RGS4 interacts with the acetylcholine receptor (63) and the opioid receptor (29). Here, we demonstrate that viral over-expression of RGS5 results in a down-regulation of hypertrophic responses to GPCR agonists (Figure 1). Using [^{3}H]-leucine incorporation as a measure of hypertrophic protein production, we demonstrate phyenylepherine (PE), endothelin-1 (ET-1), and angiotensin II (AngII)-induced hypertrophy is inhibited by approximately 25% on average (25%, 18%, and 36%, respectively). Therefore, in vSMCs, RGS5 interacts with Gα_i and Gα_q and effectively inhibits GPCR-mediated hypertrophy.

Characterization of an *in vitro* model system: expression of RGS5 in a cultured vSMC line.

Rat aortic vSMCs express RGS-R4 subfamily members.

Because of the concern with the physiologic relevance of over-expression of a regulator of signal transduction, we explored the physiologic role of RGS-R4 proteins in an *in vitro* rat aortic cell line which expresses RGS5, and other members of the RGS-R4 subfamily, at endogenous levels. Although RGS5 is the most abundant arterial RGS-R4 subfamily member (see below), vSMC cell lines derived from rodents rapidly down-regulate RGS5 expression when placed in culture. After screening a number of available cell lines, we obtained and characterized a rat aortic vSMC cell line which maintains expression of the RGS-R4 subfamily members.

Relative qPCR analysis demonstrates RGS5 and RGS4 are approximately equally expressed, while RGS2 is expressed at lower levels (Figure 2A). This closely relates to additional analyses from our laboratory demonstrating the differential expression pattern for individual members of the RGS-R4 subfamily in the rat and the mouse aorta *in vivo*: RGS5 > RGS4 > RGS2 > RGS16 (data not shown). While an absence of sensitive antibodies makes protein quantification of the RGS-R4 subfamily members difficult, we propose the modulation of RGS mRNA expression and the subsequent measurement of GPCR signaling activity is the best approach to study the functional effect of RGS-R4 expression changes.

Knock-down of RGS5 by siRNA is specific to RGS5 relative to other closely related RGS-R4 subfamily members.

RGS proteins have highly conserved structures and functions throughout evolution. This is of particular importance when comparing members of the RGS-R4 subfamily, since this family is structurally described as having short N- and C-terminal domains and the catalytic RGS domain, which comprises ~2/3 of the protein (25, 69). Therefore, when specifically targeting one member of the family with a siRNA, it is necessary to determine whether the expression of additional members is accidently modified. As demonstrated in Figure 2B, relative to RGS2, RGS4, and RGS16, we have specifically targeted RGS5 by siRNA knock-down. Furthermore, we analyzed RGS5 expression 24hr following knock-down with two additional siRNAs (*Supplemental Figures 1 and 2B*) and confirmed that multiple independent siRNAs have equivalent effects upon RGS5 expression. Therefore, in subsequent studies, we are confident we have knocked-down RGS5, and we can attribute the functional response in these cells to RGS5 expression (or loss thereof).

RGS5 expression regulates the functional response in vSMCs.

Knock-down of RGS5 activates endogenous GPCR-mediate signaling in vSMCs.

RGS proteins, as GTPase activating proteins (GAPs) (24, 27, 62, 87), function to inhibit GPCR signaling through $G\alpha_{GTP}$-dependent pathways. Since over-expression of RGS5 affected the AngII-dependent hypertrophic response, we focused on the effects of RGS5 knock-down on this signaling pathway. AngII has been shown to activate multiple signaling pathways (74, 84). Importantly, phosphorylation of mitogen-activated protein kinases (MAPKs) has been implicated in the contractile, mitogenic and trophic responses of arterial vSMCs (16, 42, 44, 47, 67, 86). Therefore, to determine whether RGS5 expression regulates AngII-dependent signaling, the effect of specific knock-down of RGS5 upon MAPK stimulation was analyzed *in vitro*.

Figure 2C demonstrates that targeted knock-down of RGS5 results in the potentiation of AngII-mediated activation of multiple downstream MAPKs. Twenty-four hours following siRNA treatment, vSMCs were stimulated with 100nM AngII. Relative to the vSMCs treated with non-specific siRNA, phosphorylated ERK (p42/p44) was markedly activated in the vSMCs treated with RGS5 siRNA. A similar response was observed for the two additional RGS5-specific siRNAs assayed (*Supplemental Figure* 2). This response is quantified in Figure 2D. This induction occurred within 2 minutes following AngII treatment and diminishes after 10 minutes of AngII treatment. Phosphorylation of two additional kinases, Akt and Jnk, was similarly activated within 2 minutes of stimulation, although the phosphorylation was not as sustained as observed for pERK. Similarly, RGS5-dependent responses were observed for additional GPCR agonists studied (ET-1, PE, Iso, S1P, NE, 5-HT; *see Supplemental Figure 3A-F*). In summary, RGS5 expression clearly controls the GPCR-mediated rapid and transient increase in kinase phosphorylation in vSMCs.

RGS5 inhibition activates the hypertrophic response in vSMCs.

To confirm the activation of functional cascades down-stream of AngII stimulation, the analysis of hypertrophic incorporation of [^{3}H]-leucine was analyzed in the presence and absence of RGS5-specific siRNA. As expected, knock-down of RGS5 resulted in an approximately 5-fold increase in hypertrophic protein production (Figure 2E). Interestingly, knock-down of RGS5 expression does not sensitize vSMCs

to the AngII-mediated hypertrophic response. Specifically, an induction of hypertrophy is only observed when vSMCs are stimulated with 100nM AngII, but not at lesser AngII concentrations (either 10nM or 50nM). As above, similar RGS5-dependent hypertrophic responses were observed for additional GPCR agonists studied (ET-1, PE, Iso, S1P, NE, 5-HT; *see Supplemental Figure 3G*). Taken together, these data indicate that in vSMCs, RGS5 expression controls both the transient signaling events (MAPK activation is largely complete 10min following AngII stimulation; Figures 2C and D) and the more long-term physiologic effects in response to GPCR stimulation (hypertrophic growth is assayed 29hr following AngII stimulation; Figure 2E), and specifically, the signaling pathways stimulated by AngII treatment.

Agonist-dependent regulation of RGS5 expression.

GPCR agonists do not directly activate RGS5 expression in vSMCs.

Expression of some members of the RGS-R4 subfamily is directly controlled by GPCR agonist stimulation. For example, RGS2 expression is up-regulated in response to AngII treatment both in cultured vSMCs (43) and in the adrenocortical carcinoma cell line (61). To determine whether RGS5 expression is similarly induced in response to GPCR stimulation, vSMCs were treated with AngII, ET-1, PE, Iso, 5-HT, NE, and S1P, and the expression of RGS5 was determined by qPCR. In contrast to the described induction of RGS2 in response to AngII stimulation, none of the GPCR agonists studied significantly affected RGS5 expression levels, following 2hrs, 6hrs, or 24hrs of stimulation (Figure 3A). As demonstrated in Figures 2C and 2D, when RGS5 is knocked down, AngII-mediated phosphorylation of ERK, Akt, and Jnk occurs rapidly. Therefore, to investigate whether short-term GPCR stimulation had any affect upon RGS5 expression, we assayed a few candidate GPCR agonists (AngII, PE, ET-1) for changes in RGS5 mRNA levels. As expected from the more extended stimulation assays, acute stimulation by these three candidate agonists had no significant effect upon RGS5 expression (Figure 3B). Taken together, this indicates an alternative mechanism(s) is controlling expression of RGS5, and potentially additional candidate RGS-R4 subfamily members, in cultured vSMCs.

PDGF-BB stimulation directly represses RGS5 expression in vSMCs.

We are interested in the possibility that PDGF might regulate RGS5 expression because RGS5 and the PDGF-R□ are expressed in pericytes, which function to stabilize neovasculature (7, 12, 13, 21, 53). The effect of PDGF upon a GPCR-mediated pathway is not unexpected because there is growing evidence of cross-talk between GPCRs and receptor tyrosine kinases (RTKs) (40, 54, 78, 81). Treatment of vSMCs with PDGF-BB resulted in the immediate and sustained down-regulation of RGS5 expression (Figure 3C). As shown, RGS5 expression is down-regulated by 25%, 50%, and 80% following 2hrs, 6hrs, and 24hrs of PDGF stimulation, respectively. Importantly, this effect is specific to PDGF, whereas additional RTK stimulants (VEGF and EGF) failed to alter RGS5 expression.

PDGF isoforms have different effects on RGS-R4 subfamily member expression.

Figure 3C clearly demonstrates that PDGF-BB treatment down-regulates RGS5 expression. Unfortunately, PDGF-BB binds all conformations of the PDGF-receptor *in vitro*: the PDGFR□ homodimer, the PDGF□ homodimer, and the PDGFR□/□ heterodimer (3, 71). Therefore, to determine which receptor is responsible for the down-regulation of RGS5, vSMCs were treated with each PDGF isoform (PDGF-AA, -BB, -CC, and -DD). In addition to RGS5 expression, the expression of both RGS4 and RGS2 was also determined by qPCR in response to each of the PDGF isoforms.

In vSMCs, the PDGF-AA and PDGF-CC isoforms did not significantly affect RGS2, RGS4, or RGS5 expression following stimulation for 2hrs, 6hrs, and 24hrs (Figure 3D). Conversely, the PDGF-BB and PDGF-DD isoforms regulated expression of these RGS-R4 subfamily members. RGS5 and RGS4 were down-regulated by both PDGF-BB and PDGF-DD throughout the stimulation time-course. Interestingly, RGS2 was acutely induced by PDGF-BB and PDGF-DD stimulation; however, expression decreases in a similar pattern to both RGS5 and RGS4 following 6hrs and 24hrs of stimulation. As with the published activation of RGS2 by AngII (43, 61), our results provide another example of different regulatory mechanisms controlling the expression of these different RGS-R4 subfamily members. Finally, since an

equivalent effect on RGS5 and RGS4 expression is observed following PDGF-BB and PDGF-DD treatment, and PDGF-BB has been shown to only signal through the PDGFR□ *in vivo* (3, 49, 73), the PDGF-mediated effect in vSMCs is most likely through PDGFR□.

RGS5 expression controls physiologic responses of vSMCs.

Inhibition of RGS5 expression enhances PDGF-mediated vSMC migration.

Classically, PDGF-BB functions to induce the migration and proliferation of vSMCs (15, 28, 57). To determine whether RGS5 expression regulates a cell's migratory capability, vSMCs were treated with RGS5-specific siRNA and exposed to increasing concentrations of PDGF-BB. As shown in Figure 4A, PDGF-dependent migration is induced approximately 1.5-fold upon knock-down of RGS5 expression. Interestingly, there is not a concentration dependence of this migratory phenotype, as an equal number of cells migrate at all concentrations of PDGF-BB assayed when RGS5 is knocked-down. To confirm that this effect was dependent upon PDGF, cells were treated with VEGF and the number of migrated cells was quantitated (Figure 4B). As expected for this negative control treatment, VEGF failed to induce vSMC migration when RGS5 was knocked-down.

PDGF-dependent inhibition of RGS5 expression activates AngII-dependent signaling in vSMCs.

Beyond vSMC migration, we determined whether PDGF-BB treatment performed the same physiologic role as knocking-down RGS5 expression by siRNA in vSMCs. Specifically, we determined whether the signaling and hypertrophic events characterized in Figure 2 could be recapitulated though the pharmacologic knock-down of RGS5 expression by PDGF-BB. As shown in Figure 5, treatment with PDGF-BB for 24hrs, followed by a short time-course of AngII stimulation, resulted in an equivalent, yet transient increase in phosphorylated MAPK (Figure 5A and *Supplemental Figure 5*). Conversely, when cells were not treated with PDGF-BB for 24 hours, AngII-dependent pERK stimulation is not observed in these $RGS5^{+}$ vSMCs. The combined effect of PDGF-BB and AngII on pERK stimulation is quantitated in

Figure 5B. This indicates the GPCR-mediated activation of pERK is dependent upon first knocking-down RGS5 expression by PDGF-BB treatment. Importantly, not only are the signaling pathways down-stream of AngII stimulated, but the hypertrophic response in vSMCs is also activated by the combination of PDGF-BB and AngII treatment. Similar to the effect in vSMCs treated with AngII and RGS5-specific siRNA, vSMCs treated with PDGF-BB for 24 hours followed by AngII treatment exhibited a 6-fold increase in hypertrophic protein production (Figure 5C). Also, as observed following specific knock-down of RGS5 by siRNA (Figure 2E), PDGF-mediated knock-down of RGS5 does not sensitize vSMCs to the AngII-mediated hypertrophic response. As predicted by the siRNA experiment, hypertrophic growth is only observed when vSMCs are stimulated with 100nM AngII, but not at the lesser AngII concentrations. To confirm RGS5 expression remained inhibited following PDGF-BB treatment, we assayed RGS5 mRNA expression at each time-point of potential agonist addition during the hypertrophy assay. As shown in *Supplemental Figure* 4, once RGS5 expression is inhibited, it remains repressed throughout the entire 53hr experimental time-course. Combined, these data provide the first evidence of RTK activation directly regulating the expression of a mediator of G□ signaling, RGS5, leading to increased cell migration and enhanced hypertrophic signaling.

DISCUSSION:

Beyond its role in controlling blood pressure (18, 22, 30, 55), RGS5 has been implicated in the control of vessel branching in normal development (7, 53), as well as in cancer (34, 51). The observations presented here suggest a mechanism by which the PDGF signaling cascade directly regulates GPCR-mediated signaling via RGS5 down-regulation, thereby linking vascular remodeling to the intricate control of RGS protein expression and the downstream physiologic responses (i.e. vSMC migration and hypertrophy).

As expected, we found that RGS5 over-expression inhibits GPCR-mediated hypertrophy in vSMCs (Figure 1). This might lead one to expect a feed-back regulation of RGS5 expression, as has been reported for AngII-mediated induction of RGS2 in both vSMCs (43) and adrenocortical cells (61). However, we found that expression of RGS5 is neither stimulated nor repressed in response to stimulation with GPCR agonists (Figures 3A and 3B). In contrast, when vSMCs are treated with PDGF, RGS5 expression is inhibited (Figures 3C and 3D). When RGS5 is inhibited, either by siRNA (Figure 2B) or pharmacologically (Figures 3C and 3D), vSMCs become more migratory (Figure 4) and GPCR-mediated signaling is induced (Figures 2 and 5). It is interesting to note that the hypertrophic response is stimulated when RGS5 is knocked-down, even in the absence of exogenous GPCR agonists (Figure 2E and *Supplemental Figure 3G*). This implies that RGS5 functions to inhibit GPCR-mediated signaling by endogenous agonists present in the culture media. Therefore, by simply knocking-out RGS5, signaling, and ultimately hypertrophic growth, is induced. However, when cells are stimulated by additional GPCR agonists, hypertrophic growth is further stimulated in the absence of RGS5. Therefore, RGS5 functions to maintain the ‘steady-state’ of the SMC

While RGS5 identifies the pericyte and its expression is down-regulated in PDGF-BB and PDGFR knock-out mice, RGS5-null animals do not have a deficiency in pericyte coverage (12, 13, 35, 55). Pericytes are SMC-like cells that function to stabilize newly formed capillaries during angiogenesis,

including tumor angiogenesis and development (4, 76). The pericyte is believed to be derived by PDGF-mediated migration of adventitial mesenchymal cells along the axis of newly formed endothelial branches. The process is dependent upon endothelial cell-derived PDGF-BB and PDGFR□(6, 10, 35, 45). PDGF-BB and PDGFR□ knock-out mice are characterized by “leaky” and unstable vessels because of the lack of pericytes. Our data suggests that at this stage of pericyte formation, RGS5 expression would be down-regulated. RGS5 expression would be up-regulated once neovessels are fully encoated by perictyes and are therefore functionally capable of distributing blood flow, as suggested by Mitchell *et al* (53). One possible function of RGS5 is the stabilization or organization of the newly formed vessels, perhaps accounting for the observation that RGS5 controls blood flow through experimental tumors in RGS5 knock-out mice (34) and the observation of RGS5 as a tumor progression marker (7, 17, 19, 51).

This hypothesis is strengthened by our observation that RGS5 also opposes PDGF function. This may open up a new and unsuspected variation on the idea of crosstalk between GPCRs and RTKs (14, 52, 54). Usually this has been thought of in terms of activation of the growth factor receptors following GPCR stimulation (23, 40, 75). Recently, Wang *et al.* demonstrated signaling through the angiotensin type I receptor (AT1R) activates the PDGFR□-dependent signaling cascade (78). However, all of these studies imply a one-way activation of RTK signaling cascades following GPCR stimulation. This mechanism has been referred to as the triple-membrane-passing-signaling (TMPS) model (77, 81). Our data showing PDGFR□ stimulation functions to down-regulate RGS5 expression establishes a link between the RTK and GPCR signaling cascade, independent of the GPCR-to-RTK connection established previously.

Taken together, our results have led us to propose the following model (Figure 6). In the quiescent arterial wall, differentiated vSMCs express RGS5, resulting in the inhibition of the GPCR-mediated signaling cascade. Therefore, $G\alpha_{q/i}$ signaling is inhibited and cells do not migrate or undergo hypertrophy, even in the presence of circulating/local GPCR agonists (Figure 6A). However, upon vascular injury, the local concentration of PDGF-BB increases, through release from platelets, activated endothelial cells, and

invading macrophages (50, 64, 72). As a result, RGS5 expression is inhibited and vSMCs become more migratory and proliferative. In addition, the inhibition of RGS5 expression enables signaling through the relevant GPCRs. The specific inhibition of RGS5 results in the phosphorylation-mediated activation of MAPKs downstream of $G_{q/i}$, and ultimately, vSMC hypertrophy/remodeling (Figure 6B). Once the injury response is complete, the platelets and macrophage dissipate and the local concentration of PDGF-BB is diminished. As a result, RGS5 expression returns to endogenous levels, and GPCR-mediated signaling is consequently inhibited.

This data correlates with our previously described expression pattern for RGS5 *in vivo*, in the remodeling response to thoracic aortic banding in the rat (79). Upon vascular injury, the expression of PDGF is induced, along with the expression of Krupple-like factor 4 (KLF4), which results in a down-regulation genes expressed in differentiated vSMCs, including smooth muscle myosin heavy chain and SM22/transgelin (26, 46, 85). Acutely, injured arteries also go into spasm, perhaps due to the combined contractile effect of PDGF and the loss of expression of RGS5 (8). In addition to stimulating contraction, PDGF also induces vSMCs to de-differentiate and become more proliferative and migratory (39), resulting in the classic vascular response to injury.

The data presented here provide a mechanism by which the combined effects of vasoactive GPCR stimulants and the circulating PDGF account for the classic vascular response to injury. Furthermore, our results establish a central role for RGS5, and potentially additional members of the RGS-R4 subfamily, in cardiovascular remodeling.

FUNDING: This work was supported by the National Institutes of Health (HL007312 and HL087513).

DISCLOSURES: none declared.

ACKNOWLEDGEMENTS: We would like to thank Dr. Mark Majesky (Seattle Children's Research Institute) for useful discussions and for critically reading this manuscript.

REFERENCES:

1. **Adams LD, Geary RL, Li J, Rossini A, and Schwartz SM.** Expression profiling identifies smooth muscle cell diversity within human intima and plaque fibrous cap: loss of RGS5 distinguishes the cap. *ArteriosclerThrombVascBiol* 26: 319-325, 2006.

2. **Adams LD, Geary RL, McManus B, and Schwartz SM.** A comparison of aorta and vena cava medial message expression by cDNA array analysis identifies a set of 68 consistently differentially expressed genes, all in aortic media. *CircRes* 87: 623-631, 2000.

3. **Andrae J, Gallini R, and Betsholtz C.** Role of platelet-derived growth factors in physiology and medicine. *Genes Dev* 22: 1276-1312, 2008.

4. **az-Flores L, Gutierrez R, Madrid JF, Varela H, Valladares F, Acosta E, Martin-Vasallo P, and az-Flores L, Jr.** Pericytes. Morphofunction, interactions and pathology in a quiescent and activated mesenchymal cell niche. *HistolHistopathol* 24: 909-969, 2009.

5. **Bansal G, Druey KM, and Xie Z.** R4 RGS proteins: Regulation of G-protein signaling and beyond. *PharmacolTher* 116: 473-495, 2007.

6. **Benjamin LE, Hemo I, and Keshet E.** A plasticity window for blood vessel remodelling is defined by pericyte coverage of the preformed endothelial network and is regulated by PDGF-B and VEGF. *Development* 125: 1591-1598, 1998.

7. **Berger M, Bergers G, Arnold B, Hammerling GJ, and Ganss R.** Regulator of G-protein signaling-5 induction in pericytes coincides with active vessel remodeling during neovascularization. *Blood* 105: 1094-1101, 2005.

8. **Berk BC, Alexander RW, Brock TA, Gimbrone MA, Jr., and Webb RC.** Vasoconstriction: a new activity for platelet-derived growth factor. *Science* 232: 87-90, 1986.

9. **Berman DM, Wilkie TM, and Gilman AG.** GAIP and RGS4 are GTPase-activating proteins for the Gi subfamily of G protein alpha subunits. *Cell* 86: 445-452, 1996.

10. **Betsholtz C, Lindblom P, and Gerhardt H.** Role of pericytes in vascular morphogenesis. *EXS*: 115-125, 2005.

11. **Bockaert J and Pin JP.** Molecular tinkering of G protein-coupled receptors: an evolutionary success. *EMBO J* 18: 1723-1729, 1999.

12. **Bondjers C, He L, Takemoto M, Norlin J, Asker N, Hellstrom M, Lindahl P, and Betsholtz C.** Microarray analysis of blood microvessels from PDGF-B and PDGF-Rbeta mutant mice identifies novel markers for brain pericytes. *FASEB J* 20: 1703-1705, 2006.

13. **Bondjers C, Kalen M, Hellstrom M, Scheidl SJ, Abramsson A, Renner O, Lindahl P, Cho H, Kehrl J, and Betsholtz C.** Transcription profiling of platelet-derived growth factor-B-deficient mouse embryos identifies RGS5 as a novel marker for pericytes and vascular smooth muscle cells. *AmJ Pathol* 162: 721-729, 2003.

14. **Booz GW and Baker KM.** Molecular signalling mechanisms controlling growth and function of cardiac fibroblasts. *CardiovascRes* 30: 537-543, 1995.

15. **Bornfeldt KE, Graves LM, Raines EW, Igarashi Y, Wayman G, Yamamura S, Yatomi Y, Sidhu JS, Krebs EG, and Hakomori S.** Sphingosine-1-phosphate inhibits PDGF-induced chemotaxis of human arterial smooth muscle cells: spatial and temporal modulation of PDGF chemotactic signal transduction. *J Cell Biol* 130: 193-206, 1995.

16. **Bornfeldt KE and Krebs EG.** Crosstalk between protein kinase A and growth factor receptor signaling pathways in arterial smooth muscle. *Cell Signal* 11: 465-477, 1999.

17. **Boss CN, Grunebach F, Brauer K, Hantschel M, Mirakaj V, Weinschenk T, Stevanovic S, Rammensee HG, and Brossart P.** Identification and characterization of T-cell epitopes deduced from RGS5, a novel broadly expressed tumor antigen. *ClinCancer Res* 13: 3347-3355, 2007.

18. **Chang YP, Liu X, Kim JD, Ikeda MA, Layton MR, Weder AB, Cooper RS, Kardia SL, Rao DC, Hunt SC, Luke A, Boerwinkle E, and Chakravarti A.** Multiple genes for essential-hypertension susceptibility on chromosome 1q. *AmJ HumGenet* 80: 253-264, 2007.

19. **Chen X, Higgins J, Cheung ST, Li R, Mason V, Montgomery K, Fan ST, van de RM, and So S.** Novel endothelial cell markers in hepatocellular carcinoma. *ModPathol* 17: 1198-1210, 2004.

20. **Cho H, Harrison K, and Kehrl JH.** Regulators of G protein signaling: potential drug targets for controlling cardiovascular and immune function. *CurrDrug TargetsImmuneEndocrMetabolDisord* 4: 107-118, 2004.

21. **Cho H, Kozasa T, Bondjers C, Betsholtz C, and Kehrl JH.** Pericyte-specific expression of Rgs5: implications for PDGF and EDG receptor signaling during vascular maturation. *FASEB J* 17: 440-442, 2003.

22. **Cho H, Park C, Hwang IY, Han SB, Schimel D, Despres D, and Kehrl JH.** Rgs5 Targeting Leads to Chronic Low Blood Pressure and a Lean Body Habitus. *Mol Cell Biol*, 2008.

23. **Daub H, Weiss FU, Wallasch C, and Ullrich A.** Role of transactivation of the EGF receptor in signalling by G-protein-coupled receptors. *Nature* 379: 557-560, 1996.

24. **De Vries L and Gist FM.** RGS proteins: more than just GAPs for heterotrimeric G proteins. *Trends Cell Biol* 9: 138-144, 1999.

25. **De Vries L, Zheng B, Fischer T, Elenko E, and Farquhar MG.** The regulator of G protein signaling family. *AnnuRevPharmacolToxicol* 40: 235-271, 2000.

26. **Deaton RA, Gan Q, and Owens GK.** Sp1-dependent activation of KLF4 is required for PDGF-BB-induced phenotypic modulation of smooth muscle. *AmJPhysiol Heart CircPhysiol* 296: H1027-H1037, 2009.

27. **Druey KM.** Bridging with GAPs: receptor communication through RGS proteins. *SciSTKE* 2001: RE14, 2001.

28. **Ferns GA, Sprugel KH, Seifert RA, Bowen-Pope DF, Kelly JD, Murray M, Raines EW, and Ross R.** Relative platelet-derived growth factor receptor subunit expression determines cell migration to different dimeric forms of PDGF. *Growth Factors* 3: 315-324, 1990.

29. **Georgoussi Z, Leontiadis L, Mazarakou G, Merkouris M, Hyde K, and Hamm H.** Selective interactions between G protein subunits and RGS4 with the C-terminal domains of the mu- and delta-opioid receptors regulate opioid receptor signaling. *Cell Signal* 18: 771-782, 2006.

30. **Grayson TH, Ohms SJ, Brackenbury TD, Meaney KR, Peng K, Pittelkow YE, Wilson SR, Sandow SL, and Hill CE.** Vascular microarray profiling in two models of hypertension identifies Cav-1, Rgs2 and Rgs5 as antihypertensive targets. *BMCGenomics* 8: 404, 2007.

31. **Gross V, Tank J, Obst M, Plehm R, Blumer KJ, Diedrich A, Jordan J, and Luft FC.** Autonomic nervous system and blood pressure regulation in RGS2-deficient mice. *AmJ Physiol RegulIntegrComp Physiol* 288: R1134-R1142, 2005.

32. **Gu S, Cifelli C, Wang S, and Heximer SP.** RGS proteins: identifying new GAPs in the understanding of blood pressure regulation and cardiovascular function. *ClinSci(Lond)* 116: 391-399, 2009.

33. **Hague C, Bernstein LS, Ramineni S, Chen Z, Minneman KP, and Hepler JR.** Selective inhibition of alpha1A-adrenergic receptor signaling by RGS2 association with the receptor third intracellular loop. *J BiolChem* 280: 27289-27295, 2005.

34. **Hamzah J, Jugold M, Kiessling F, Rigby P, Manzur M, Marti HH, Rabie T, Kaden S, Grone HJ, Hammerling GJ, Arnold B, and Ganss R.** Vascular normalization in Rgs5-deficient tumours promotes immune destruction. *Nature* 453: 410-414, 2008.

35. **Hellstrom M, Kalen M, Lindahl P, Abramsson A, and Betsholtz C.** Role of PDGF-B and PDGFR-beta in recruitment of vascular smooth muscle cells and pericytes during embryonic blood vessel formation in the mouse. *Development* 126: 3047-3055, 1999.

36. **Hendriks-Balk M, van Loenen P, Hajji N, Michel M, Peters S, and Alewijnse A.** S1P receptor signalling and RGS proteins; expression and function in vascular smooth muscle cells and transfected CHO cells. *Eur J Pharmacol* 600: 1-9, 2008.

37. **Hendriks-Balk MC, Peters SL, Michel MC, and Alewijnse AE.** Regulation of G protein-coupled receptor signalling: focus on the cardiovascular system and regulator of G protein signalling proteins. *EurJ Pharmacol* 585: 278-291, 2008.

38. **Heximer SP, Knutsen RH, Sun X, Kaltenbronn KM, Rhee MH, Peng N, Oliveira-Dos-Santos A, Penninger JM, Muslin AJ, Steinberg TH, Wyss JM, Mecham RP, and Blumer KJ.** Hypertension and prolonged vasoconstrictor signaling in RGS2-deficient mice. *J ClinInvest* 111: 445-452, 2003.

39. **Holycross BJ, Blank RS, Thompson MM, Peach MJ, and Owens GK.** Platelet-derived growth factor-BB-induced suppression of smooth muscle cell differentiation. *CircRes* 71: 1525-1532, 1992.

40. **Kalmes A, Daum G, and Clowes AW.** EGFR transactivation in the regulation of SMC function. *AnnNYAcadSci* 947: 42-54, 2001.

41. **Li H, He C, Feng J, Zhang Y, Tang Q, Bian Z, Bai X, Zhou H, Jiang H, Heximer SP, Qin M, Huang H, Liu PP, and Huang C.** Regulator of G protein signaling 5 protects against cardiac hypertrophy and fibrosis during biomechanical stress of pressure overload. *ProcNatlAcadSciUSA* 107: 13818-13823, 2010.

42. **Li S, Moon JJ, Miao H, Jin G, Chen BP, Yuan S, Hu Y, Usami S, and Chien S.** Signal transduction in matrix contraction and the migration of vascular smooth muscle cells in three-dimensional matrix. *JVascRes* 40: 378-388, 2003.

43. **Li Y, Hashim S, and Anand-Srivastava MB.** Angiotensin II-evoked enhanced expression of RGS2 attenuates Gi-mediated adenylyl cyclase signaling in A10 cells. *Cardiovasc Res* 66: 503-511, 2005.

44. **Liang KW, Ting CT, Yin SC, Chen YT, Lin SJ, Liao JK, and Hsu SL.** Berberine suppresses MEK/ERK-dependent Egr-1 signaling pathway and inhibits vascular smooth muscle cell regrowth after in vitro mechanical injury. *BiochemPharmacol* 71: 806-817, 2006.

45. **Lindblom P, Gerhardt H, Liebner S, Abramsson A, Enge M, Hellstrom M, Backstrom G, Fredriksson S, Landegren U, Nystrom HC, Bergstrom G, Dejana E, Ostman A, Lindahl P, and**

Betsholtz C. Endothelial PDGF-B retention is required for proper investment of pericytes in the microvessel wall. *Genes Dev* 17: 1835-1840, 2003.

46. **Liu Y, Sinha S, McDonald OG, Shang Y, Hoofnagle MH, and Owens GK.** Kruppel-like factor 4 abrogates myocardin-induced activation of smooth muscle gene expression. *JBiolChem* 280: 9719-9727, 2005.

47. **Liu Y, Suzuki YJ, Day RM, and Fanburg BL.** Rho kinase-induced nuclear translocation of ERK1/ERK2 in smooth muscle cell mitogenesis caused by serotonin. *CircRes* 95: 579-586, 2004.

48. **Livak KJ and Schmittgen TD.** Analysis of relative gene expression data using real-time quantitative PCR and the 2(-Delta Delta C(T)) Method. *Methods* 25: 402-408, 2001.

49. **Majack RA, Grieshaber NA, Cook CL, Weiser MC, McFall RC, Grieshaber SS, Reidy MA, and Reilly CF.** Smooth muscle cells isolated from the neointima after vascular injury exhibit altered responses to platelet-derived growth factor and other stimuli. *J Cell Physiol* 167: 106-112, 1996.

50. **Majesky MW.** Neointima formation after acute vascular injury. Role of counteradhesive extracellular matrix proteins. *Tex Heart Inst J* 21: 78-85, 1994.

51. **Manzur M and Ganss R.** Regulator of g protein signaling 5: a new player in vascular remodeling. *Trends CardiovascMed* 19: 26-30, 2009.

52. **Mehta PK and Griendling KK.** Angiotensin II cell signaling: physiological and pathological effects in the cardiovascular system. *AmJ Physiol Cell Physiol* 292: C82-C97, 2007.

53. **Mitchell TS, Bradley J, Robinson GS, Shima DT, and Ng YS.** RGS5 expression is a quantitative measure of pericyte coverage of blood vessels. *Angiogenesis* 11: 141-151, 2008.

54. **Natarajan K and Berk BC.** Crosstalk coregulation mechanisms of G protein-coupled receptors and receptor tyrosine kinases. *Methods MolBiol* 332: 51-77, 2006.

55. **Nisancioglu MH, Mahoney WM, Jr., Kimmel DD, Schwartz SM, Betsholtz C, and Genove G.** Generation and characterization of rgs5 mutant mice. *Mol Cell Biol* 28: 2324-2331, 2008.

56. **Obst M, Tank J, Plehm R, Blumer KJ, Diedrich A, Jordan J, Luft FC, and Gross V.** NO-dependent blood pressure regulation in RGS2-deficient mice. *AmJ Physiol RegulIntegrComp Physiol* 290: R1012-R1019, 2006.

57. **Raines EW.** PDGF and cardiovascular disease. *Cytokine Growth Factor Rev* 15: 237-254, 2004.

58. **Riddle EL, Schwartzman RA, Bond M, and Insel PA.** Multi-tasking RGS proteins in the heart: the next therapeutic target? *CircRes* 96: 401-411, 2005.

59. **Rogers JH, Tamirisa P, Kovacs A, Weinheimer C, Courtois M, Blumer KJ, Kelly DP, and Muslin AJ.** RGS4 causes increased mortality and reduced cardiac hypertrophy in response to pressure overload. *J ClinInvest* 104: 567-576, 1999.

60. **Rogers JH, Tsirka A, Kovacs A, Blumer KJ, Dorn GW, and Muslin AJ.** RGS4 reduces contractile dysfunction and hypertrophic gene induction in Galpha q overexpressing mice. *JMolCell Cardiol* 33: 209-218, 2001.

61. **Romero DG, Plonczynski MW, Gomez-Sanchez EP, Yanes LL, and Gomez-Sanchez CE.** RGS2 is regulated by angiotensin II and functions as a negative feedback of aldosterone production in H295R human adrenocortical cells. *Endocrinology* 147: 3889-3897, 2006.

62. **Ross EM and Wilkie TM.** GTPase-activating proteins for heterotrimeric G proteins: regulators of G protein signaling (RGS) and RGS-like proteins. *AnnuRevBiochem* 69: 795-827, 2000.

63. **Roy AA, Lemberg KE, and Chidiac P.** Recruitment of RGS2 and RGS4 to the plasma membrane by G proteins and receptors reflects functional interactions. *Mol Pharmacol* 64: 587-593, 2003.

64. **Sapienza P, di Marzo L, Cucina A, Corvino V, Mingoli A, Giustiniani Q, Ziparo E, and Cavallaro A.** Release of PDGF-BB and bFGF by human endothelial cells seeded on expanded polytetrafluoroethylene vascular grafts. *J Surg Res* 75: 24-29, 1998.

65. **Seger R, Seger D, Reszka AA, Munar ES, Eldar-Finkelman H, Dobrowolska G, Jensen AM, Campbell JS, Fischer EH, and Krebs EG.** Overexpression of mitogen-activated protein kinase kinase

(MAPKK) and its mutants in NIH 3T3 cells. Evidence that MAPKK involvement in cellular proliferation is regulated by phosphorylation of serine residues in its kinase subdomains VII and VIII. *J Biol Chem* 269: 25699-25709, 1994.

66. **Semplicini A, Lenzini L, Sartori M, Papparella I, Calo LA, Pagnin E, Strapazzon G, Benna C, Costa R, Avogaro A, Ceolotto G, and Pessina AC.** Reduced expression of regulator of G-protein signaling 2 (RGS2) in hypertensive patients increases calcium mobilization and ERK1/2 phosphorylation induced by angiotensin II. *J Hypertens* 24: 1115-1124, 2006.

67. **Servant MJ, Giasson E, and Meloche S.** Inhibition of growth factor-induced protein synthesis by a selective MEK inhibitor in aortic smooth muscle cells. *JBiolChem* 271: 16047-16052, 1996.

68. **Shimizu RT, Blank RS, Jervis R, Lawrenz-Smith SC, and Owens GK.** The smooth muscle alpha-actin gene promoter is differentially regulated in smooth muscle versus non-smooth muscle cells. *JBiolChem* 270: 7631-7643, 1995.

69. **Sierra DA, Gilbert DJ, Householder D, Grishin NV, Yu K, Ukidwe P, Barker SA, He W, Wensel TG, Otero G, Brown G, Copeland NG, Jenkins NA, and Wilkie TM.** Evolution of the regulators of G-protein signaling multigene family in mouse and human. *Genomics* 79: 177-185, 2002.

70. **Sun X, Kaltenbronn KM, Steinberg TH, and Blumer KJ.** RGS2 is a mediator of nitric oxide action on blood pressure and vasoconstrictor signaling. *Mol Pharmacol* 67: 631-639, 2005.

71. **Tallquist M and Kazlauskas A.** PDGF signaling in cells and mice. *Cytokine Growth Factor Rev* 15: 205-213, 2004.

72. **Tani K, Ogushi F, Takahashi H, Kawano T, Endo T, and Sone S.** Thrombin stimulates platelet-derived growth factor release by alveolar macrophages in rats--significance in bleomycin-induced pulmonary fibrosis. *J Med Invest* 44: 59-65, 1997.

73. **Thomas JA, Deaton RA, Hastings NE, Shang Y, Moehle CW, Eriksson U, Topouzis S, Wamhoff BR, Blackman BR, and Owens GK.** PDGF-DD, a novel mediator of smooth muscle cell

phenotypic modulation, is upregulated in endothelial cells exposed to atherosclerosis-prone flow patterns. *AmJ Physiol Heart CircPhysiol* 296: H442-H452, 2009.

74. **Touyz RM and Schiffrin EL.** Signal transduction mechanisms mediating the physiological and pathophysiological actions of angiotensin II in vascular smooth muscle cells. *PharmacolRev* 52: 639-672, 2000.

75. **Ushio-Fukai M, Griendling KK, Becker PL, Hilenski L, Halleran S, and Alexander RW.** Epidermal growth factor receptor transactivation by angiotensin II requires reactive oxygen species in vascular smooth muscle cells. *ArteriosclerThrombVascBiol* 21: 489-495, 2001.

76. **von TD, Armulik A, and Betsholtz C.** Pericytes and vascular stability. *ExpCell Res* 312: 623-629, 2006.

77. **Wallasch C, Crabtree JE, Bevec D, Robinson PA, Wagner H, and Ullrich A.** Helicobacter pylori-stimulated EGF receptor transactivation requires metalloprotease cleavage of HB-EGF. *BiochemBiophysResCommun* 295: 695-701, 2002.

78. **Wang C, Wu LL, Liu J, Zhang ZG, Fan D, and Li L.** Crosstalk between angiotensin II and platelet derived growth factor-BB mediated signal pathways in cardiomyocytes. *Chin MedJ(Engl)* 121: 236-240, 2008.

79. **Wang X, Adams LD, Pabon LM, Mahoney WM, Jr., Beaudry D, Gunaje J, Geary RL, deBlois D, and Schwartz SM.** RGS5, RGS4, and RGS2 expression and aortic contractibility are dynamically co-regulated during aortic banding-induced hypertrophy. *JMolCell Cardiol* 44: 539-550, 2008.

80. **Wang X, Zeng W, Soyombo AA, Tang W, Ross EM, Barnes AP, Milgram SL, Penninger JM, Allen PB, Greengard P, and Muallem S.** Spinophilin regulates Ca2+ signalling by binding the N-terminal domain of RGS2 and the third intracellular loop of G-protein-coupled receptors. *NatCell Biol* 7: 405-411, 2005.

81. **Wetzker R and Bohmer FD.** Transactivation joins multiple tracks to the ERK/MAPK cascade. *NatRevMol Cell Biol* 4: 651-657, 2003.

82. **Wieland T, Lutz S, and Chidiac P.** Regulators of G protein signalling: a spotlight on emerging functions in the cardiovascular system. *CurrOpinPharmacol* 7: 201-207, 2007.

83. **Wieland T and Mittmann C.** Regulators of G-protein signalling: multifunctional proteins with impact on signalling in the cardiovascular system. *Pharmacol Ther* 97: 95-115, 2003.

84. **Yin G, Yan C, and Berk BC.** Angiotensin II signaling pathways mediated by tyrosine kinases. *IntJ BiochemCell Biol* 35: 780-783, 2003.

85. **Yoshida T, Kaestner KH, and Owens GK.** Conditional deletion of Kruppel-like factor 4 delays downregulation of smooth muscle cell differentiation markers but accelerates neointimal formation following vascular injury. *CircRes* 102: 1548-1557, 2008.

86. **Zhang H, Chalothorn D, Jackson LF, Lee DC, and Faber JE.** Transactivation of epidermal growth factor receptor mediates catecholamine-induced growth of vascular smooth muscle. *CircRes* 95: 989-997, 2004.

87. **Zhou J, Moroi K, Nishiyama M, Usui H, Seki N, Ishida J, Fukamizu A, and Kimura S.** Characterization of RGS5 in regulation of G protein-coupled receptor signaling. *Life Sci* 68: 1457-1469, 2001.

FIGURE LEGENDS:

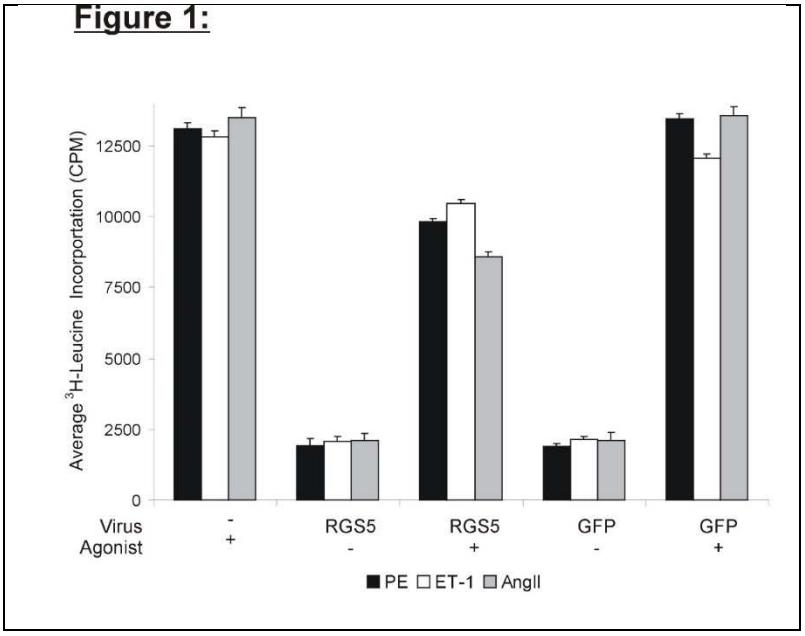

Figure 1. *RGS5 over-expression inhibits hypertrophy in vSMCs.* Rat aortic vSMCs were infected with retrovirus over-expressing either RGS5 or GFP (control). Following stimulation with the GPCR agonists (10□M PE, 100nM ET-1, 100nM AngII) for 24hrs and pulsed with 1□Ci [^{3}H]-leucine for 5hrs, the amount of [^{3}H]-leucine incorporated into new protein was quantitated to assess hypertrophic growth. Each GPCR agonist assayed stimulated hypertrophic growth of vSMCs. When RGS5 was over-expressed, but not when GFP was over-expressed, hypertrophic growth was inhibited. (error bars are SEM; n=3.)

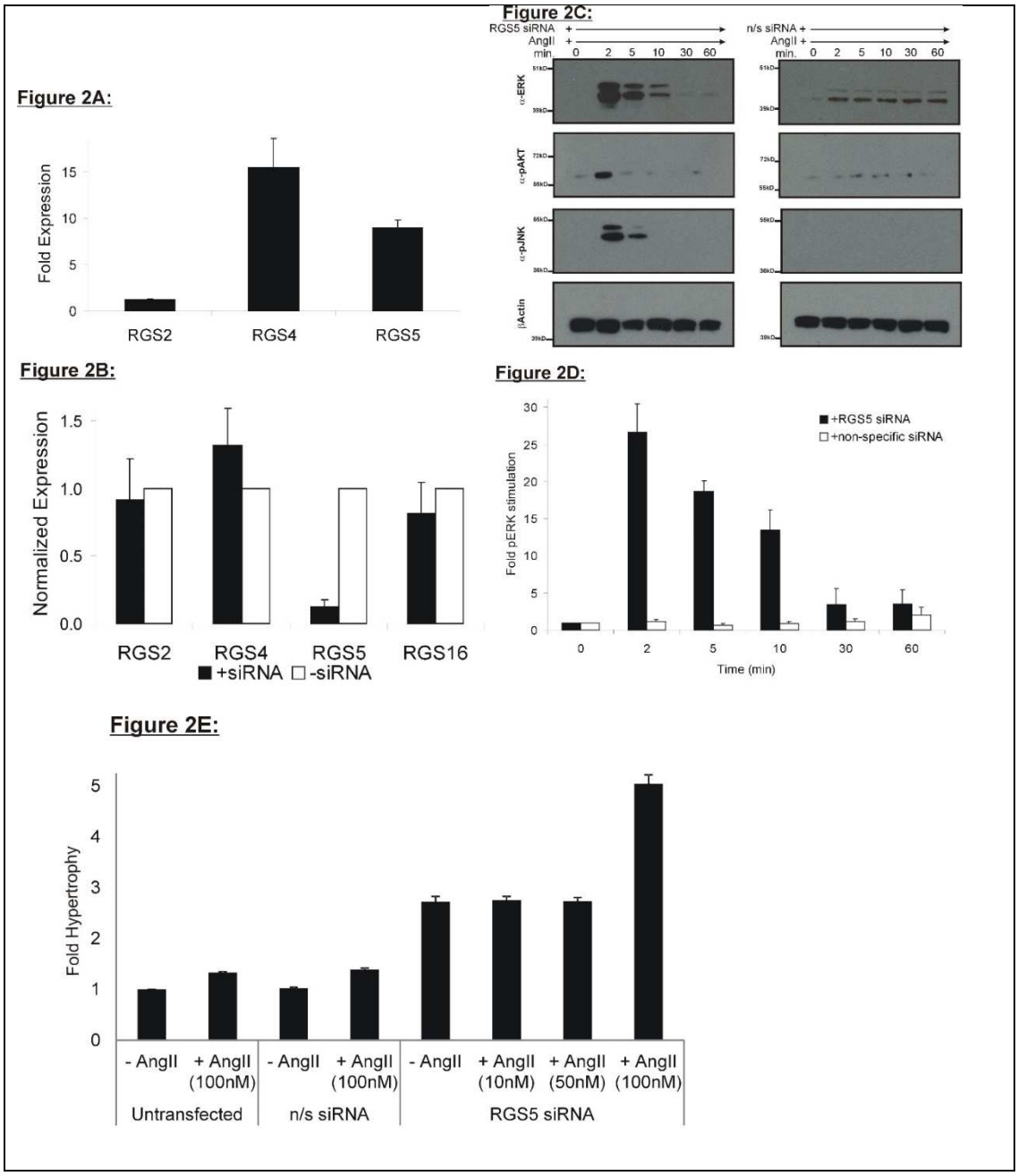

Figure 2. *RGS5 expression regulates AngII stimulated signaling pathways.* (A.) The relative expression of RGS-R4 subfamily members was assessed in rat aortic vSMCs by qPCR. In multiple rat aortic vSMC isolates, the expression RGS2, RGS4, and RGS5 was determined, and normalized to the relative expression of RGS2 ($2^{-\Box\Box Ct}$) (error bars are SEM; n=4). (B.) The specificity of the RGS5 siRNA was assessed by qPCR. As shown, the siRNA specifically down-regulates RGS5, independently from other

RGS-R4 subfamily members (error bars are SEM; n=3). (C.) Knock-down of RGS5 expression stimulates AngII-stimulated phosphorylation cascades. vSMCs were stimulated with AngII (100nM) in the presence of either RGS5 siRNA (*left*) or non-specific siRNA (*right*). Whole-cell extracts were prepared and immunoblotted. The phosphorylation of ERK, AKT, and JNK is stimulated when RGS5 is specifically knocked-down. □Actin is shown as a control for equivalent protein loading. (D.) Quantitation of immunoblots (error bars are SEM; n=3) demonstrating RGS5 knock-down stimulates AngII-mediated phosphorylation of ERK. (E.) RGS5 knock-down induces AngII-stimulated hypertrophy. vSMCs were transfected with either RGS5 siRNA or non-specific siRNA, stimulated with AngII (0, 10nM, 50nM, and 100nM) for 24 hrs, pulsed with 1□Ci [^{3}H]-leucine for 5hrs, and the amount of ^{3}H-leucine incorporated into new protein was quantitated to assess hypertrophic growth. (error bars are SEM; n=3.)

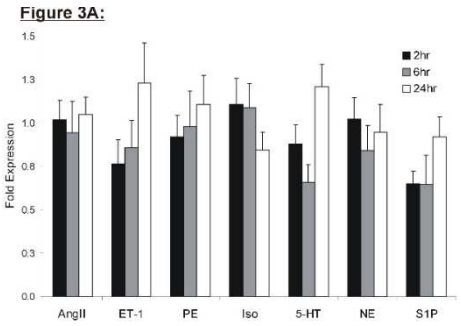

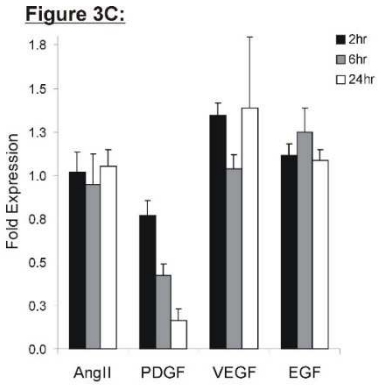

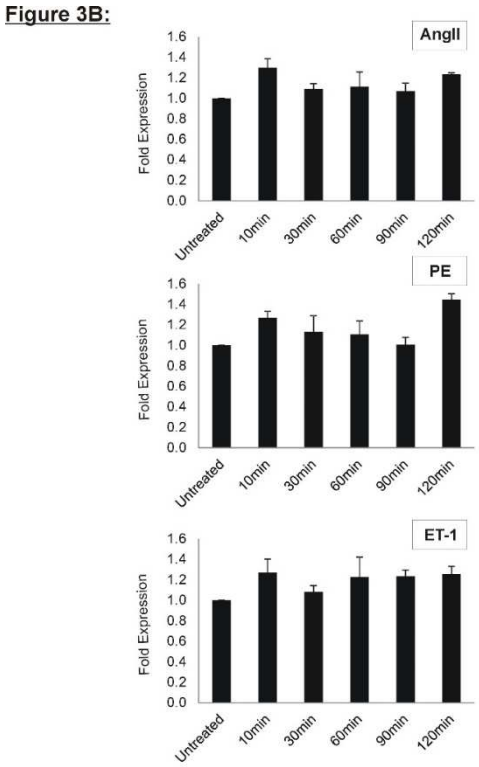

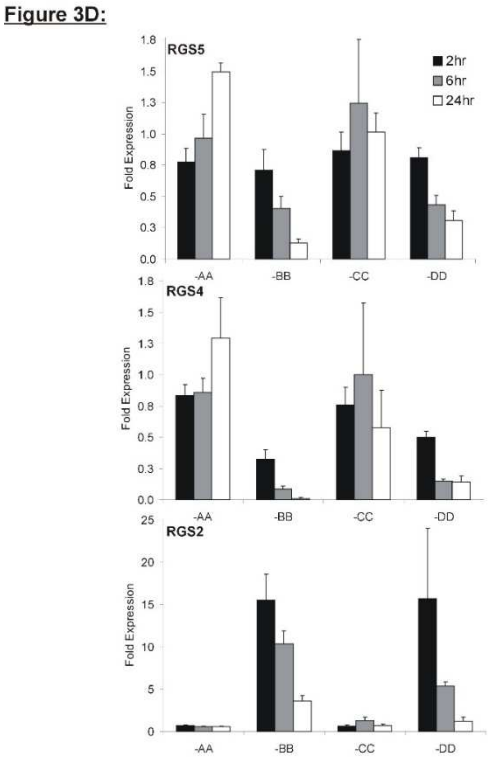

Figure 3. *The effect of GPCR- and RTK-stimulation on RGS-R4 subfamily expression.* (A.) vSMCs were stimulated, for 2hrs, 6hrs, and 24hrs, with GPCR agonists: AngII (100nM), ET-1 (100nM), PE (10□M), Iso(10□M), 5-HT (5□M), NE (10□M), and S1P (1□M). The expression of RGS5 was quantitated by qPCR, and normalized to the relative expression of RGS5 in untreated cells. (B) vSMCs were stimulated for 10min, 30min, 60min, 90min, and 120min with candidate GPCR agonists: AngII (100nM), PE (10mM), and ET-1 (100nM). The expression of RGS5 was quantitated by qPCR, and

normalized to the relative expression of RGS5 in untreated cells. (C.) vSMCs were stimulated, for 2hrs, 6hrs, and 24hrs, with RTK agonists: PDGF (10ng/mL), VEGF (10ng/mL), and EGF (10ng/mL),. The expression of RGS5 was quantitated by qPCR, and normalized to the relative expression of RGS5 in untreated cells. (D.) vSMCs were stimulated, for 2hrs, 6hrs, and 24hrs, with each PDGF isoform: PDGF-AA, -BB, -CC, -DD. The relative expression of RGS5 (*top*), RGS4 (*middle*), and RGS2 (*lower*) was quantitated by qPCR, and normalized to the relative expression of RGS5, RGS4 and RGS2 in untreated cells, respectively. (error bars are SEM; n=4.)

Figure 4A:

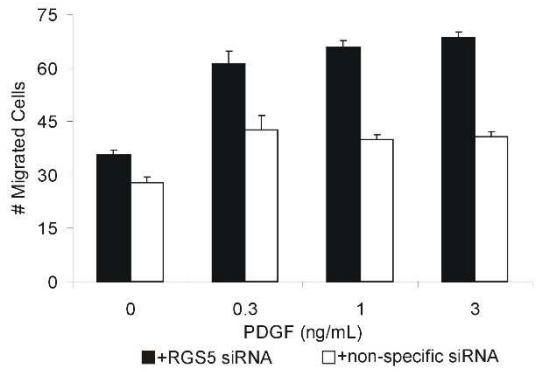

Figure 4B:

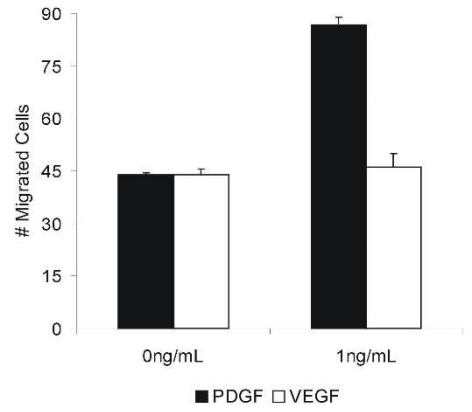

Figure 4. *Knock-down of RGS5 expression by siRNA induces PDGF-induced vSMC migration*. (A.) A migration assay was performed in the presence of either RGS5 siRNA or non-specific siRNA. At each concentration of PDGF-BB (0.3ng/mL, 1ng/mL, and 3ng/mL), vSMCs are more migratory when RGS5 has been specifically knocked-down. (B.) The migration assay was performed in the presence of PDGF-BB or VEGF in vSMCs, where RGS5 is specifically knocked-down. Only PDGF-BB stimulates migration in vSMCs. (error bars are SEM; n=3.)

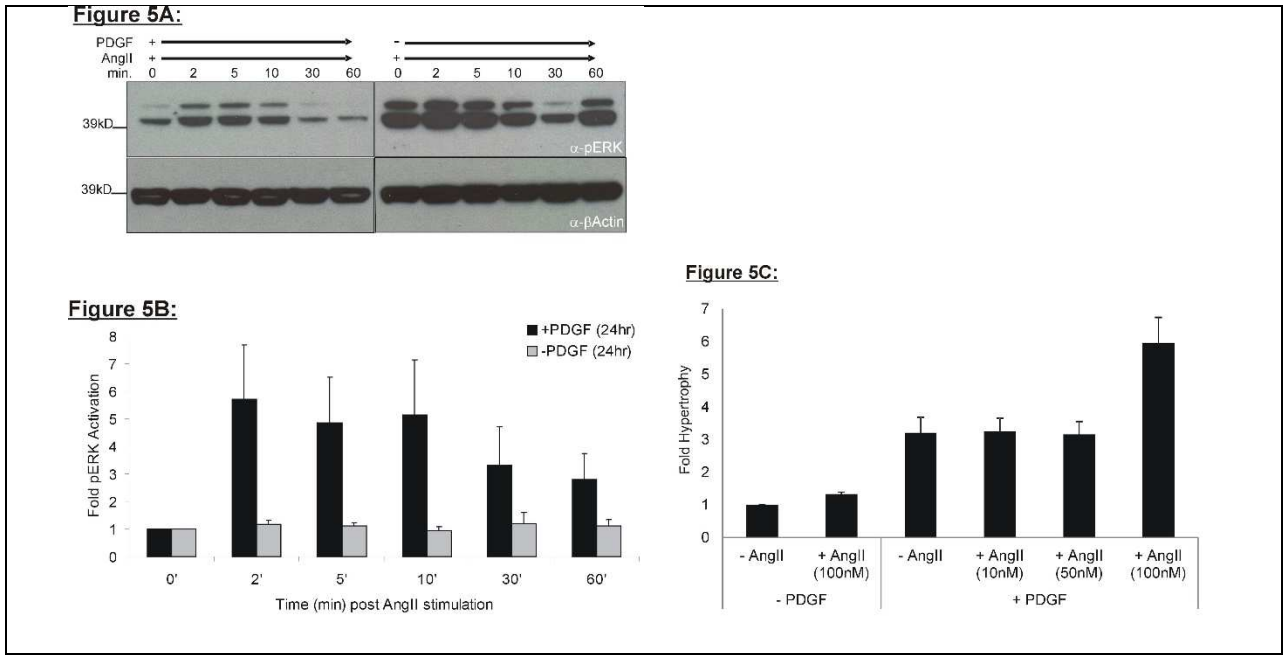

Figure 5. *PDGF-BB stimulates RGS5 knock-down, induces AngII-mediated ERK phosphorylation, and induces Ang-II mediated hypertrophy.* (A.) vSMCs were stimulated with AngII (100nM) for the indicated times, following 24hrs treatment of PDGF-BB (10ng/mL; *left*) or without PDGF-BB treatment (*right*). Whole-cell extracts were prepared and immunoblotted for the expression of phosphorylated ERK. Actin is shown as a control for equivalent protein loading. (*Note: For comparison, the pERK blot is over-exposed relative to the + non-specific siRNA blot (Figure 2E*). (B.) Quantitation of immunoblots (n=4) demonstrating PDGF-BB treatment stimulates AngII-mediated phosphorylation of ERK. (C.) PDGF-BB induces AngII-stimulated hypertrophy. vSMCs were treated with or without PDGF-BB for 24hrs, stimulated with AngII (0, 10nM, 50nM, and 100nM) for 24hrs, pulsed with 1 Ci [^{3}H]-leucine for 5hrs, and the amount of [^{3}H]-leucine incorporated into new protein was quantitated to assess hypertrophic growth. (error bars are SEM; n=3.)

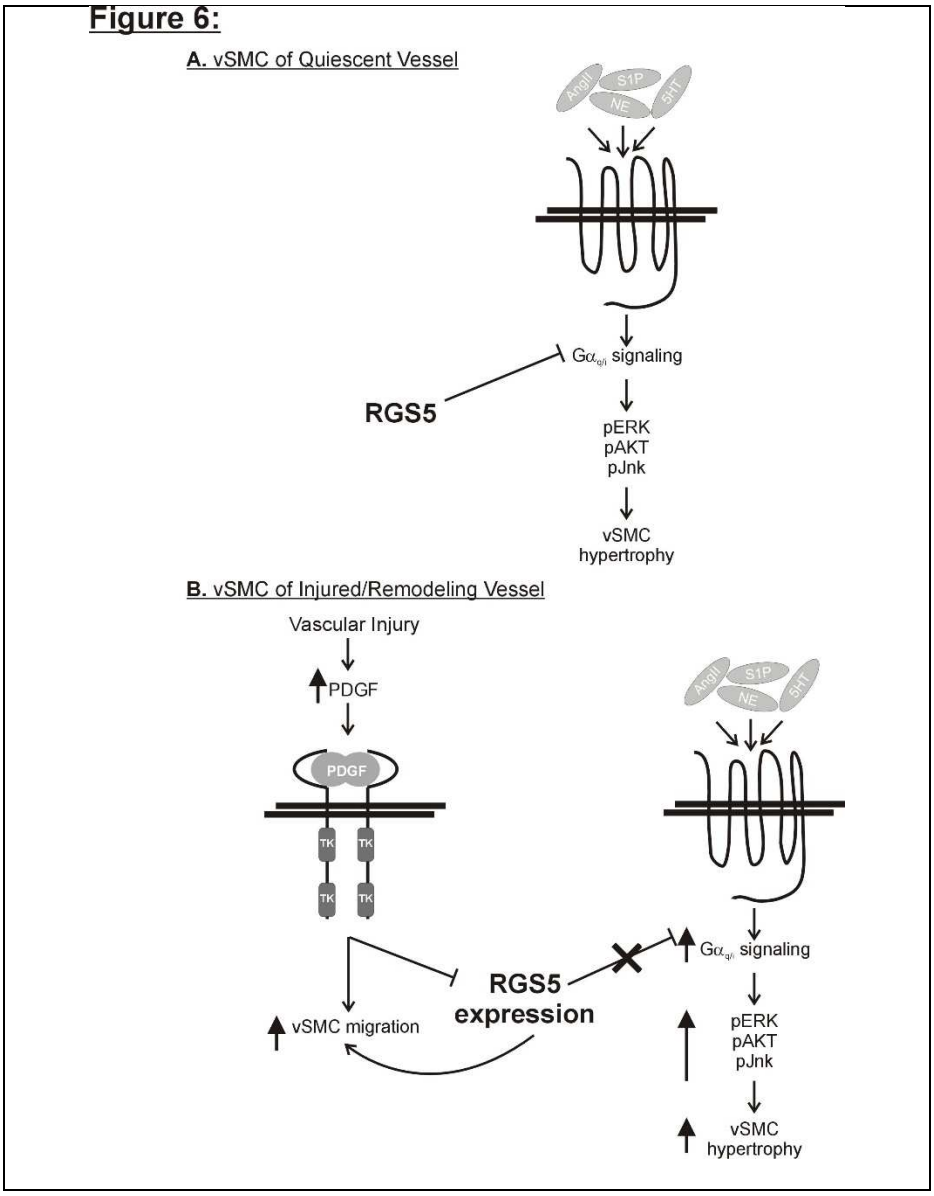

Figure 6. *The role of RGS5 in regulating vSMC signaling.* (A.) RGS5 normally represses GPCR signaling. (B.) In response to vascular injury, local concentrations of PDGF increase, thereby repressing RGS5 expression. Upon inhibition of RGS5 expression, vSMC migration and GPCR-stimulated signaling cascades are activated, leading to enhanced vSMC hypertrophy and vascular remodeling.